5-2016

# AEROBIC BACTERIAL TRANSFORMATIONS OF LIGNIN-DERIVED AROMATIC COMPOUNDS

Ashley Marie Frank
*University of Tennessee - Knoxville*, afrank3@vols.utk.edu

To the Graduate Council:

I am submitting herewith a dissertation written by Ashley Marie Frank entitled "AEROBIC BACTERIAL TRANSFORMATIONS OF LIGNIN-DERIVED AROMATIC COMPOUNDS." I have examined the final electronic copy of this dissertation for form and content and recommend that it be accepted in partial fulfillment of the requirements for the degree of Doctor of Philosophy, with a major in Microbiology.

Alison Buchan, Major Professor

We have read this dissertation and recommend its acceptance:

Erik R. Zinser, Frank E. Löffler, Joseph J. Bozell

Accepted for the Council:

Carolyn R. Hodges

Vice Provost and Dean of the Graduate School

(Original signatures are on file with official student records.)

# AEROBIC BACTERIAL TRANSFORMATIONS OF LIGNIN-DERIVED AROMATIC COMPOUNDS

A Dissertation Presented for the

Doctor of Philosophy

Degree

The University of Tennessee, Knoxville

Ashley Marie Frank

May 2016

# ACKNOWLEDGEMENTS

I would like to extend my most gracious thanks and appreciation to family and friends who have supported me throughout my life, and particularly during the arduous years of graduate school. I would specifically like to extend gratitude to my mother, Robin; my father, Ray; and my sister, Tammy for their kind words, thoughts, and encouragement.

One of the most fulfilling aspects of graduate school has been the incredible people that I have met and became friends with. This local network of support was has been critical to my happiness and achievements, both academic and personal. So thank you so very much to my team of cheerleaders, comic relievers, listeners, idea-sculptors, instigators and supporters; Nathan Cude, Chris Gulvik, Nana Ankrah, Jackson Gainer, Jeremy Chandler, Abby Smartt, Lauren Quigley, Jonelle Basso and Steven Higgins.

I would be remiss if I did not also extend my most sincere gratitude to mentors who have helped cultivate an enthusiasm for science. One of the most inspiring scientists I have had the pleasure to meet is my undergraduate genetics and molecular biology instructor at Elmhurst College, Dr. Kent Kerby. Dr. Kerby was the first person to encourage me to pursue science and went out of his way to support me with kind words and scholarship opportunities. For all of his enthusiasm, dedication, and encouragement I would like to offer my most genuine thanks.

Lastly, I would like to extend a heartfelt thanks and appreciation to my Ph.D. advisor, Dr. Alison Buchan, who has provided the necessary guidance for me to improve and complete my doctoral training. I admire Alison for many reasons that extend beyond academics, as she is likely one of the most well balanced and fair individuals I have ever met. Alison, I would like to offer a gracious thanks to you for your support.

# ABSTRACT

Lignin, the most abundant aromatic polymer on earth, has been estimated to contribute ~20% of the total carbon deposited in nature and thus imparts a large influence on carbon cycling in the environment. The extraordinary abundance of carbon stored in this material renders it a desirable source of renewable carbon for a variety of applications including hydrocarbon fuels and industrial chemicals. Due to its incredibly stable architecture and entanglement with cell wall polysaccharides, however, efforts toward the conversion of lignin to high value commodities have historically been impeded. Despite this obstacle, many microbes in nature are capable of degrading lignin for use as a carbon and energy source. Microbial lignin depolymerization is typically initiated by the activity of extracellular peroxidases produced by fungi and a limited number of bacteria. This deconstruction liberates a pool of lower molecular weight aromatic compounds that can be subsequently catabolized by bacteria in the environment. The work presented here investigates the diverse reactions involved in the bacterial transformation of lignin-derived compounds, with a strong focus on conversions with potential to deliver valuable products. Insights into the bacterial transformation of ferulic acid, an abundant lignin-derived compound, are provided through mutagenesis studies with the model marine roseobacter strain, *Sagittula stellata* E-37. This study specifically interrogates the role of two annotated feruloyl-CoA synthase genes in the catabolism of ferulic acid. Results unveil the possible misannotation of genes and incite intrigue concerning substrate promiscuity across aromatic acyl-CoA synthases. Additional evidence is provided for the utilization and transformation of a pretreated organosolv lignin by another roseobacter species, *Citreicella* sp. SE45. This work highlights the potential application of lignolytic bacteria to upgrade residual lignin from a biorefinery. Finally, biotransformation studies with bacterial ring-hydroxylating dioxygenases present evidence for the transformation of lignin model compounds to a highly valuable *cis*-dihydrodiol intermediate that can be chemical converted to an array of synthetic chemicals. Collectively, this work provides

an enhanced understanding of bacterial reactions with lignin-derived compounds and offers new insights and suggestions for continued studies in this field.

# TABLE OF CONTENTS

# LIST OF TABLES

# LIST OF FIGURES

# CHAPTER ONE - INTRODUCTION

# I. Lignin

Lignocellulose, the matrix supporting vascular plant cell walls, is considered one of the most renewable sources of carbon on earth. This material comprises three recalcitrant biopolymers, cellulose, hemicellulose, and lignin, all of which harbor potential to yield high-value products of commercial and/or industrial interest (1). The monomeric sugars in the polysaccharides can be converted into ethanol, whereas the aromatic lignin can be transformed into hydrocarbon fuels and various aromatic chemicals of industrial application. Although all three polymers contain valuable chemical potential, the cellulose and hemicellulose have been more heavily targeted due to their relative ease of conversion to ethanol and the concomitant need for alternative fuel energies. General practices for bioethanol production include an initial pretreatment of the biomass to partially degrade and fractionate the lignin from the sugars, followed by an enzymatic saccharification and fermentation of the sugars to ethanol (2). In this process, the refractory lignin is commonly considered a waste product and is burned for disposal. While this method is successful in liberating fermentable sugars in plant cell walls, it fails to exploit the energy-rich bonds within lignin's heteropolymeric network of aromatic compounds.

The work detailed in this dissertation focuses on the underutilized, but highly valuable lignin component of lignocellulose. Accordingly, the sections below discuss the structure and composition of lignin, its role in the biorefinery, as well as useful products that can be extracted and/or generated from this material.

### *A. Structure and function of lignin*

Lignocellulose has been heavily studied since the mid 1800s, however, it was not until the 1930s that researchers were able to optimize procedures enough to isolate lignin from proteins and carbohydrates and begin to resolve features (3-5). Anselme Payen is credited with the first chemical biomass fractionation in 1838 (5) whereby he

sequentially treated wood with nitric acid and washed with sodium hydroxide to yield an insoluble “cellulose” and a dissolved fraction later termed “lignin” by Schulze in 1857 (5). From here, interest in technologies to “delignify” wood increased as an effort to isolate cellulose for production of cellulose fibers used in the paper industry. As delignification technologies advanced, fundamental chemical features of lignin began to emerge, amassing the repertoire of knowledge that we currently exploit for lignin research today. The experiments supporting this foundational insight to lignin structure and composition have been thoroughly documented (5-8).

Thanks to almost 200 years of research, we now have a strong (but not comprehensive) understanding of the chemical composition and structure of the lignin polymer. It is currently understood that all lignins are formed through the polymerization of three 4-hydroxycinnamyl alcohols (monolignols): *p*-coumaryl, coniferyl, and sinapyl alcohol. In their polymerized form, these residues are referred to as 4-hydroxyphenyl (H), guaiacyl (G), and syringyl (S) phenylpropanoid units, respectively (Figure 1.1). All units are similar in structure but differ in the degree of ring methoxylation. While there is some contention regarding the process of lignification *in planta*, the most supported theory of polymerization involves a radical coupling of monolignols driven by peroxidase-$H_2O_2$ which facilitates the dehydrogenation of monolignol units into di- and oligo-lignols (9). This idea is supported by the studies of many different research groups who approached the concept from a variety of angles. Dating back to 1965 (10) Freudenberg demonstrated that the addition of peroxidase and $H_2O_2$ to coniferyl alcohol generated a dehydrogenated polymer (DHP) consistent with lignin from spruce. Similarly, Musel *et al*. showed that addition of $H_2O_2$ to plant tissue resulted in an increase of lignin content, suggesting the involvement of hydrogen peroxide in lignification (11). More recently, others have more directly investigated the role of peroxidase activity through assessment of transgenic plants that down regulate peroxidases, resulting in decreased lignification (12, 13).

Due to electron delocalization across the aromatic ring and side chains of the 4-hydroxycinnamyl alcohols, radical species are generated at a variety of positions on each monolignol. The combination of these radicals across the monolignols results in different radical coupling combinations, and ultimately different linkages across the lignin polymer. For instance, coniferyl alcohol can form a radical at the 4-C and 5-C ring positions as well as the β carbon of the side chain, generating β-O-4 (β-ether), β-5 (β-dimer), and β-β (pinoresinol) interunit linkages (5-5 and 4-O-5 have not been observed from *in vitro* dehydrogenations but exist in nature) (9) (Figure 1.2). The sinapyl alcohol residues form radicals at the 4-C position and β-carbon of the side chain, yielding β-O-4 and β-β linkages. Due to the plethora of radical positions across all 3 monolignols and the somewhat stochastic nature of radical coupling (governed by the environmental conditions and deposition of reactants), it is not surprising that lignin structure and composition is extremely diverse between, and even within plant species (14). Despite the variability of lignin composition, general characteristics regarding common lignin content and composition of different plant classes have been observed. For any given plant, the lignin content constitutes 15-30% of the dry weight of the plant cell wall (15). Gymnosperms (softwoods) contain mostly G-units with a small proportion of H units, whereas angiosperms (hardwoods) contain predominantly G- and S- units. Grasses (monocots) generally consist of equal amounts of G- and S- units, with a higher proportion of H than dicots (16). Due to these differences, the S:G:H (more often S:G) ratio is used to classify different sources of biomass, and applied as a metric to determine relative recalcitrance and/or complexity, usually in the context of sugar accessibility/release from a particular plant (17).

Collectively, the composition and arrangement of stable phenylpropanoid units in lignin confer structural and protective properties to the plant, rendering it the most recalcitrant component of plant cell walls. Most obviously, lignin's network of aromatic constituents affords UV protection to the plant tissues (18) and an incredibly strong infrastructure capable of supporting massive tree weights. Lignin also serves as a primary defense mechanism against invading pathogens. Studies have shown an accumulation of lignin

in plant tissue at the site of fungal attack, strengthening the physical barrier to fungal penetration (19). Similarly, RNAi silencing of monolignol biosynthesis genes has demonstrated an increased susceptibility of wheat leaf tissue to infection by powdery mildew fungus (20). Not only does lignin present a physical barrier to cellular invasion, but it also impedes the attack of hydrolytic enzymes, particularly cellulases, produced by microbes. This impediment is the crux of the challenges faced in bioethanol refineries. Cellulases are instrumental in generating fermentable sugars from cellulose, however, if cellulose access is denied through lignin interference, ethanol cannot be effectively and economically produced. For this purpose, bioethanol industries have applied various strategies to circumvent the lignin barrier, including biomass pretreatments to remove the lignin (21), biomass engineering to reduce the lignin content of the plant (22), and other approaches to be discussed in the proceeding section.

### *B. Lignin in the biorefinery*

Since its infancy, the bioethanol industry has sought to advance technologies for superior biomass conversion efficiencies and economic viability. This involves efforts to overcome the inherent recalcitrance of lignocellulose, including optimizing biomass pretreatment practices, engineering plant biomass to enhance its depolymerization (23), and engineering enzymes for sugar hydrolysis and fermentation (2, 24). The historical biomass fractionation chemistries from Payen and others have been adapted over time to provide the scaffolding for biomass pretreatment practices applied in today's biorefineries. Prior to chemical pretreatments, biomass can be physically degraded through chipping, milling and grinding to increase the surface area of the material prior to further treatments. Chemical pretreatments are generally categorized by the solvents applied during the process and broadly include alkaline, acid, and organic solvent (organosolv) methods. Alkaline pretreatments typically involve soaking the biomass in calcium or sodium hydroxide with moderate heat to increase porosity and disrupt lignification and lignin-carbohydrate bonds. This approach co-solubilizes the lignin and hemicelluloses, leaving mostly cellulose behind for enzymatic saccharification (25).

Acid pretreatments are usually performed with either dilute or concentrated acid. Dilute sulfuric acid pretreatments at 160-220°C hydrolyze only the hemicellulose, allowing increased enzymatic access to the cellulose (26). Treatment with concentrated acids such as sulfuric or hydrochloric acid, however, will disrupt both the hemicellulose and cellulose without affecting the lignin. While this generates a relatively high yield of monomeric sugars for fermentation, it also generates a large amount of toxic material and need for acid recycling to reduce costs. Organic solvent (organosolv) pretreatments react the biomass with an acid catalyst in an organic solvent (ethanol, methanol, acetone, etc.) at high temperatures to facilitate the hydrolysis of bonds within lignin and between lignin and hemicellulose. The lignin is separated from the remaining biomass (mostly cellulose) through extraction of the organic phase. This approach is particularly attractive, as it provides a relatively clean separation of lignin and cellulose, generating two carbon pools from which valuable products can be derived. The cellulose is obviously targeted for ethanol production, whereas the fairly pure lignin extract offers opportunities for conversion to hydrocarbon fuels and drop in chemicals. Recent studies have demonstrated success in optimizing organosolv reaction conditions for switchgrass, highlighting the utility of this pretreatment as a viable and advantageous method for use in the biorefinery (27). Much attention has been paid to comparing pretreatments for various biomass sources (21, 28), however, most recent investigations point to the organosolv method as the most attractive and tractable option for increasing cellulose saccharification and generating value-added products from lignin (29).

Because biomass pretreatments tend to be one of the largest costs of bioethanol production, additional efforts have been made to reduce the need for intense delignifying pretreatments by genetically manipulating the biomass source to make it more amenable to fractionation. The most obvious modification to increase ethanol would be to limit the production of lignin. Accordingly, studies have engineered plants to produce sub-basal levels of lignin and found an associated increase in sugar release from polysaccharide hydrolysis (30). However, decreases in lignin content may not be

the only determinant of polysaccharide accessibility. Clint Chapple's group at Purdue University has dedicated much effort towards generating lines of transgenic plants for enhanced cell wall digestibility. Studies from this team have recently found that changes to the composition (not abundance) of lignin yields plants with enhanced cell wall digestibility (31). Here, transgenic lines of *Arabidopsis thaliana* were generated with disruptions in the phenylpropanoid biosynthesis pathway to enrich the plants in either G- or S- aldehydes (aldehydes are non tradition lignin components). In all instances, plants were viable and produced comparable amounts of lignin, but were more amenable to saccharification. These results suggest that the lignin unit composition may be more important to cell wall deconstruction than total lignin content. Work on these gene disruptions and others have been summarized and additional manipulations proposed for further plant digestibility (22).

### *C. Lignin products and applications*

There exists a long-standing joke among lignin researchers that "you can make anything from lignin except money (32)." Unfortunately there is an unsettling truth to this as although the value of lignin has been long recognized, harnessing the potential from lignin has been challenging. Upon appropriate isolation, however, lignin can be transformed into an array of useful materials, which perpetuates a strong interest in continued lignin research. Many potential lignin-derived products have been considered (32) and are worth examination; however, only the most prevalent will be discussed here. One grand valorization of lignin would be a conversion to carbon fiber to replace heavier materials, such as steel in cars, however, the technology for this conversion is in its infancy and the projected successes from a lignin-based material are unclear (1). Nevertheless, efforts are being put forth to generate lignins that are compatible with effective conversion to carbon fibers (33, 34). Another promising family of lignin-derived products includes plastics and related polyurethanes. Recent advancements on polyurethane foam technology has allowed substituting 12% of the standard fossil polyol

starting material with commercial lignin, offering potential for integration into industry (35).

The most historically pursued potentials of lignin include production of hydrocarbon fuels and valuable chemicals. The research presented in Chapters 3 and 4 of this document were motivated by the prospect of generating lignin-derived materials for conversion into liquid transportation fuels and chemicals of industrial relevance. Transformation of the lignin polymer involves an initial depolymerization typically mediated by reductive catalysis for hydrogenolysis and hydrodeoxygenation (36). In addition to fuel products, many valuable aromatic monomers can be liberated from lignin. Nonselective lignin deconstruction approaches can yield products such as benzene, toluene, xylene, and phenol. These chemicals can easily be integrated into current chemistry technologies to produce other industrially relevant chemicals (32). Other high-value aromatics such as vanillin could also be liberated from lignin, however, this would require a much more selective type of chemical pretreatment. While this is not a completely unmanageable approach, perhaps a more effective route would be the application of microbial enzymes known to produce vanillin and similar products from lignin substrates (37, 38). Due to the heterogeneity and recalcitrance of lignin, unlocking its imprisoned chemical potential has presented a major obstacle, however, technologies are advancing to make these practices more fruitful and economical. Perhaps soon the saying “you can make anything from lignin except money” will no longer be so relevant.

## II. Microbial transformations of lignin and its derivatives

Lignocellulose has been claimed to account for 70% of terrestrial plant biomass, contributing 120–140 x $10^9$ tons of carbon-rich biomass per year (39). The aromatic lignin portion of this material typically constitutes about 20-30% of the plant cell wall, suggesting that lignin is responsible for depositing about 20% (or up to 28 x $10^9$ tons) of

carbon material to the earth annually. Understanding the microbial reactions that facilitate the release of this carbon aids in our comprehension of carbon cycling related to climate control, and may also elucidate enzymes of industrial interest for the conversion of lignin into valuable products. The degradation of lignin in nature is predominantly initiated by the activity of fungal enzymes, with a few instances of bacterial lignolytic activity. This primary degradation yields a variety of low molecular weight aromatics that are subsequently utilized by bacteria as carbon and energy sources. Historically, most research on microbial lignin degradation has focused on soil environments; however, other plant-rich environments such as coastal salt marshes have recently received due attention (40, 41). The following sections outline our current knowledge of microbial degradation of lignin and its aromatic constituents.

### *A. Degradation of lignin*

The degradation of lignocellulose in nature proceeds through an initial biomass oxidation mediated by fungal (and sometimes bacterial) enzymes, releasing aromatic monomers for further microbial consumption. Lignolytic fungi are classified as either "white rot" or "brown rot" species depending on their method and extent of lignin degradation. White rot fungi are capable of performing a complete degradation of lignin, leaving a "white" cellulose-rich material, whereas the brown rot fungi only partially degrade lignin, resulting in a brown residue. The enzymes produced by both of these groups of fungi vary; however, both generate aromatic monomers from lignin that can be further catabolized by bacteria. White rot fungi like *Phanerochaete chrysosporium*, have been extensively studied with respect to the abundance and activity of extracellular oxidoreductase enzymes they produce. Generally, white rot species produce several different peroxidases to oxidize lignin. Fungal peroxidases include lignin peroxidase (LiP), manganese peroxidase (MnP), and versatile peroxidase (VP), all of which oxidize the substrate through reduction of hydrogen peroxide but differ in substrate range. Lignin peroxidases (E.C. 1.11.1.14) oxidize the non-phenolic units in lignin (which generally comprise over 90% of the polymer) while the manganese

peroxidases (E.C. 1.11.1.13) convert both phenolic and non-phenolics through oxidation of $Mn^{2+}$ to $Mn^{3+}$, which can oxidize surrounding lignin material. Versatile peroxidase represents the most recently discovered lignin oxidoreductase and exhibits hybrid features of the LiP and MnP enzymes (42).

Another class of fungal enzymes that have been implicated in lignin degradation is the copper-containing laccases (E.C.1.10.3.2), which oxidize phenols through the reduction of oxygen to water. Although laccases have been demonstrated to react with lignin model compounds (43), there is conflicting evidence regarding its role in lignin oxidation in nature (44). While some studies show a prevention of lignolysis in laccase-deficient fungi (45), others report no loss in lignin degradation when laccases are inhibited by the copper-chelating chemical thioglycolate (46). Furthermore, antibody inhibition studies suggest that laccase-mediated lignin degradation may be an artifact of *in vitro* experiments, as the inhibited enzyme did not impair lignin degradation in pure cultures (47). Thus the contributions of laccases to lignin degradation remain unclear and require additional studies to support their true activity in nature. In contrast to the plethora of enzymes generated by white-rot fungi, brown-rot species are believed to partially degrade lignin through Fenton chemistry ($Fe^{2+} + H_2O_2 + H^+ \rightarrow Fe^{3+} + H_2O +$ •OH), although a precise mechanism has not been defined. Current research proposes a quinone-mediated reduction of $Fe^{3+}$ to $Fe^{2+}$ that subsequently reacts with hydrogen peroxide to generate a hydroxyl radical capable of oxidizing lignin (48).

To a limited extent, bacteria also present evidence of lignolysis through utilization of extracellular enzymes similar to those produced by fungi (49, 50). Knowledge to date suggests these activities are mostly limited to select members of the actinobacteria, γ-proteobacteria, and α-proteobacteria classes, with most insight provided by studies from the α-proteobacterium, *Sphingobium* sp. SYK-6 (50). The first bacterial lignin peroxidase was identified and experimentally validated in the actinobacterium *Streptomyces veridosporus* T7A in 1998. A purified peroxidase from this organism was used to successfully cleave diaryl-propane and beta-aryl ether lignin models in a

hydrogen peroxide-dependent manner, suggesting a degradation approach consistent with fungi (51). Additionally, a manganese ($Mn^{2+}$)-activated peroxidase, DypB (Dye-decolorizing Peroxidase), has been identified and structurally characterized (PDB 3QNR and 3QNS) in another actinomycete, *Rhodococcus jostii* RHA1 (52). Both this strain as well as the γ-proteobacterium, *Pseudomonas putida* mt-2, were found to transform lignin as evidenced by spectrophotometric assays employing both fluorescently modified lignin and nitrated lignin (53). The same study provided additional support for lignin degradation through incubation studies detecting the appearance of monomeric phenols after growth on milled miscanthus. Studies on the α-proteobacterium, *Sphingobium paucimobilis* sp. SYK-6, focus on the degradation of β-aryl-ether linkages (refer to Figure 1.1). The initial conversion of this substrate proceeds through the oxidation of the side chain α-hydroxyl group to a ketone through the activity of LigD, an NAD-dependent dehydrogenase (54). The subsequent bond cleavage steps are conducted through a pair of β-etherase glutathione-S-transferases (LigEF) and a glutathione lyase (LigF) to yield the cleavage products β-hydroxypropiovanillone and guaiacol (55).

Lignin cleavage studies like those mentioned above offer an opportunity to assess the degradation products of lignin, revealing substrates that can be utilized by other bacteria in the environment. Of course, the array of compounds liberated from any biomass will depend on the structure and composition of its source as well as the enzymes involved; however, many common structures arise from these oxidations. For instance, analysis of products from *Phanerochaete chrysosporium* degradation of spruce lignin revealed 10 different benzoic acid derivatives (50) many of which were also present from degradations of kraft lignin with the bacterium *Aneurinibacillus aneurinilyticus (56)* . Another important class of aromatics that regularly appears from degradation studies are the cinnamic acids, *p*-coumaric and ferulic acid derived from H- and G- lignin units, respectively. These have been reported from the degradations with *Bacillus sp*., *Pseudomonas putida*, and *Rhodococcus jostii* RHA1 (50). The generation of ferulic acid is of particular interest due to its subsequent conversion to commercially valuable

products like anti-inflammatories and vanillin (38, 57), which will be discussed in more detail in Chapter 2. Most of the above products have been generated from terrestrial plants and pretreated biomass, however, degradation products from coastal grasses have also been examined. In a study aiming to determine the contribution of lignocellulose to salt marsh dissolved organic carbon (DOC), the coastal cord grass *Spartina alterniflora* was $^{14}C$ radiolabeled and degraded by its associated fungus, *Phaeosphaeria spartinicola* (58). Gas chromatography of the resulting lignin phenols suggested an increase in vanillin and related compounds, with a decrease in ferulic acid and *p*-coumaric acid, suggesting a relative preference for transformation of these hydroxycinnamic acids.

### *B. Degradation of lignin-derived aromatics*

Once the initial lignocellulosic material is oxidized, the low molecular weight aromatics serve as carbon and energy sources for the surrounding bacterial communities. While Fuchs and others have described four recognized aromatic catabolism pathways (59, 60), only those that proceed under oxic conditions will be addressed here, as these are directly relevant to the research herein. The microbial degradation of aromatic compounds generally proceeds through a catabolic funneling process whereby an array of aromatic substrates are transformed into a limited number of central intermediates (peripheral pathways) that are then subject to ring cleavage (lower pathways) for central metabolism. Several different ring-cleaving pathways have been documented for plant-derived aromatic compounds, however, most have been shown to utilize one of the two branches of the classical β-ketoadipate pathway, proceeding through either a catechol or protocatechuate intermediate prior to ring fission (61). In this classical aerobic pathway, compounds are initially hydroxylated through incorporation of 1 or 2 oxygen atoms (from $O_2$) through monooxygenase or dioxygenase activity, respectively. Monoxygenases perform a single hydroxylation, whereas the dioxygenase adds a pair of vicinal hydroxyl groups to yield a reactive *cis*-dihydrodiol intermediate that is quickly oxidized by a dehydrogenase to form a rearomatized product. *Special attention will be*

*paid to the cis-dihydrodiol of ring-hydroxylating dioxygenases in Chapter 4.* Some of the common central intermediates from classical ring hydroxylations include catechol, protocatechuate, and gentisate (62). The addition of electron-rich hydroxyl groups at the *ortho* and *para* ring positions prepares the ring for subsequent cleavage by *ring-cleaving* dioxygenases, which can act between hydroxyls (ortho cleavage) or adjacent to the hydroxyl groups (meta cleavage).

In addition to the ring hydroxylating approach, hybrid pathways have been observed that combine elements of traditional aerobic and anaerobic catabolism reactions (60). Due to the electron poor conditions of anoxic or low oxygen environments, microbes in these conditions employ a reducing reaction to initiate ring cleavage. This requires the addition of electron-withdrawing groups, such as Coenzyme A (CoA) to the ring to facilitate further reduction. Typically this is performed through CoA thiolation of a carboxylic acid side group. The canonical example of this type of reaction is the carboxyl-CoA thiolation of benzoate to yield benzoyl-CoA (63), but has also been observed with other compounds including phenylacetate (64), anthranilate (2-aminobenzoate) (65), *p*-coumarate (66), and ferulate (67). The CoA addition mediated by a CoA synthetase/ligase requires ATP and is therefore more energetically expensive than the oxidative approach. Aerobic hybrid pathways employ this initial CoA thiolation of the substrate, followed by standard ring cleavage mediated by oxygenases (anthraniliate with *Pseudomonas sp.*) (68), or may alternatively proceed through previously overlooked reactions facilitated by CoA-epoxidases (benzoate with *Azoarcus evansii*) (69, 70), and/or enoyl-CoA hydratases (ferulate with *Sphingobium* SYK-6) (67). As research expands on aromatic degradation, previously unseen approaches are being elucidated, providing additional insight into the enzymology and physiology of plant-degrading microorganisms. Continued studies promise to inflate this knowledge to provide a more comprehensive understanding of the mechanisms by which microbes process aromatic compounds. This insight may lead to the unveiling of novel enzymes for industrial application or for guidance biomimetic chemistries.

## III. Roseobacter catabolism of aromatics

Studies on bacterial degradation of lignin-derived aromatic compounds have historically focused on soil environments that are known for their wealth of carbon-rich plant material. An important environment that is often overlooked for these studies, however, is the highly productive coastal salt marsh system whose grasses contribute significantly to the marine dissolved organic carbon pools. Among the most well studied marsh systems are those along the southeastern United States. Analyses from Moran and Hodson suggest that up to 75% of the dissolved humic substances in this region, as determined by lignin-phenol content, is deposited by vascular plant material derived from the surrounding marshes and the adjacent riverine inputs (71). The dominant vascular plant in this particular region is the cordgrass *Spartina alterniflora*. Microcosm experiments with $^{14}C$ lignocellulose from *S. alterniflora* incubated with natural bacterial communities from salt marsh water suggest that bacteria mineralize 30% of the lignocellulose after 3 months (72). These data present preliminary evidence to support the notion that coastal marine bacteria are adapted to degrade lignocellulose, suggesting that this system may provide important information regarding bacterial degradation of plant material to supplement what is known from soil studies.

Among the most abundant bacteria found in southeastern coastal marsh systems are members of the Roseobacter lineage (α-proteobacteria of the *Rhodobacteracea* family), for which there are currently 32 genome sequences available (as of 2008). The Roseobacter clade contains > 35 different species, all of which share >89% 16S rRNA gene sequence identity (73). Although roseobacters are ubiquitous across the oceans, they dominate in coastal regions where they can account for ~30% of the bacterial community in southeastern coastal seawater as indicated by 16S rRNA gene analysis (74). Members of this clade are readily culturable and exhibit a diversity of ecologically relevant physiologies, arguing their importance as model organisms for a broad range of marine microbial research. Among some of the most notable phenotypes demonstrated

by roseobacter representatives are sulfur cycling through transformations of the algal and plant osmolyte dimethylsulfopropionate (DMSP) (75), symbioses with marine eukaryotes (76), production of secondary metabolites (77, 78) and associated surface colonization (77), and the degradation of plant-derived aromatic compounds (79), which is the primary focus of the work herein.

Knowing that roseobacters are abundant in coastal salt marsh systems where there are large inputs of plant-derived carbon, the isolation of cultured representatives capable of degrading plant-derived aromatic compounds was not a surprise. One of the most prolific accounts of aromatic catabolism in roseobacters arrived in 1996 when Gonzalez *et al*. isolated an organism, later named *Sagittula stellata* E-37, from a lignin enrichment from pulp mill effluent (80). Subsequent studies documented this organism's ability to mineralize synthetic DHP lignin and selectively attach to lignocellulose particles (81). Evidence for aromatic catabolism was soon expanded when Buchan *et al.* documented growth on aromatic compounds across 6 roseobacter isolates and verified the activity of protocatechuate 3,4-dioxygenase (PcaHG), a ring-cleaving enzyme of the β-ketoadipate pathway, in two of these isolates. This particular study reported growth on anthranilate, benzoate, *p*-hydroxybenzoate, protocatechuate, salicylate, *p*-coumarate, vanillate, and ferulate (82). Subsequent PCR-based assays for *pcaH* from Georgia salt marsh samples identified 149 *pcaH* clones, of which 52% were homologous to roseobacter sequences, suggesting that roseobacters are not only numerically dominant in coastal systems, but also likely carry a majority of the aromatic ring-cleaving capacity (83).

While aromatic catabolism is widespread across the roseobacter lineage, the wealth of information emerging from studies with *Sagittula stellata* E-37 (referred to as E-37 from here out) render this isolate an important model organism for studying aromatic catabolism in marine systems (84). Among the 32 sequenced roseobacters which collectively harbor 1-6 ring-cleaving pathways, E-37 is one of four isolates that exhibits evidence for all six ring-cleaving pathways (85), strengthening its potential to unveil new information on a diversity of aromatic pathways. Some paradigm-shifting physiologies

and exceptional genomic features are also being documented in this organism with respect the utilization of plant-derived aromatic compounds. In 2013, Gulvik *et al*. reported a growth advantage from the simultaneous catabolism of two plant-derived compounds (*p*-hydroxybenzoate and benzoate) that are processed through different ring-cleaving pathways, protocatechuate (pca) and benzoyl-CoA oxidation (box) (40). This concurrent substrate utilization contradicts the paradigm of hierarchical substrate utilization that is typically observed with soil bacteria. Another set of genetic and phenotypic features that has not been described until now includes a unique approach to ferulate catabolism through the joint effort of two annotated feruloyl CoA synthase homologs (42% identity, 96% coverage, expected value of e-148). Recent evidence from the work presented within also suggests the necessity of these two genes for the degradation of *p*-coumarate (Chapter 2). The insight provided from the work in this document helps to expand the growing repertoire of information regarding the utilization of plant-derived aromatics in coastal marine bacteria. These new findings will help guide future studies and may reveal novel enzymes and pathways that could be of used for industrial applications regarding the valorization of lignin.

## IV. Objectives

The work described in this dissertation collectively aims to expand upon our knowledge regarding bacterial transformations of lignin-derived material. The first research chapter focuses on the transformation of ferulate, a highly valuable lignin compound, by the model aromatic-degrading roseobacter, *Sagittula stellata* E-37, whose genomic architecture and composition suggests a unique approach to ferulate catabolism. The interest in this study lies in the value of the substrate and its intermediates as well as the potential to uncover new information on reactions involved in ferulate catabolism. The second research chapter focuses on roseobacter transformations of pretreated (organosolv) lignin in effort to demonstrate utilization of a modified lignin as a sole carbon source and to elucidate potential structural changes to the lignin that might be of

industrial interest as many valuable compounds can be liberated from lignin. The final research chapter examines the efficacy of a specific class of enzymes, ring-hydroxylating dioxygenases (RHDs), to generate a highly valuable *cis*-dihydrodiol intermediate from lignin models for downstream chemical conversion to hydrocarbon fuels and synthetic chemicals. The goals of this project are very targeted as they reflect a sub-aim of a high-risk high-reward DOE grant concerning a more comprehensive utilization of biomass from a biorefinery. The novelty in this particular study is derived from the screening of well-characterized recombinant RHDs with a set of *non-native* substrates, the lignin models compounds. The assays performed examine whether or not these enzymes are capable of accepting lignin models as substrates and their relative abilities to generate the desired *cis*-dihydrodiol product.

# V. References


1. **Ragauskas AJ, Beckham GT, Biddy MJ, Chandra R, Chen F, Davis MF, Davison BH, Dixon RA, Gilna P, Keller M, Langan P, Naskar AK, Saddler JN, Tschaplinski TJ, Tuskan GA, Wyman CE.** 2014. Lignin valorization: improving lignin processing in the biorefinery. Science **344:**1246843.
2. **Himmel ME, Ding SY, Johnson DK, Adney WS, Nimlos MR, Brady JW, Foust TD.** 2007. Biomass recalcitrance: engineering plants and enzymes for biofuels production. Science **315:**804-807.
3. **Norman AG, Jenkins SH.** 1934. The determination of lignin: Errors introduced by the presence of certain carbohydrates. Biochem J **28:**2147-2159.
4. **Norman AG, Jenkins SH.** 1934. The determination of lignin: Errors introduced by the presence of proteins. Biochem J **28:**2160-2168.
5. **McCarthy JL, Islam A.** 1999. Lignin chemistry, technology, and utilization: A brief history, p 2-99, Lignin: Historical, Biological, and Materials Perspectives, vol 742. American Chemical Society.
6. **Adler E.** 1977. Lignin chemistry- past, present and future. Wood Science and Technology **11:**169-218.
7. **Glasser WG.** 1985. Lignin, p 61-76. *In* Overend RP, Milne TA, Mudge LK (ed), Fundamentals of thermochemical biomass conversion. Springer Netherlands, Dordrecht.
8. **Lin SY, Dence CW.** 1992. Methods in Lignin Chemistry. Springer-Verlag Berlin Heidelberg.
9. **Ralph J, Lundquist K, Brunow G, Lu F, Kim H, Schatz PF, Marita JM, Hatfield RD, Ralph SA, Christensen JH, Boerjan W.** 2004. Lignins: Natural polymers from oxidative coupling of 4-hydroxyphenyl- propanoids. Phytochem Rev **3:**29-60.
10. **Freudenberg K, Chen CL, Harkin JM, Nimz H, Renner H.** 1965. Observation on lignin. Chemical Communications (London)**:**224-225.

11. **Musel G, Schindler T, Bergfeld R, Ruel K, Jacquet G, Lapierre C, Speth V, Schopfer P.** 1997. Structure and distribution of lignin in primary and secondary cell walls of maize coleoptiles analyzed by chemical and immunological probes. Planta **201:**146-159.
12. **Talas-Oğraş T, Kazan K, Gözükırmızı N.** 2001. Decreased peroxidase activity in transgenic tobacco and its effect on lignification. Biotech Lett **23:**267-273.
13. **Li Y, Kajita S, Kawai S, Katayama Y, Morohoshi N.** 2003. Down-regulation of an anionic peroxidase in transgenic aspen and its effect on lignin characteristics. J Plant Res **116:**175-182.
14. **Atalla RH, Agarwal UP.** 1986. Recording Raman spectra from plant cell walls. J Raman Spectrosc **17:**229-231.
15. **Sjostrom E.** 1993. Lignin, p 71-89, Wood Chemistry (Second Edition). Academic Press, San Diego.
16. **Boerjan W, Ralph J, Baucher M.** 2003. Lignin biosynthesis. Ann Rev Plant Biol **54:**519-546.
17. **Novaes E, Kirst M, Chiang V, Winter-Sederoff H, Sederoff R.** 2010. Lignin and biomass: A negative correlation for wood formation and lignin content in trees. Plant Physiol **154:**555-561.
18. **Austin AT, Ballare CL.** 2010. Dual role of lignin in plant litter decomposition in terrestrial ecosystems. Proc Natl Acad Sci U S A **107:**4618-4622.
19. **Vance CP, Kirk TK, Sherwood RT.** 1980. Lignification as a mechanism of disease resistance. Annu Rev Phytopathol **18:**259-288.
20. **Bhuiyan NH, Selvaraj G, Wei Y, King J.** 2009. Role of lignification in plant defense. Plant Signal Behav **4:**158-159.
21. **Galbe M, Zacchi G.** 2007. Pretreatment of lignocellulosic materials for efficient bioethanol production. Adv Biochem Eng Biotechnol **108:**41-65.
22. **Wang P, Dudareva N, Morgan JA, Chapple C.** 2015. Genetic manipulation of lignocellulosic biomass for bioenergy. Curr Opin Chem Biol **29:**32-39.
23. **Chapple C, Ladisch M, Meilan R.** 2007. Loosening lignin's grip on biofuel production. Nat Biotechnol **25:**746-748.

24. **Margeot A, Hahn-Hagerdal B, Edlund M, Slade R, Monot F.** 2009. New improvements for lignocellulosic ethanol. Curr Opin Biotechnol **20:**372-380.
25. **Kim S, Holtzapple MT.** 2005. Lime pretreatment and enzymatic hydrolysis of corn stover. Bioresour Technol **96:**1994-2006.
26. **Kim KH, Tucker M, Nguyen Q.** 2005. Conversion of bark-rich biomass mixture into fermentable sugar by two-stage dilute acid-catalyzed hydrolysis. Bioresour Technol **96:**1249-1255.
27. **Bozell JJ, O'Lenick CJ, Warwick S.** 2011. Biomass fractionation for the biorefinery: heteronuclear multiple quantum coherence-nuclear magnetic resonance investigation of lignin isolated from solvent fractionation of switchgrass. J Agric Food Chem **59:**9232-9242.
28. **Chaturvedi V, Verma P.** 2013. An overview of key pretreatment processes employed for bioconversion of lignocellulosic biomass into biofuels and value added products. 3 Biotech **3:**415-431.
29. **Zhang Z, Harrison MD, Rackemann DW, Doherty WOS, O'Hara IM.** 2016. Organosolv pretreatment of plant biomass for enhanced enzymatic saccharification. Green Chem **18:**360-381.
30. **Chen F, Dixon RA.** 2007. Lignin modification improves fermentable sugar yields for biofuel production. Nat Biotechnol **25:**759-761.
31. **Anderson NA, Tobimatsu Y, Ciesielski PN, Ximenes E, Ralph J, Donohoe BS, Ladisch M, Chapple C.** 2015. Manipulation of guaiacyl and syringyl monomer biosynthesis in an *Arabidopsis* cinnamyl alcohol dehydrogenase mutant results in atypical lignin biosynthesis and modified cell wall structure. Plant Cell **27:**2195-2209.
32. **Bozell JJ, Holladay JE, Johnson D, White JF.** 2007. Top value added chemicals from biomass. Volume II - results of screening for potential candidtates from biorefinery lignin. Pacific Northwest National Laboratory, Richland.
33. **Lindsey K, Johnson A, Kim P, Jackson S, Labbé N.** 2013. Monitoring switchgrass composition to optimize harvesting periods for bioenergy and value-added products. Biomass Bioenergy **56:**29-37.

34. **Chatterjee S, Jones EB, Clingenpeel AC, McKenna AM, Rios O, McNutt NW, Keffer DJ, Johs A.** 2014. Conversion of lignin precursors to carbon fibers with nanoscale graphitic domains. ACS Sustain Chem Eng **2:**2002-2010.
35. **Bernardini J, Anguillesi I, Coltelli M-B, Cinelli P, Lazzeri A.** 2015. Optimizing the lignin based synthesis of flexible polyurethane foams employing reactive liquefying agents. Polym Int **64:**1235-1244.
36. **Parsell TH, Owen BC, Klein I, Jarrell TM, Marcum CL, Haupert LJ, Amundson LM, Kenttamaa HI, Ribeiro F, Miller JT, Abu-Omar MM.** 2013. Cleavage and hydrodeoxygenation (HDO) of C-O bonds relevant to lignin conversion using Pd/Zn synergistic catalysis. Chem Sci **4:**806-813.
37. **Sainsbury PD, Hardiman EM, Ahmad M, Otani H, Seghezzi N, Eltis LD, Bugg TD.** 2013. Breaking down lignin to high-value chemicals: the conversion of lignocellulose to vanillin in a gene deletion mutant of *Rhodococcus jostii* RHA1. ACS Chem Biol **8:**2151-2156.
38. **Priefert H, Rabenhorst J, Steinbuchel A.** 2001. Biotechnological production of vanillin. Appl Microbiol Biotechnol **56:**296-314.
39. **Pauly M, Keegstra K.** 2008. Cell-wall carbohydrates and their modification as a resource for biofuels. Plant J **54:**559-568.
40. **Gulvik CA, Buchan A.** 2013. Simultaneous catabolism of plant-derived aromatic compounds results in enhanced growth for members of the Roseobacter lineage. Appl Environ Microbiol **79:**3716-3723.
41. **Bergbauer M, Newell SY.** 1992. Contribution to lignocellulose degradation and DOC formation from a salt marsh macrophyte by the ascomycete *Phaeosphaeria spartinicola*. FEMS Microbiol Lett **86:**341-347.
42. **Heinfling A, Ruiz-Dueñas FJ, Martínez MaJ, Bergbauer M, Szewzyk U, Martínez AT.** 1998. A study on reducing substrates of manganese-oxidizing peroxidases from *Pleurotus eryngii* and *Bjerkandera adusta*. FEBS Lett **428:**141-146.
43. **Bourbonnais R, Paice MG.** 1990. Oxidation of non-phenolic substrates. An expanded role for laccase in lignin biodegradation. FEBS Lett **267:**99-102.

44. **Thurston CF.** 1994. The structure and function of fungal laccases. Microbiol **140:**19-26.
45. **Bermek H, Li K, Eriksson KE-L.** 1998. Laccase-less mutants of the white-rot fungus *Pycnoporus cinnabarinus* cannot delignify kraft pulp. J Biotech **66:**117-124.
46. **Haars A, Hüttermann A.** 1980. Function of laccase in the white-rot fungus *Fomes annosus*. Arch Microbiol **125:**233-237.
47. **Evans CS.** 1985. Laccase activity in lignin degradation by *Coriolus versicolor* in vivo and in vitro studies. FEMS Microbiol Lett **27:**339-343.
48. **Jensen KA, Jr., Houtman CJ, Ryan ZC, Hammel KE.** 2001. Pathways for extracellular Fenton chemistry in the brown rot basidiomycete *Gloeophyllum trabeum*. Appl Environ Microbiol **67:**2705-2711.
49. **Brown ME, Chang MCY.** 2014. Exploring bacterial lignin degradation. Curr Opin Chem Biol **19:**1-7.
50. **Bugg TD, Ahmad M, Hardiman EM, Rahmanpour R.** 2011. Pathways for degradation of lignin in bacteria and fungi. Nat Prod Rep **28:**1883-1896.
51. **Ramachandra M, Crawford DL, Hertel G.** 1988. Characterization of an extracellular lignin peroxidase of the lignocellulolytic actinomycete *Streptomyces viridosporus*. Appl Environ Microbiol **54:**3057-3063.
52. **Roberts JN, Singh R, Grigg JC, Murphy ME, Bugg TD, Eltis LD.** 2011. Characterization of dye-decolorizing peroxidases from *Rhodococcus jostii* RHA1. Biochemistry **50:**5108-5119.
53. **Ahmad M, Taylor CR, Pink D, Burton K, Eastwood D, Bending GD, Bugg TD.** 2010. Development of novel assays for lignin degradation: comparative analysis of bacterial and fungal lignin degraders. Mol Biosyst **6:**815-821.
54. **Masai E, Kubota S, Katayama Y, Kawai S, Yamasaki M, Morohoshi N.** 1993. Characterization of the C alpha-dehydrogenase gene involved in the cleavage of beta-aryl ether by *Pseudomonas paucimobilis*. Biosci Biotechnol Biochem **57:**1655-1659.

55. **Masai E, Ichimura A, Sato Y, Miyauchi K, Katayama Y, Fukuda M.** 2003. Roles of the enantioselective glutathione S-transferases in cleavage of beta-aryl ether. J Bacteriol **185:**1768-1775.

56. **Raj A, Chandra R, Reddy MMK, Purohit HJ, Kapley A.** 2006. Biodegradation of kraft lignin by a newly isolated bacterial strain, *Aneurinibacillus aneurinilyticus* from the sludge of a pulp paper mill. World J Microbiol Biotechnol **23:**793-799.

57. **Kumar N, Pruthi V.** 2014. Potential applications of ferulic acid from natural sources. Biotechnology Reports **4:**86-93.

58. **Bergbauer M, Newell SY.** 1992. Contribution to lignocellulose degradation and DOC formation from a salt marsh macrophyte by the ascomycete *Phaeosphaeria spartinicola*. FEMS Microbiol Lett **86:**341-348.

59. **Fuchs G, Boll M, Heider J.** 2011. Microbial degradation of aromatic compounds - from one strategy to four. Nat Rev Microbiol **9:**803-816.

60. **Fuchs G.** 2008. Anaerobic metabolism of aromatic compounds. Ann N Y Acad Sci **1125:**82-99.

61. **Harwood CS, Parales RE.** 1996. The beta-ketoadipate pathway and the biology of self-identity. Annu Rev Microbiol **50:**553-590.

62. **Fuenmayor SL, Wild M, Boyes AL, Williams PA.** 1998. A gene cluster encoding steps in conversion of naphthalene to gentisate in *Pseudomonas* sp. strain U2. J Bacteriol **180:**2522-2530.

63. **Harwood CS, Burchhardt G, Herrmann H, Fuchs G.** 1998. Anaerobic metabolism of aromatic compounds via the benzoyl-CoA pathway. FEMS Microbiol Rev **22:**439-458.

64. **Olivera ER, Minambres B, Garcia B, Muniz C, Moreno MA, Ferrandez A, Diaz E, Garcia JL, Luengo JM.** 1998. Molecular characterization of the phenylacetic acid catabolic pathway in *Pseudomonas putida* U: the phenylacetyl-CoA catabolon. Proc Natl Acad Sci U S A **95:**6419-6424.

65. **Schuhle K, Jahn M, Ghisla S, Fuchs G.** 2001. Two similar gene clusters coding for enzymes of a new type of aerobic 2-aminobenzoate (anthranilate) metabolism in the bacterium *Azoarcus evansii*. J Bacteriol **183:**5268-5278.

66. **Hirakawa H, Schaefer AL, Greenberg EP, Harwood CS.** 2012. Anaerobic p-coumarate degradation by *Rhodopseudomonas palustris* and identification of CouR, a MarR repressor protein that binds p-coumaroyl coenzyme A. J Bacteriol **194:**1960-1967.
67. **Masai E, Harada K, Peng X, Kitayama H, Katayama Y, Fukuda M.** 2002. Cloning and characterization of the ferulic acid catabolic genes of *Sphingomonas paucimobilis* SYK-6. Appl Environ Microbiol **68:**4416-4424.
68. **Buder R, Ziegler K, Fuchs G, Langkau B, Ghisla S.** 1989. 2-Aminobenzoyl-CoA monooxygenase/reductase, a novel type of flavoenzyme. Studies on the stoichiometry and the course of the reaction. Eur J Biochem **185:**637-643.
69. **Rather LJ, Bill E, Ismail W, Fuchs G.** 2011. The reducing component BoxA of benzoyl-coenzyme A epoxidase from *Azoarcus evansii* is a [4Fe-4S] protein. Biochim Biophys Acta **1814:**1609-1615.
70. **Rather LJ, Knapp B, Haehnel W, Fuchs G.** 2010. Coenzyme A-dependent aerobic metabolism of benzoate via epoxide formation. J Biol Chem **285:**20615-20624.
71. **Moran MA, Hodson RE.** 1994. Dissolved humic substances of vascular plant origin in a coastal marine environment. Limnol Oceanogr **39:**762-771.
72. **Moran MA, Hodson RE.** 1989. Formation and bacterial utilization of dissolved organic carbon derived from detrital lignocellulose. Limnol Oceanogr **34:**1034-1047.
73. **Buchan A, Gonzalez JM, Moran MA.** 2005. Overview of the marine roseobacter lineage. Appl Environ Microbiol **71:**5665-5677.
74. **Gonzalez JM, Moran MA.** 1997. Numerical dominance of a group of marine bacteria in the alpha-subclass of the class Proteobacteria in coastal seawater. Appl Environ Microbiol **63:**4237-4242.
75. **Moran MA, Gonzalez JM, Kiene RP.** 2003. Linking a bacterial taxon to sulfur cycling in the sea: Studies of the marine Roseobacter group. Geomicrobiol J **20:**375-388.

76. **Alavi M, Miller T, Erlandson K, Schneider R, Belas R.** 2001. Bacterial community associated with Pfiesteria-like dinoflagellate cultures. Environmental Microbiol **3:**380-396.

77. **Cude WN, Mooney J, Tavanaei AA, Hadden MK, Frank AM, Gulvik CA, May AL, Buchan A.** 2012. Production of the antimicrobial secondary metabolite indigoidine contributes to competitive surface colonization by the marine roseobacter Phaeobacter sp. strain Y4I. Appl Environ Microbiol **78:**4771-4780.

78. **Geng HF, Bruhn JB, Nielsen KF, Gram L, Belas R.** 2008. Genetic dissection of tropodithietic acid biosynthesis by marine roseobacters. Appl Environ Microbiol **74:**1535-1545.

79. **Buchan A, Collier LS, Neidle EL, Moran MA.** 2000. Key aromatic-ring-cleaving enzyme, protocatechuate 3,4-dioxygenase, in the ecologically important marine Roseobacter lineage. Appl Environ Microbiol **66:**4662-4672.

80. **González JM, Whitman WB, Hodson RE, Moran MA.** 1996. Identifying numerically abundant culturable bacteria from complex communities: an example from a lignin enrichment culture. Appl Environ Microbiol **62:**4433-4440.

81. **Gonzalez JM, Mayer F, Moran MA, Hodson RE, Whitman WB.** 1997. *Sagittula stellata* gen. nov., sp. nov., a lignin-transforming bacterium from a coastal environment. Int J Syst Bacteriol **47:**773-780.

82. **Buchan A, Collier LS, Neidle EL, Moran MA.** 2000. Key aromatic-ring-cleaving enzyme, protocatechuate 3,4-dioxygenase, in the ecologically important marine Roseobacter lineage. Appl Environ Microbiol **66:**4662-4672.

83. **Buchan A, Neidle EL, Moran MA.** 2001. Diversity of the ring-cleaving dioxygenase gene pcaH in a salt marsh bacterial community. Appl Environ Microbiol **67:**5801-5809.

84. **Gulvik CA.** 2013. Ecology and Physiology of Aerobic Aromatic Catabolism in Roseobacters. PhD Dissertation. University of Tennessee.

85. **Newton RJ, Griffin LE, Bowles KM, Meile C, Gifford S, Givens CE, Howard EC, King E, Oakley CA, Reisch CR, Rinta-Kanto JM, Sharma S, Sun S,**

**Varaljay V, Vila-Costa M, Westrich JR, Moran MA.** 2010. Genome characteristics of a generalist marine bacterial lineage. ISME J **4:**784-798.

# VI. Appendix: Figures

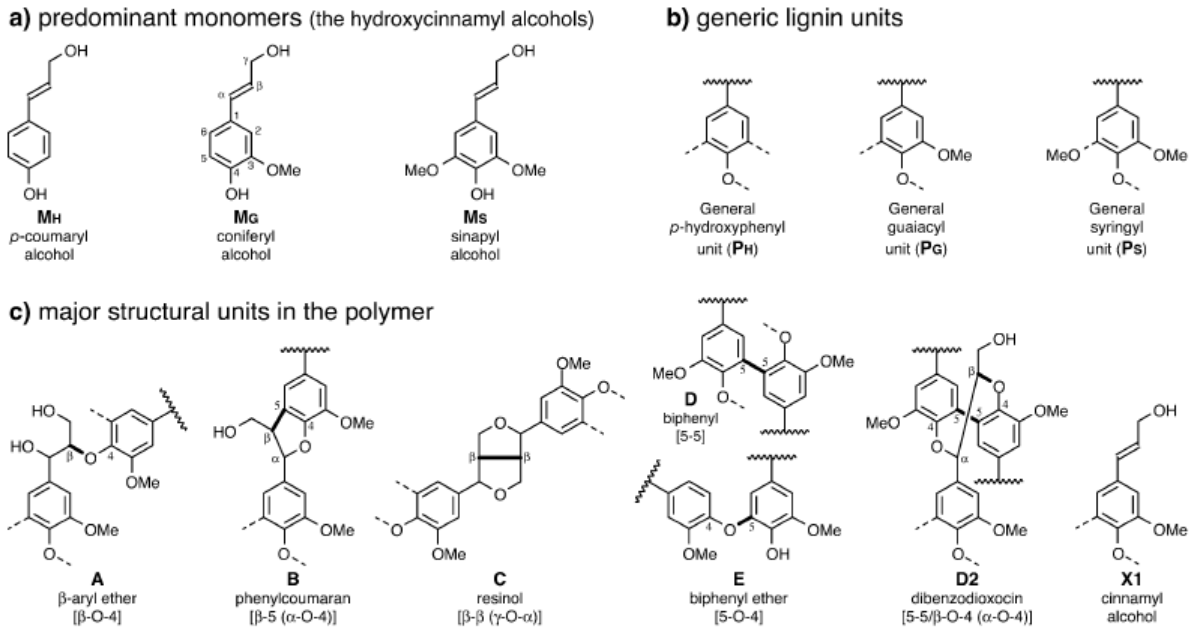


**Figure 1.1**. Monolignols (a), phenylpropanoid units (b), and major linkages found in lignin (c). (From Ralph *et al*. 2004)

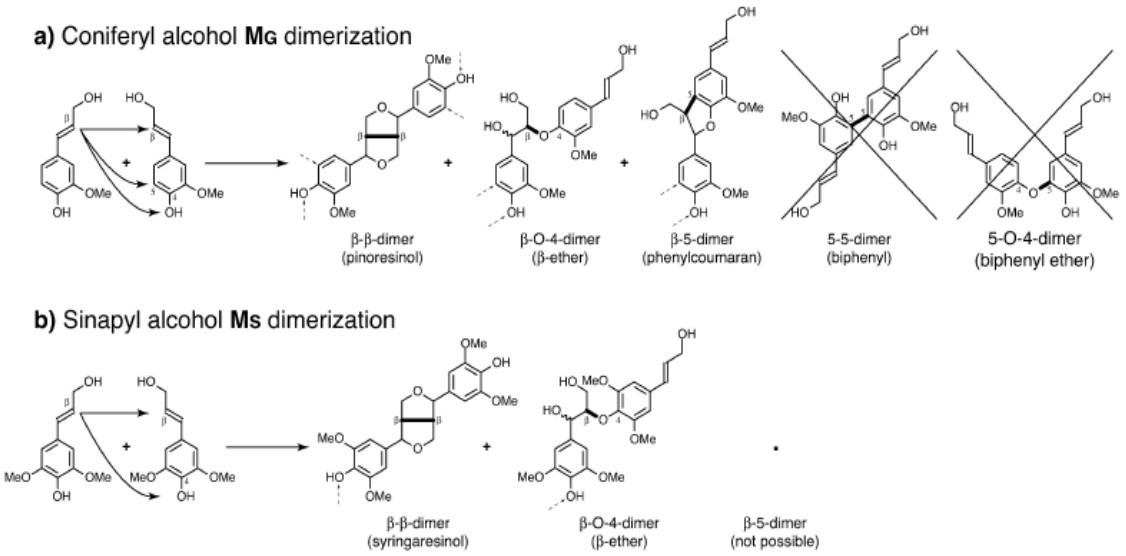


**Figure 1.2**. Radical polymerization of monolignols, (a) coniferyl alcohol. (b) sinapyl alcohol.

# CHAPTER TWO - GENETIC INVESTIGATION OF FERULIC ACID CATABOLISM IN THE MARINE BACTERIUM *SAGITTULA STELLATA* E-37

# I. Abstract

Ferulic acid is among the most abundant constituents of lignin and imparts an enhanced structural rigidity to plant biomass through its notorious cross-linking to hemicellulose in plant cell walls. This aromatic compound is particularly abundant in grasses where it may account for 3% of the cell wall dry weight. Interest in ferulic acid studies has historically been driven by its bacterial conversion to the highly valuable flavor compound, vanillin. Thus, insight into the bacterial degradation of ferulic acid harbors potential to advance efforts for the biotechnological production of vanillin and provide a more comprehensive understanding of reactions involved in the degradation of lignin-derived compounds. To date, three major pathways have been described for the bacterial degradation of ferulic acid, two of which are initiated through coenzyme A activation of the compound via feruloyl-CoA synthase/ligase activity. Of these CoA-dependent pathways, only one has been demonstrated to proceed through a vanillin intermediate. Here we investigate the catabolism of ferulic acid by *Sagittula stellata* E-37, a member of the roseobacter lineage of marine bacteria that is capable of growth on ferulic acid, vanillin, and vanillic acid and possesses two annotated feruloyl-CoA (*fcs*) synthase homologs in its genome. In effort to elucidate the role of both *fcs* genes in ferulate catabolism, mutagenesis techniques were implemented to generate single and double mutant strains. Phenotypic analyses of the mutant strains suggest only a partial involvement of either *fcs* gene in ferulate catabolism, as growth of all mutant strains was only slightly impaired on this compound compared to wildtype. Instead, a complete growth deficiency was observed with the double mutant strain when provided *p*-coumaric acid as a substrate. These findings indicate that both of the annotated *fcs* genes are required for growth on *p*-coumaric acid suggesting a misannotation of these genes and possible enzyme promiscuity leading the partial phenotypes that were observed. Additional insights could be provided from functional studies with purified hydroxycinnamoyl-CoA synthases as well as a metabolite analysis during growth on *p*-coumaric acid and ferulic acid.

# II. Introduction

Plant-derived carbon has been estimated to contribute ~50% of the dissolved organic carbon in coastal regions of the southeastern United States (1), highlighting its importance in carbon cycling in this environment. The carbon liberated from this material is derived from the lignocellulose in plant cell walls, which contains the polysaccharides cellulose and hemicellulose, as well as the highly recalcitrant lignin polymer. Lignin is a heterogeneous aromatic polymer generated from the radical polymerization of three monolignols; *p*-coumaryl alcohol, coniferyl alcohol, and sinapyl alcohol, resulting in a variety of stable carbon-carbon and ether interunit linkages (2). Due to its structural heterogeneity and chemical stability, lignin serves as a physiochemical barrier to many sources of damage including UV degradation (3), insect and herbivore predation (4), fungal penetration (5) and enzymatic hydrolysis (6). Thus, due to its protective architecture, lignin acts at the gatekeeper for plant carbon release and is therefore instrumental in mediating carbon cycling in nature.

Constituting up to 30% of the plant cell wall, lignin represents the most abundant aromatic polymer on earth and offers potential as a highly valuable source of renewable carbon for various applications including hydrocarbon fuels (7) and synthetic chemicals (8). Accessing the potential of this polymer from a practical perspective however, remains a large obstacle due to its refractory nature and entanglement with cellulose and hemicellulose. Despite such recalcitrance, many fungi and a limited number of bacteria have been demonstrated to degrade lignin in nature (9). Most knowledge of lignin degradation has been extracted from reports on the white-rot fungus, *Phanerochaete chrysosporium*, for which many different lignolytic enzymes have been described (10). Primary depolymerization of lignin is typically accomplished through enzymatic oxidation driven by extracellular oxidoreductases, namely lignin peroxidases (11) and manganese peroxidases (12, 13). This reaction liberates a pool of low

molecular weight aromatics that can serve as carbon and energy sources for the surrounding microbial community.

Among the most abundant and valuable aromatic compounds embedded in (and liberated from) lignin is ferulic acid. Ferulic acid is a hydroxycinnamic acid (related to coniferyl alcohol) that cross-links lignin to hemicellulose in plant cell walls (14). This connectivity provides additional reinforcement to the plant, and has been recently accused as the main source of recalcitrance in grasses (15). Ferulic acid was initially isolated from *Ferula feotida*, a relative of the fennel plant (16, 17), and has since been extracted from a wide variety of sources. Levels of ferulic acid are generally highest in grasses, where it accounts for ~3% of the cell wall dry weight, but is also commonly found in other crops such as rice, wheat, grains, vegetables, fruits, flowers, and coffee (18, 19). Due to its occurrence in common dietary foods, ferulic acid and its derivatives have been investigated for their potential medicinal properties. The phenolic structure and resonance across the conjugated aromatic ring and carboxylic side chain generates a system capable of scavenging radicals, and thus elicits anti-oxidant and anti-inflammatory properties (17). Aside from the interest in ferulic acid itself, it has value in its transformation to vanillin, a desirable commercial flavoring product. Many microbes that utilize ferulic acid generate vanillin as an intermediate, a reaction that has been pursued for the industrial production of commercial vanillin (20-22).

To date, there have been 3 major pathways described for the degradation of ferulic acid. The oldest documented pathway involves a direct enzymatic decarboxylation (C1-removal) of ferulic acid, generating 4-vinylguaiacol. A literature review by Rossazza *et al*. suggests that this pathway may be the most widely observed, as 4-vinylguaiacol was demonstrated as a metabolite of ferulic acid catabolism across 45 of the 67 surveyed microbial strains. While ferulic acid decarboxylation has been reported across many genera of bacteria (23-26) and fungi (27, 28), it was first observed in *Bacillus pumilus* for which the most information is available (24). Crystal structures of ferulic acid decarboxylases are available for *Bacillus pumilus* (PDB ID 3NAD) (29), *Enterobacter sp*.

PxG-4 (PDB ID 3NX1) (23), *Saccharomyces cerevisiae* (PDB ID 4S13) (27), and *Aspergillus niger* (PDB ID 4ZAA) (28). The second and third pathways for ferulic acid catabolism are both initiated by a CoA addition to the ferulic acid carboxylate side chain to generate feruloyl-CoA, followed by deacetylation (C2 removal of acetate). The difference in these two pathways lies in the methods employed for removal of the acetate moiety, with one pathway proceeding through a β-oxidative pathway and the other through a non-β-oxidative pathway that generates vanillin intermediate, thus these two pathways can be differentiated by the presence or absence of vanillin. Evidence for the CoA-dependent β-oxidative pathway has been described for *Agrobacterium fabrum* (30) whereas evidence for the CoA-dependent non-β-oxidative pathway (with a vanillin intermediate) has been much more frequently reported for organisms including *Delftia acidovorans* (31), *Pseudomonas fluorescens* AN103 (32), *Pseudomonas sp.* HR199 (33), *Acinetobacter* ADP1 (34) and *Sphingobium* SYK-6 (35). For both of these pathways, the initial conversion of ferulic acid to feruloyl-CoA is mediated by a feruloyl-CoA synthase or ligase (E.C. 6.2.1.34), for which there is currently not a deposited crystal structure.

While a strong understanding of aromatic compound degradation has been established with soil bacteria like those above, studies with bacteria from other lignin-rich environments such as coastal marshes, is less well documented. Members of the roseobacter lineage of marine bacteria, particularly those isolated from coastal regions, have been documented to utilize a variety of lignin-derived aromatic compounds as sole carbon and energy sources including anthranilate, benzoic acid, *p*-hydroxybenzoic acid, protocatechuic acid, salicylic acid, *p*-coumaric acid, vanillic acid, and ferulic acid (36-38). Among the many isolates capable of degrading aromatic compounds, *Sagittula stellata* E-37 serves as a particularly suitable model for the degradation of plant-derived aromatic compounds in coastal regions due to its amenability to cultivation, evidence for multiple aromatic ring-cleaving pathways (39), and ability to mineralize a synthetic lignin (40). This isolate shows robust growth on ferulic acid and presents some unique genetic features with respect to its catabolism. The genome of this isolate harbors two

annotated feruloyl-CoA synthases (FCS) that share 42% amino acid identity (96% coverage, 2e-151), indicating that this organism likely utilizes a CoA-dependent pathway for the conversion of ferulic acid to feruloyl-CoA. The presence of 2 *fcs* homologs is intriguing as this phenomenon is not observed in other species and may imply that E-37 requires simultaneous use of these two genes for ferulic acid catabolism or balances their expression under different conditions. Another possible explanation for the presence of two *fcs* homologs is the misannotation of these genes, which can only be verified through genetic and functional studies. In addition to the catabolism of ferulic acid, E-37 can also use vanillin and vanillic acid as sole carbon substrates, which suggests the processing of ferulic acid through a vanillin intermediate through a non-β-oxidative pathway. Together these features help to generate the hypothesis that E-37 degrades ferulic acid through the joint use of two feruloyl-coA synthases and proceeds through CoA-dependent, non-β-oxidative pathway.

In effort to elucidate the method by which E-37 degrades ferulic acid, a molecular approach was employed targeting the disruption of ferulic acid-related genes. Both random and targeted mutagenesis was performed in effort to capture a more comprehensive understanding of the genes involved in ferulic acid conversions. Construction of a random Tn5 mutant library yielded mutants in an enoyl-CoA hydratase that has been implicated in the conversion of feruloyl-CoA to vanillin; however, mutants in other suspected genes were not identified with this approach, including either of the annotated *fcs* genes, which are the main source of intrigue in this organism. To assess the contribution of both *fcs* genes to ferulic acid catabolism, individual and double mutants were generated using a targeted marker exchange mutagenesis approach as well as a targeted insertional (pKNOCK) mutagenesis approach using pKNOCK plasmids. The application of multiple methods for genetic mutation expands our genetic toolbox for roseobacters which has historically been limited to a handful of methods with selected strains (41). This work demonstrates the first documented set of genetic mutations in *Sagittula stellata* E-37 and the first use of targeted pKNOCK mutagenesis in a roseobacter. Results of these mutagenesis studies demonstrate an involvement,

but not a requirement, of both *fcs* genes in the catabolism of ferulic acid as a double mutant strain exhibited depressed growth and activity, but not a complete loss of activity. Alternatively, the interruptions of both *fcs* genes facilitates the loss of growth and activity on *p*-coumaric acid, suggesting that the genes may be misannotated as feruloyl-CoA synthases, when in fact they are *p*-coumaryl-CoA synthases. Further functional studies with the expressed enzymes are required to support the new hypothesis emerging from this work.

## III. Materials and methods

*Strains and Plasmids*

Strains and plasmids used in this study are described in Table 2.1. Primers used for validation of cloning inserts and chromosomal integrations are described in Table 2.2.

*Media and Culture Conditions*

*Sagittula stellata* E-37 was previously isolated from pulp mill effluent and enriched on indulin as described by Gonzalez *et al*. (40). Unless otherwise noted, wildtype E-37 and its mutant strains were maintained at 30°C in YTSS medium (per liter, 2.5g yeast extract, 4 g tryptone, 15 g sea salts [Sigma-Aldrich, St. Louis, MO]). *E. coli* strains used for cloning and mating experiments (Table 2.1) were maintained at 37°C in Luria Broth (per liter, 10 g tryptone, 5 g yeast extract, 10 g NaCl). Antibiotics were added to the growth medium when necessary to maintain selective pressure (25-50 µg/mL kanamycin, 5-10 µg/mL tetracycline). Growth assays were routinely performed in Marine Basal Medium containing 1.5% (wt/vol) sea salts, 225 nM $K_2HPO_4$, 13.35 µM $NH_4Cl$, 71 mM Tris-HCl (pH 7.5), 68 µM Fe-EDTA, trace metals, vitamins and carbon (2mM aromatic and 10mM acetate unless otherwise noted). Glassware used for carbon studies was combusted for 4-24 hours prior to use to eliminate trace carbon that could yield false positives for growth assays. All plastic materials used for screening were either autoclaved or UV-sterilized prior to use.

*Molecular techniques*

All PCR purifications, plasmid extractions, and gel extractions were performed with the appropriate Qiagen kit and executed per manufacturer protocol, performing all elutions with pre-warmed (60°C) elution buffer. Restriction enzymes and buffers, unless otherwise noted, were purchased from New England Biolabs and applied as suggested by manufacturer. Cloning inserts were routinely verified through PCR amplification followed by sequencing and sequence alignments (Geneious 8.1.3) to the relevant reference sequences for E-37 (taxonomy ID 388399), pKNOCK-Km (Addgene 46262), pKNOCK-Tc (Addgene 46259 ). PCR mixtures for all reactions included the following unless otherwise noted: 1x GoTAQ buffer (Promega), 200 µM deoxynucleotide triphostphates (dNTPs, Promega), 0.4 µM forward and reverse primers, 0.025 U/µl GoTaq DNA Polymerase (Promega), and 1-2 ng/µl template DNA. Thermocycling for site-directed mutagenesis approaches was generally performed using an initial denaturation at 95°C for 2 minutes, followed by 30 cycles of 95°C denaturation for 30 seconds, 55°C annealing for 30 seconds, 72°C elongation for 30 seconds, and a final extension at 72°C for 5 minutes. All non-TA (ie TOPO) ligation reactions were performed by first co-precipitating a 50:1 molar ratio of the insert and plasmid. One tenth volume (0.1% v:v) ammonium acetate (7.5M) was added to the DNA mixture before incubating in 95% ethanol at -20°C for 2 hours. The DNA was then pelleted at 4°C for 15 minutes at 13,000 rpm and resuspended in 8 µl elution buffer. The co-precipitated DNA was then ligated with 1 µl 10x T4 DNA ligase buffer (Promega) and 1 µl T4 DNA Ligase (1 unit) and incubated on ice overnight.

*Random transposon mutagenesis*

A mini-Tn5 random transposon mutant library was constructed from wildtype *Sagittula stellata* E-37 via conjugal mating with the diaminopimelate (DAP) auxotroph *Escherichia coli* EA145 pRL27::mini-Tn5-Kmr-oriR6K following the methods of Larsen *et al*. (42). Briefly, 1 mL of overnight cultures of E-37 and *E. coli* EA145 pRL27::mini-Tn5-KanR-oriR6K were used to inoculate 10 mL YTSS and LB/DAP (1 mM), respectively. Cultures were grown to an $OD_{540}$ of ~0.4 before setting up the mating mixtures which consisted

of 200 µl of both recipient E-37 and donor *E. coli* strains. Mating mixtures were pelleted, washed in 1 mL YTSS, pelleted again, and resuspended in 15 µl YTSS before spot plating onto YTSS/DAP (1 mM) agar plates. Mating spots were incubated at 30°C until robust growth (~24 hours) at which time the spots were transferred to 1 mL YTSS, resuspended, diluted, and plated onto YTSS/Kan (50 ug/mL) agar plates to establish the entire mutant library. Tn5 mutant screening was performed on 1.5% solid agar; either YTSS or a marine basal medium containing 25 mM acetate, 10 mM POB, 2 mM ferulic acid, 5 mM vanillin, or 5 mM vanillic aicd. All media used for Tn5 mutants contained cycloheximide (25 µg/mL) to inhibit fungal contamination and kanamycin (50 µg/mL) to maintain selective pressure for the KanR Tn5 mutants.

*Arbitrary PCR, sequencing, and identifying Tn5 insertion sites*

Arbitrary PCR was used to identify the location of the Tn5 insertions of selected E-37 mutants as described by O'Toole *et al*. (43) and Cude *et al*. (44). Briefly, crude cell lysates were used as DNA templates for arbitrary PCR. The first round of PCR was performed with the transposon-specific forward primer TNPR13Out (5'-CAG CAA CAC CTT CTT CAC GA-3') and the arbitrary reverse primer Arb6 (5'-GGC CAC GCG TCG ACT AGT ACN NNN NNN NNN ACG CC-3') to amplify the region downstream of the transposon. Thermocycling conditions consisted of a 5 minute initial denaturation at 95°C, followed by 5 cycles of 94°C for 30 sec, 30°C for 30 sec, and 72°C for 1 minute and 30 cycles of 94°C for 30 sec, 45°C for 30 sec, 72°C for 1 minute and a final extension of 72°C for 5 minutes. A secondary nested PCR was then performed using the product from the first round of PCR as the DNA template. This reaction utilized the Arb2 primer (5'-GGC CAC GCG TCG ACT AGT AC-3') which nests within the Arb6 arm of the product, and TNPR13Nest (5'-CTA GAG TCG ACC TGC AGG CAT-3'), which nests within the TNPR13Out arm of the PCR product. Thermocycling conditions for the nested PCR included a 5 minute initial denaturation at 95°C, followed by 30 cycles of 94°C for 30 sec, 45°C for 30 sec, and 72°C for 1 minute and a final extension of 72°C for 10 minutes. PCR products were then purified and sequenced with the TNPR13Nest primer.

*Marker exchange mutagenesis*

Methods for marker exchange mutagenesis of SSE37_12324 were optimized from previously described procedures (45-47). PCR was used to amplify a 402 bp region upstream and a 585 bp region downstream of the gene of interest, generating "A" and "B' amplicons, respectively (Figure 2.1). During these first amplifications, a 21 bp scar sequence was added to the internal A primer (5'-gattcgaggagcgatagagct*GTCGAC*TTCTCCTCCTGGCGTTTTAG-3', scar underlined) and internal B primer (5'-agctctatcgctcctcgaatcGACCGGCGCCCGGTT-3'), generating complementary appendages for overlap extension PCR. PCR mixtures for each A and B reaction included 1x GoTaq Buffer (Promega), 200 µM deoxynucleotide triphosphates (Promega), 6 µM internal primer, 0.6 µM external primer, 0.025 U/µl GoTaq DNA Polymerase (Promega) and 1-2 ng/µl E-37 genomic DNA. Thermocylcing conditions consisted of a 3 minute denaturation at 95°C followed by 31 cycles of 30 seconds at 95°C, 30 seconds at 56°C, 30 seconds at 72°C and a final extension for 5 minutes at 72°C. The A and B amplicons were subsequently used as template DNA during overlap extension PCR to generate a fused "AB" product. This PCR was performed with 1x FailSafe Buffer F (Epicentre), 6 µM external primer A, 6 µM external primer B, 0.05 U/µl FailSafe enzyme mix (Epicenter), 1-2 ng/µl amplicon A, and 1-2 ng/µl amplicon B. Thermocycling conditions were the same as previous, except with a 10 minute final extension. The resulting AB product was cloned into pCR2.1-TOPO (Invitrogen) and transformed into TOP10 chemically competent cells per manufacturer instructions, generating plasmid pCR2.1_12324. Positive clones were selected on LB/Kanamycin (50 µg/mL) agar and verified through M13 amplification of the insert and sequencing of the product with M13 primers. The AB insert was then subcloned from pCR2.1_12324 to the mobilizable suicide plasmid, pARO180 (ATCC 77123), through shared *HindIII* (New England Biolabs) and *XbaI* sites, generating plasmid pARO_12324, and transformed into chemically competent *E. coli* JM109. Positive clones were selected on LB/ampicillin (50 µg/mL) agar and verified through amplification and sequencing of the insert. The *sacBkanR* cassette from pRMJ1 (47) was inserted into the middle of the AB insert through a *SalI* site that was designed into the internal A primer (Figure 2.2, Table

2.1), generating plasmid pARO_12324_SK. The completed A- *sacBkanR* -B construct in pARO_12324_SK was then transformed into the mating strain, *E. coli* S17-1. Conjugal mating of *E. coli* S17-1 (pARO_12324_SK) with wildtype E-37 was initiated by creating a mating mixture containing 200 µl of each strain (OD540 ~ 0.5 for each strain). The mating mixture was pelleted for 2 minutes at 10,000rpm, washed in 1 mL YTSS, and resuspended in 15 µl YTSS. The entire volume of mating mixture was spot plated onto YTSS agar and incubated at 30°C. To select for successful E-37 transconjugants, the grown mating spot was washed in 500 µl 1.5% sea salts and resuspended in another 500 µl 1.5% seas salts before plating 1:10 dilutions onto MBM agar containing 5 mM POB (to select against S17-1) and 50 µg/mL kanamycin (to select for E-37 transconjugants). DNA was extracted from selected E-37 transconjugants (DNeasy blood and tissue kit, Qiagen) and screened for allelic replacement of SSE37_12324 with *sacBkanR* through PCR amplifications across the chromosomal region of interest using primers Asac_F/Bkm_R (Table 2.2). PCR for this amplification was performed through LongRange PCR (Qiagen) according to manufacturer instructions with the following thermocycling conditions: initial denaturation at 93°C for 3 minutes, followed by 30 cycles of 93°C denaturation for 15 seconds, 57°C annealing for 30 seconds, 68°C elongation for 12 minutes with no final extension.

*Insertional mutagenesis with pKNOCK plasmids*

Construction of SSE37_24399 mutant was performed through insertional mutagenesis with the pKNOCK-Km (kanamycin marker) plasmid (48). A 231 bp internal region of SSE37_24399 was cloned into pCR2.1-TOPO and transformed into commercial Top10 chemically competent cells (Invitrogen). The insert was subsequently transferred from pCR2.1-TOPO into pKNOCK-Km through their shared *BamHI* and *XhoI* sites in the multiple cloning sites, generating plasmid pKNOCKKm_24399. The plasmid was then transformed into the chemically competent cells of the *E. coli* mating strain BW20767 (49). Conjugation of BW20767 (pKNOCKKM_24399) with wildtype E-37 was performed as described earlier. Positive E-37 transconjugants were selected on MBM agar with 5mM POB and 50 µg/mL kanamycin as previous. The *fcs1*/*fcs2* double mutant was

generated by cloning the same 231 bp fragment of *fcs2* into pKNOCK-Tc (tetracycline marker), transforming into the mating strain *E. coli* BW201767, and mating with the *fcs1*- strain of E-37.

*Biolog™ phenotypic microarrays of* fsc *mutants*

Custom phenotypic microarrays were performed to assay for redox activity of all strains when incubated with various carbon sources (10 mM acetate, 2 mM *p*-hydroxybenzoic acid, ferulic acid, vanillin, vanillic acid, *p*-coumaric acid). All *fcs* mutants and wildtype E-37 were pre-cultured in MBM with 10 mM acetate (supplemented with kanamycin and tetracycline when necessary) prior to initiation of the assay. Assays were performed in 96 well flat-bottom plates (Costar) containing 1x MBM, 1x Biolog™ Dye Mix G (Hayward, Ca), $10^7$ cells/mL, and desired carbon source. Plates were incubated at 30°C in the Omnilog reader where digital colorimetric readings were captured every 30 minutes to monitor the intensity of dye reduction over time, recorded in Omnilog units/time.

*Growth assays of* fsc *mutants*

All *fcs* mutants and wildtype E-37 were pre-cultured in MBM with 10 mM acetate (supplemented with kanamycin and tetracycline when necessary) prior to initiation of the growth curve. Pre-cultures were used to inoculate growth curve cultures (~$10^7$ cells/mL) containing 10 mL MBM with 2mM aromatic carbon (p-hydroxybenzoic acid, ferulic acid, vanillin, vanillic acid) or 10mM acetate in 18 mm tubes. Cultures were incubated at 30°C with shaking (200 rpm) throughout with $OD_{540}$ measurements taken every 3-4 hours for 3 days.

# IV. Results

*Random Tn5 library identifies gene involved in conversion of feruloyl-Co*A

>6,000 member random Tn5 transposon mutant library was created from the E-37 wildtype strain to identify transposon insertions in genes involved in ferulic acid, vanillin, and vanillic acid degradation. For practical purposes, only half of the library was screened. A primary plating on acetate was performed to eliminate any auxotrophs generated from insertions in required nutrient biosynthesis genes. A second filtration screen was performed to reduce the library to only those mutants capable of utilizing the protocatechuate pathway, through which ferulic acid, vanillin, and vanillic acid are degraded. Protocatechuate 3,4-dioxygenase enzyme assays (37) were performed prior to library construction (C.A. Gulvik, unpublished data) to verify that all assayed compounds were funneled through the protocatechuate (PCA) pathway. Screening on *p*-hydroxybenzoate (POB), a non-ferulic acid related aromatic known to be degraded through the PCA pathway, allowed for the reduction of the library to 2,909 mutants (37, 38). All remaining mutants were subsequently replica plated onto 2mM ferulic acid, 5mM vanillin, and 5mM vanillic acid, for which concentrations were determined based on ability to generate robust colony growth. These screens yielded 5 ferulic acid- mutants, 23 vanillin- mutants, and 3 vanillic acid- mutants. Due to the strong interest in recovering insertions in the two anomalous *fcs* homologs, only those mutants deficient on ferulate were pursued. Arbitrary PCR and sequencing analysis of the 5 ferulic acid mutants unveiled 2 mutants of direct interest, both of which contained a single Tn5 insertion in the annotated enoyl-coA hydratase (SSE37_12349) near one of the *fcs* genes (SSE37_12324). Subsequent growth assays in liquid culture confirmed the inability of this mutant to grow on ferulic acid. The enoyl-coA hydratase has been demonstrated to be involved in both the β-oxidative (30) and non-β-oxidative (33) pathways for ferulic acid degradation.

*Targeted mutagenesis successfully generates fcs- mutants*

In effort to assess the relative contributions of the annotated *fcs* homologs and expand our molecular tools for E-37, a set of targeted mutagenesis techniques were applied to generate the resulting *fcs1*-, *fcs2*-, and *fcs1*-/*fcs2*- mutants. The first *fcs* gene ("*fcs1*", SSE37_12324) was generated using a marker exchange mutagenesis technique whereby the entire gene was replaced with a ::*sacBkanR* cassette for selection in the E-37 genome. The replacement of this gene was verified through multiple PCR-based assays to detect the entire gene region (Figure 2.3), and parts of the *sacB* and *kanR* cassette (data not shown). For each of the described PCRs, the amplicons were sequenced and confirmed through alignment to the E-37 genome when applicable as well as the available sequences for *sacB* and *kanR*.

The second *fcs* gene ("*fcs2*", SSE37_24399) was interrupted through insertional mutagenesis with a pKNOCK-Km plasmid in which a 231 bp region internal to the gene of interest was cloned. This small gene fragment served as a region of homology with the *fcs2* in the E-37 genome allowing for the single homologous recombination event that resulted in incorporation of the entire plasmid into the middle of the *fcs2* gene. Transconjugants were screened via PCR for the integration of the 2.1 kb plasmid into the gene of interest using primers (Table 2.2) that flank the 231bp region of homology on the E-37 genome. Results from this screen yielded one clone (now the *fcs2*- strain) that exhibited a band consistent with integration of the plasmid (Figure 2.4). Sequencing of this PCR product and alignments to the E-37 genome and pKNOCK-Km sequence confirmed the anticipated sequence.

The double *fcs* mutant (*fcs1*-/*fcs2*-) was generated by interrupting the *fcs2* gene in the previously constructed *fcs*1- strain. Because the base *fcs*1- strain already contained a *kanR* gene, the *fcs2* mutation required a different selection. For this the same 231 bp region of the *fcs*2 single mutant was cloned into a pKNOCK-Tc plasmid, (containing a tetracycline marker) and transferred through conjugation to the E-37 *fcs1*- strain where it underwent homologous recombination to integrate into the *fcs2* gene. Verification of

both mutations (*fcs1* marker exchange mutation and *fcs2* pKNOCK-Tc mutation) was verified through PCR amplification as done previously. Results confirmed the maintenance of the original *fcs*1 mutation (*sacBkanR* replacement) and new integration of pKNOCK-Tc into the *fcs2* gene (Figure 2.5). PCR products were again sequenced and aligned to the relevant DNA templates to confirm successful mutations.

*Phenotypic and growth assays suggest* fcs genes are *required for p-coumaric acid catabolism*

Upon successful construction of all desired *fcs* mutants, Biolog™ redox assays and culture-based growth assays were performed with a variety of plant-derived aromatic compounds to assess differences in response to these compounds. Biolog™ assays detect cellular respiration through monitoring the cell-mediated reduction of a tetrazolium dye (50). The dye reduction is accomplished through transfer of electrons from the carbon source to NADH, and finally to the tetrazolium salt eliciting a color change that can be detected (51). Surprisingly, results do not show a complete loss of activity for any of the *fcs* mutants when incubated with ferulic acid (Figure 2.6). Instead, a differential response is observed with all mutant strains, with a slight impairment exhibited by the double mutant and a stronger impairment exhibited by both individual mutants. Even more interestingly, a complete loss of redox activity is noted for the double mutant when incubated with *p*-coumarate, a compound that shares a similar structure to ferulate but is lacking the o-methoxyl group. A delayed activity is noted with the *fcs*1- strain on *p*-coumarate, whereas the *fcs*2- strain responds similar to wildtype. Another interesting phenotype revealed by this assay is the loss of activity of the *fcs2*- strain on vanillin, whereas the *fcs1*- strain is congruent with wildtype activity. All of the above phenotypes are corroborated by growth assays, suggesting the respiration responses are correlated with growth (Figure 2.7).

# V. Discussion

*Expanding insight into hydroxycinnamic acid catabolism in E-37*

Findings from the redox and growth assays present some interesting and unexpected results regarding the degradation of ferulic acid and *p*-coumaric acid. These assays demonstrate that neither of the annotated feruloyl-CoA synthase homologs is necessarily required for the utilization of ferulic acid. This is supported by the maintenance of growth and activity in the presence of ferulic acid for the *fcs1*-, *fcs2*- and *fcs1*-/*fcs2*- strains. While all three of these strains exhibit a suppressed response relative to wildtype, none are nullified by their mutation(s), suggesting another enzyme could be recruited for the catabolism of ferulic acid in their absence. Although no other genes are annotated as feruloyl-CoA synthases in this genome, there are 9 other CoA-synthases or ligases with homology to these proteins that could possibly compensate for these enzymes, although none of the protein homologs exhibit particularly strong amino acid identity and coverage to either *fcs* gene (coverage <65%, expected value e-<$10^{-20}$) (Table 2.3). A potential candidate for recovering any potential lost *fcs* functionality could be the benzoyl-CoA ligase (locus tag SSE37_24404, accession EBA09441) which is situated adjacent to *fcs2* on the E-37 chromosome. Due to the proximity and consistent orientation of the *fcs2* gene to the benzoate-CoA ligase and its corresponding benzoyl-CoA oxidation (box) operon (which harbors other genes implicated in ferulic acid catabolism including an enoyl-coA hydratase (SSE37_24454) and thioesterase (SSE37_24444)), it is feasible that these two proteins could have interchangeable functions and/or accept a variety of similar substrates. Small deviations in substrate specificity has been documented previously for the benzoyl-CoA ligase from *Thauera aromatica* from which the purified benzoyl-CoA ligase was capable of transforming benzoate and 2-aminobenzoate (52). Another instance of CoA ligase promiscuity is demonstrated in *Acinetobacter* ADP1 whose CoA ligase (Hca*C*) was found to transfer CoA to caffeic acid, *p*-coumaric acid, and ferulic acid (34). Similarly,

the annotated feruloyl-CoA ligase (FerA) from *Sphingobium* SYK-6 has been demonstrated to convert caffeic acid, *p*-coumaric, sinapic acid, and ferulic acid (35).

The proximity and consistent orientation of the *fcs2* gene to the *box* genes might also imply polar effects of the insertional mutation, truncating expression of the annotated benozoyl-CoA ligase and adjacent *box* operon. If the *box* genes are misannotated and/or involved in the degradation of other hydroxycinnamic acids, like ferulic acid and *p*-coumaric, the polar disruption of these genes might also contribute to the given phenotype. Although growth and activity on benzoic acid was not affected by any of these mutations (data not shown), a second benzoyl-CoA ligase (locus tag SSE37_02644, accession EBA07214) and a 2-aminobenzoate-CoA ligase (locus tag SSE37_00175, accession EBA06840) are annotated in the genome which could potentially provide the required benzoate transformations if the other gene is impaired. While a polar effect would represent an undesired outcome of the intended *fcs2* mutation, it could serendipitously uncover previous misunderstandings regarding the aromatic catabolome of E-37 and encourage future studies to provide a more comprehensive understanding of aromatic catabolism. Although less satisfying, another explanation for these data is simply a misannotation of both *fcs* genes in the available draft genome of E-37, assigning the ferulic acid substrate to enzymes with other preferred substrates. While protein BLAST analyses aligning Fcs1 and Fcs2 to sequences in Genbank overwhelmingly yields hits to other annotated feruloyl-CoA synthase and ligases from various bacteria (data not shown), the homology of these two proteins to functionally annotated feruloyl-CoA synthase/ligases is fairly low. Alignment of E-37's Fcs1 to the functionally validated FerA protein of *Sphingobium* SYK-6 (for which there are multiple substrates) (35) provides an alignment covering only 12% of the amino acids for Fcs1 and 22% of the amino acids for Fcs2 (recall that Fcs1 and Fcs2 only share 42% identity, but with a strong coverage of 96%). This supports the concept that these two proteins are distinct from a characterized feruloyl-CoA synthase, suggesting a different function or substrate for these enzymes, despite their evidence of diagnostic sequence motifs, including AMP and CoA binding sites.

Given the current level of information offered from the studies at hand, it would be overly presumptuous to propose a defined mechanism for the involvement of *fcs* genes in the degradation of ferulic acid in E-37, however additional information was elucidated regarding the involvement of these genes in *p*-coumarate degradation that are a bit more interpretable. Results from the Biolog assay and growth studies indicated a complete loss of activity and growth on *p*-coumaric acid for the *fcs1*/*fcs2* double mutant. These data indicate that both annotated *fcs* genes are required for the utilization of *p*-coumaric acid in E-37. This phenotype was not observed with either of the individual mutants, suggesting a synergistic contribution of both enzymes for the degradation of *p*-coumarate. As mentioned earlier, perhaps the ability of a feruloyl-CoA synthase to transform a related substrate like *p*-coumaric acid is not surprising given the documentation of the substrate-variable HcaC CoA ligase in *Acinetobacter* (34). While these findings provide strong circumstantial evidence for the use of *p*-coumaric acid by both *fcs* genes, it would be hasty to assign such specific function to these genes without the proper functional enzyme studies and chemical analyses of intermediates. Future work on this project would benefit from focusing on defining substrates for these enzymes through binding assays with purified proteins. Additional insight on the overall cellular response to aromatic compounds could be provided by q-RT-PCR experiments to monitor and quantify gene expression during growth. At present, we understand that the two annotated *fcs* genes are involved, but not required for ferulic acid utilization, however both genes are required for the degradation of *p*-coumaric acid, suggesting a genomic misannotation or enzyme promiscuity.

*Contributions to roseobacter genetics*

In addition to providing insight to the roles of *fcs* genes in aromatic catabolism in E-37, this work was also instrumental in establishing a more comprehensive set of molecular tools to employ in E-37 and possibly other roseobacters for future genetic studies. The approaches employed include random transposon mutagenesis, marker exchange mutagenesis, and plasmid insertion mutagenesis. While the Tn5-based random transposon mutagenesis has already been documented for some roseobacter strains

(*Phaeobacter* sp. Y4I (44) and others (41)), this is the first report of its implementation in *Sagittula stellata* E-37 which is taxonomically and functionally distinct from strains who have previously been genetically manipulated (39, 53). Additionally, this work demonstrates successful application of marker exchange mutagenesis which has only recently been described in the roseobacter *Ruegeria pomeroyi* DSS-3 (45). Lastly, the generation of chromosomal interruptions through single homologous recombination with a pKNOCK plasmid demonstrates the first application of this approach in a roseobacter strain. Given the environmental importance of E-37 in coastal systems, the establishment of a strong genetic system in this organism vows to provide a fruitful future of molecular-based studies that can be applied toward any function of interest.

## VI. Acknowledgements

I would like to acknowledge the help of Michelle Chua for aiding in the generation of growth curve data to assess mutant phenotypes on various aromatic compounds.

# VII. References


1. **Moran MA, Hodson RE.** 1990. Contributions of degrading *Spartina alterniflora* lignocellulose to the dissolved organic carbon pool of a salt marsh. Mar Ecol Prog Ser **62:**161-168.
2. **Ralph J, Lundquist K, Brunow G, Lu F, Kim H, Schatz PF, Marita JM, Hatfield RD, Ralph SA, Christensen JH, Boerjan W.** 2004. Lignins: Natural polymers from oxidative coupling of 4-hydroxyphenyl- propanoids. Phytochem Rev **3:**29-60.
3. **Austin AT, Ballare CL.** 2010. Dual role of lignin in plant litter decomposition in terrestrial ecosystems. Proc Natl Acad Sci U S A **107:**4618-4622.
4. **Johnson MT, Smith SD, Rausher MD.** 2009. Plant sex and the evolution of plant defenses against herbivores. Proc Natl Acad Sci U S A **106:**18079-18084.
5. **Vance CP, Kirk TK, Sherwood RT.** 1980. Lignification as a mechanism of disease resistance. Annu Rev Phytopathol **18:**259-288.
6. **Yang Q, Pan X.** 2015. Correlation between lignin physicochemical properties and inhibition to enzymatic hydrolysis of cellulose. Biotechnol Bioeng**:**[Epub ahead of print].
7. **Laskar DD, Yang B, Wang H, Lee J.** 2013. Pathways for biomass-derived lignin to hydrocarbon fuels. Biofuels, Bioprod Biorefin **7:**602-626.
8. **Ragauskas AJ, Beckham GT, Biddy MJ, Chandra R, Chen F, Davis MF, Davison BH, Dixon RA, Gilna P, Keller M, Langan P, Naskar AK, Saddler JN, Tschaplinski TJ, Tuskan GA, Wyman CE.** 2014. Lignin valorization: improving lignin processing in the biorefinery. Science **344:**1246843.
9. **Bugg TD, Ahmad M, Hardiman EM, Rahmanpour R.** 2011. Pathways for degradation of lignin in bacteria and fungi. Nat Prod Rep **28:**1883-1896.
10. **Levasseur A, Piumi F, Coutinho PM, Rancurel C, Asther M, Delattre M, Henrissat B, Pontarotti P, Asther M, Record E.** 2008. FOLy: an integrated database for the classification and functional annotation of fungal

oxidoreductases potentially involved in the degradation of lignin and related aromatic compounds. Fungal Genet Biol **45:**638-645.

11. **Tien M, Kirk TK, Bull C, Fee JA.** 1986. Steady-state and transient-state kinetic studies on the oxidation of 3,4-dimethoxybenzyl alcohol catalyzed by the ligninase of *Phanerocheate chrysosporium* Burds. J Biol Chem **261:**1687-1693.
12. **Kuwahara M, Glenn JK, Morgan MA, Gold MH.** 1984. Separation and characterization of two extracelluar H2O2-dependent oxidases from ligninolytic cultures of *Phanerochaete chrysosporium*. FEBS Lett **169:**247-250.
13. **Kirk TK, Farrell RL.** 1987. Enzymatic "combustion": the microbial degradation of lignin. Annu Rev Microbiol **41:**465-505.
14. **Carpita NC.** 1996. Structure and biogenesis of the cell walls of grasses. Annu Rev Plant Physiol Plant Mol Biol **47:**445-476.
15. **de Oliveira DM, Finger-Teixeira A, Rodrigues Mota T, Salvador VH, Moreira-Vilar FC, Correa Molinari HB, Craig Mitchell RA, Marchiosi R, Ferrarese-Filho O, Dantas Dos Santos W.** 2015. Ferulic acid: a key component in grass lignocellulose recalcitrance to hydrolysis. Plant Biotechnol J **13:**1224-1232.
16. **Hlasiwetz H, Barth L.** 1866. Mittheilungen aus dem chemischen Laboratorium in Innsbruck I)Ueber einige Harze [Zersetzungsproducte derselben durch schmelzendes Kali]. Justus Liebigs Annalen der Chemie **138:**61-76.
17. **Graf E.** 1992. Antioxidant potential of ferulic acid. Free Radic Biol Med **13:**435-448.
18. **Kumar N, Pruthi V.** 2014. Potential applications of ferulic acid from natural sources. Biotechnology Reports **4:**86-93.
19. **Zhao Z, Moghadasian MH.** 2008. Chemistry, natural sources, dietary intake and pharmacokinetic properties of ferulic acid: A review. Food Chem **109:**691-702.
20. **Priefert H, Rabenhorst J, Steinbuchel A.** 2001. Biotechnological production of vanillin. Appl Microbiol Biotechnol **56:**296-314.
21. **Plaggenborg R, Overhage J, Loos A, Archer JA, Lessard P, Sinskey AJ, Steinbuchel A, Priefert H.** 2006. Potential of *Rhodococcus* strains for

biotechnological vanillin production from ferulic acid and eugenol. Appl Microbiol Biotechnol **72:**745-755.

22. **Muheim A, Lerch K.** 1999. Towards a high-yield bioconversion of ferulic acid to vanillin. Appl Microbiol Biotechnol **51:**456-461.
23. **Gu W, Yang J, Lou Z, Liang L, Sun Y, Huang J, Li X, Cao Y, Meng Z, Zhang KQ.** 2011. Structural basis of enzymatic activity for the ferulic acid decarboxylase (FADase) from *Enterobacter* sp. Px6-4. PLoS One **6:**e16262.
24. **Degrassi G, Polverino De Laureto P, Bruschi CV.** 1995. Purification and characterization of ferulate and p-coumarate decarboxylase from *Bacillus pumilus*. Appl Environ Microbiol **61:**326-332.
25. **Chai L-y, Zhang H, Yang W-c, Zhu Y-h, Yang Z-h, Zheng Y, Chen Y-h.** 2013. Biodegradation of ferulic acid by a newly isolated strain of *Cupriavidus* sp. B-8. J Cent South Univ **20:**1964-1970.
26. **Huang Z, Dostal L, Rosazza JP.** 1994. Purification and characterization of a ferulic acid decarboxylase from *Pseudomonas fluorescens*. J Bacteriol **176:**5912-5918.
27. **Bhuiya MW, Lee SG, Jez JM, Yu O.** 2015. Structure and mechanism of ferulic acid decarboxylase (FDC1) from *Saccharomyces cerevisiae*. Appl Environ Microbiol **81:**4216-4223.
28. **Payne KA, White MD, Fisher K, Khara B, Bailey SS, Parker D, Rattray NJ, Trivedi DK, Goodacre R, Beveridge R, Barran P, Rigby SE, Scrutton NS, Hay S, Leys D.** 2015. New cofactor supports alpha,beta-unsaturated acid decarboxylation via 1,3-dipolar cycloaddition. Nature **522:**497-501.
29. **Matte A, Grosse S, Bergeron H, Abokitse K, Lau PC.** 2010. Structural analysis of *Bacillus pumilus* phenolic acid decarboxylase, a lipocalin-fold enzyme. Acta Crystallogr Sect F Struct Biol Cryst Commun **66:**1407-1414.
30. **Campillo T, Renoud S, Kerzaon I, Vial L, Baude J, Gaillard V, Bellvert F, Chamignon C, Comte G, Nesme X, Lavire C, Hommais F.** 2014. Analysis of hydroxycinnamic acid degradation in *Agrobacterium fabrum* reveals a coenzyme

A-dependent, beta-oxidative deacetylation pathway. Appl Environ Microbiol **80:**3341-3349.

31. **Plaggenborg R, Steinbuchel A, Priefert H.** 2001. The coenzyme A-dependent, non-beta-oxidation pathway and not direct deacetylation is the major route for ferulic acid degradation in *Delftia acidovorans*. FEMS Microbiol Lett **205:**9-16.
32. **Narbad A, Gasson MJ.** 1998. Metabolism of ferulic acid via vanillin using a novel CoA-dependent pathway in a newly-isolated strain of *Pseudomonas fluorescens*. Microbiol **144 ( Pt 5):**1397-1405.
33. **Overhage J, Priefert H, Steinbuchel A.** 1999. Biochemical and genetic analyses of ferulic acid catabolism in *Pseudomonas* sp. strain HR199. Appl Environ Microbiol **65:**4837-4847.
34. **Parke D, Ornston LN.** 2003. Hydroxycinnamate (hca) catabolic genes from *Acinetobacter* sp. strain ADP1 are repressed by HcaR and are induced by hydroxycinnamoyl-coenzyme A thioesters. Appl Environ Microbiol **69:**5398-5409.
35. **Masai E, Harada K, Peng X, Kitayama H, Katayama Y, Fukuda M.** 2002. Cloning and characterization of the ferulic acid catabolic genes of *Sphingomonas paucimobilis* SYK-6. Appl Environ Microbiol **68:**4416-4424.
36. **Buchan A, Gonzalez JM, Moran MA.** 2005. Overview of the marine roseobacter lineage. Appl Environ Microbiol **71:**5665-5677.
37. **Buchan A, Collier LS, Neidle EL, Moran MA.** 2000. Key aromatic-ring-cleaving enzyme, protocatechuate 3,4-dioxygenase, in the ecologically important marine Roseobacter lineage. Appl Environ Microbiol **66:**4662-4672.
38. **Gulvik CA, Buchan A.** 2013. Simultaneous catabolism of plant-derived aromatic compounds results in enhanced growth for members of the Roseobacter lineage. Appl Environ Microbiol **79:**3716-3723.
39. **Newton RJ, Griffin LE, Bowles KM, Meile C, Gifford S, Givens CE, Howard EC, King E, Oakley CA, Reisch CR, Rinta-Kanto JM, Sharma S, Sun S, Varaljay V, Vila-Costa M, Westrich JR, Moran MA.** 2010. Genome characteristics of a generalist marine bacterial lineage. ISME J **4:**784-798.

40. **Gonzalez JM, Mayer F, Moran MA, Hodson RE, Whitman WB.** 1997. *Sagittula stellata* gen. nov., sp. nov., a lignin-transforming bacterium from a coastal environment. Int J Syst Bacteriol **47:**773-780.
41. **Piekarski T, Buchholz I, Drepper T, Schobert M, Wagner-Doebler I, Tielen P, Jahn D.** 2009. Genetic tools for the investigation of Roseobacter clade bacteria. BMC Microbiol **9:**265.
42. **Larsen RA, Wilson MM, Guss AM, Metcalf WW.** 2002. Genetic analysis of pigment biosynthesis in *Xanthobacter autotrophicus* Py2 using a new, highly efficient transposon mutagenesis system that is functional in a wide variety of bacteria. Arch Microbiol **178:**193-201.
43. **O'Toole GA, Pratt LA, Watnick PI, Newman DK, Weaver VB, Kolter R.** 1999. Genetic approaches to study of biofilms. Methods Enzymol **310:**91-109.
44. **Cude WN, Mooney J, Tavanaei AA, Hadden MK, Frank AM, Gulvik CA, May AL, Buchan A.** 2012. Production of the antimicrobial secondary metabolite indigoidine contributes to competitive surface colonization by the marine roseobacter *Phaeobacter* sp. strain Y4I. Appl Environ Microbiol **78:**4771-4780.
45. **Lidbury I, Murrell JC, Chen Y.** 2014. Trimethylamine N-oxide metabolism by abundant marine heterotrophic bacteria. Proc Natl Acad Sci U S A **111:**2710-2715.
46. **Stibitz S.** 1994. Use of conditionally counterselectable suicide vectors for allelic exchange. Methods Enzymol **235:**458-465.
47. **Jones RM, Williams PA.** 2003. Mutational analysis of the critical bases involved in activation of the AreR-regulated sigma54-dependent promoter in *Acinetobacter* sp. strain ADP1. Appl Environ Microbiol **69:**5627-5635.
48. **Alexeyev MF.** 1999. The pKNOCK series of broad-host-range mobilizable suicide vectors for gene knockout and targeted DNA insertion into the chromosome of gram-negative bacteria. Biotechniques **26:**824-826, 828.
49. **Metcalf WW, Jiang W, Daniels LL, Kim SK, Haldimann A, Wanner BL.** 1996. Conditionally replicative and conjugative plasmids carrying lacZ alpha for cloning, mutagenesis, and allele replacement in bacteria. Plasmid **35:**1-13.

50. **Borglin S, Joyner D, DeAngelis KM, Khudyakov J, D'Haeseleer P, Joachimiak MP, Hazen T.** 2012. Application of phenotypic microarrays to environmental microbiology. Curr Opin Biotechnol **23:**41-48.
51. **Bochner BR, Gadzinski P, Panomitros E.** 2001. Phenotype microarrays for high-throughput phenotypic testing and assay of gene function. Genome Res **11:**1246-1255.
52. **Schuhle K, Gescher J, Feil U, Paul M, Jahn M, Schagger H, Fuchs G.** 2003. Benzoate-coenzyme A ligase from *Thauera aromatica*: an enzyme acting in anaerobic and aerobic pathways. J Bacteriol **185:**4920-4929.
53. **Brinkhoff T, Giebel HA, Simon M.** 2008. Diversity, ecology, and genomics of the Roseobacter clade: a short overview. Arch Microbiol **189:**531-539.

# VIII. Appendix: Tables

**Table 2.1**. Plasmids and strains used in this study

| **Plasmids** | **Description** | **Source** |
|---|---|---|
| pCR2.1 TOPO | TA plasmid for cloning | Invitrogen |
| pRMJ1 | Plasmid harboring *sacBkanR* cassette for marker exchange mutagenesis | Jones & Williams 2003 |
| pARO180 | Mobilizable suicide plasmid for marker exchange mutagenesis | D. Park (ATCC 77123) |
| pARO180_12343 | pARO180 containing fused flanking regions of *fcs1* (SSE37_12324) cloned into the *XbaI* and *HindIII* sites of the MCS | This study |
| pARO180_12324_SK | pARO180_12324 with *sacBkanR* from pRMJ1 inserted into the middle of the *fcs1* insert through the designed *SalI* site | This study |
| pKNOCK-Km | Mobilizable suicide plasmid harboring kanamycin resistance gene. Used for site-directed mutagenesis via chromosomal integration | M.Alexeyev 1999 (Addgene 46262) |
| pKNOCK-Km_24399 | pKNOCK-Km with small internal region (231 bp) of *fcs2* cloned into the *BamHI* and *XhoI* sites of the MCS | This study |
| pKNOCK-Tc | Mobilizable suicide plasmid harboring tetracycline resistance gene. Used for site-directed mutagenesis via chromosomal integration | M.Alexeyev 1999 (Addgene 46259) |
| pKNOCK-Tc_24399 | pKNOCK-Tc with small internal region (231 bp) of *fcs2* cloned into the *BamHI* and *XhoI* sites of the MCS | This study |
| **Strains** | | |
| E-37 | Wildtype *Sagitulla stellata* E-37 | Gonzalez *et al*. 1997 |
| E-37 Δ*fsc1*::*sacBkanR* | E-37 *fcs1* mutant where *fcs1* (SE37_12324) is replaced with *sacBkanR* from pARO180_12324_SK | This study |
| E-37 *fcs2*::pKNOCK-Km | E-37 *fcs2* mutant where *fcs2* (SSE37_24399) is interrupted by pKNOCK-Km_24399 | This study |
| E-37 Δ*fsc1*::*sacBkanR* *fcs2*::pKNOCK-Tc | E-37 *fcs1*/*fcs2* double mutant generated by interrupting *fcs2* (SSE37_24399) with pKNOCK-Tc_24399 in strain E-37 Δ*fsc1*::*sacBkanR* | This study |
| *E. coli* TOP10 | Cloning strain for pCR2.1 TOPO plasmid | Invitrogen |
| *E. coli* JM109 | Subcloning and transformation strain | gift |
| *E. coli* S17-1 | Mating strain for marker exchange mutagenesis | ATCC 47055 |
| *E. coli* BW20767 | Mating strain for pKNOCK mutagenesis, derived from S17-1 | Metcalf *et al*. 1996 ATCC 47084 |

**Table 2.2**. Primers used in this study

| Name | Sequence | Function |
|---|---|---|
| E37_12324_A_ex<br>E37_12324_A_in | GATCACTGCGCCGATCTT<br>gattcgaggagcgatagagctGTCGACTTCTCCTCC TGGCGTTTTAG* | Primer pair amplifies A region (402 bp upstream of 12324) with 21 bp scar *SalI* site appended to the 3' end. A_ex primer is also use with B_ex for cross-over pCR to generate the A-scar-B product |
| E37_12324_B_ex<br>E37_12324_A_in | GGAGCCCAACAGCATCAT<br>agctctatcgctcctcgaatcGACCGGCGCCCGGTT* | Primer pair amplifies B region (585 bp downstream of 12324) with 21 bp scar appended to the 5' end. B_ex primer is also use with A_ex for cross-over PCR to generate the A-scar-B product |
| E37_12324_Asac_F<br>E37_12324_Bkm_R | GGATCAGGATGTCGTCGTTC<br>CAGCTTCTCCTCGATTCGCT | Amplifies region upstream and downstream of *fcs1* to verify replacement of gene with *sacBkanR* cassette |
| 24399_int_F<br>24399_int_R | TGGTGTTTTATGCAGGCGCG<br>TTTCGCAGCGCATGTCTTCG | Primer pair amplifies 231 bp internal region of *fcs2* (SSE37_24399) used for cloning into pKNOCK plasmids |
| pKNOCKKm_752_F<br>pKNOCKKm_901_R | ACGGCTGACATGGGAATTCC<br>GCGGAATTAATTCGACGCGTC | Primer pair binds around MCS of pKNOCK-Km to amplify inserts off of plasmid |
| pKNOCKTc_425_F<br>pKNOCKTc_558_R | GAATTCCCCTCCACCGCGG<br>TGATCAAGCTGACGCGTCCT | Primer pair binds around MCS of pKNOCK-Tc to amplify inserts off of plasmid |
| 24399_884_F<br>24399_1383_R | GAACGCTGGCCTTCAACGTG<br>GAAATCCTCCGAAATCCGCCC | Primer pair binds E-37 DNA upstream and downstream of the 231 bp internal region of *fcs2*. Used to verify insertion of pKNOCK plasmids in *fcs2* of E-37 |

***** 21 bp scar sequence indicated in lower case. *SalI* site underlined.

**Table 2.3**. Fcs1 homologs in the E-37 genome. Results were generated from BLASTing the E-37 Fcs1 amino acid sequence against the *Sagittula stellata* E-37 genome.

| Description | Accession ID | % Identity | % Query coverage | Expected value |
|---|---|---|---|---|
| Fcs1 (SSE37_12324) | WP_005859342.1 | 100 | 100 | 0 |
| Fcs2 (SSE37_24399) | WP_005857142.1 | 42 | 96 | 5.07E-148 |
| Long-chain fatty acid CoA ligase | WP_005859196.1 | 24 | 64 | 3.53E-17 |
| Malonyl-CoA synthase | WP_005858701.1 | 29 | 39 | 6.54E-14 |
| 4-hydroxybenzoate-CoA ligase | WP_005857144.1 | 26 | 50 | 2.78E-13 |
| Benzoate-CoA ligase | WP_005860777.1 | 23 | 58 | 2.59E-08 |
| AMP-dependent synthetase | WP_005857435.1 | 27 | 34 | 2.78E-07 |
| Benzoate-CoA ligase | EBA06840 | 23 | 69 | 8.50E-06 |
| 2-aminobenzoate-CoA ligase | WP_040604889.1 | 23 | 37 | 8.56E-06 |
| Long-chain fatty acid CoA ligase | WP_005861161.1 | 25 | 20 | 5.37E-05 |
| AMP-dependent synthetase | WP_005863246.1 | 32 | 39 | 1.35E-04 |

# IX. Appendix: Figures

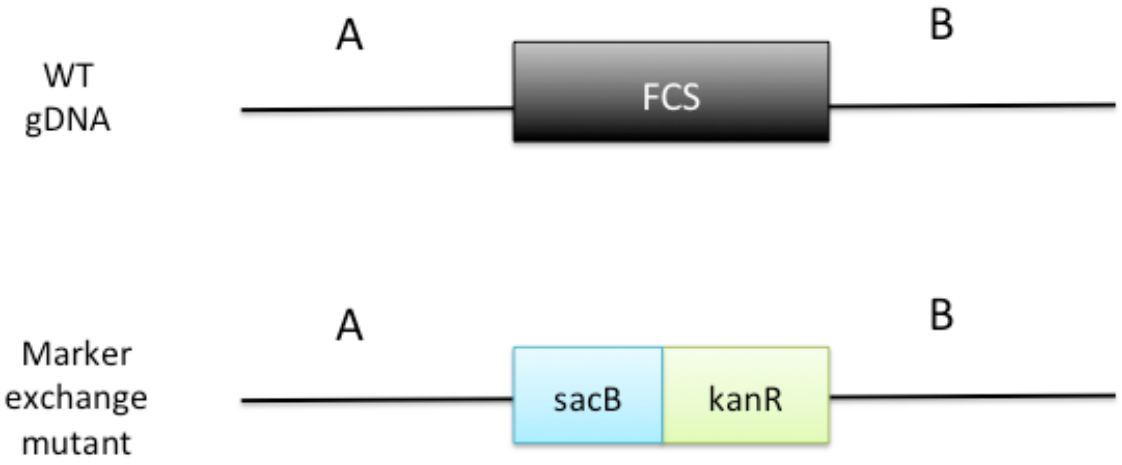


**Figure 2.1**. Conceptual depiction of the marker exchange mutagenesis approach used to generate the *fcs1* mutant. A and B regions surrounding the *fcs* gene represent the regions used for overlap extension PCR eventually serving as regions of homology for homologous recombination in the E-37 genome

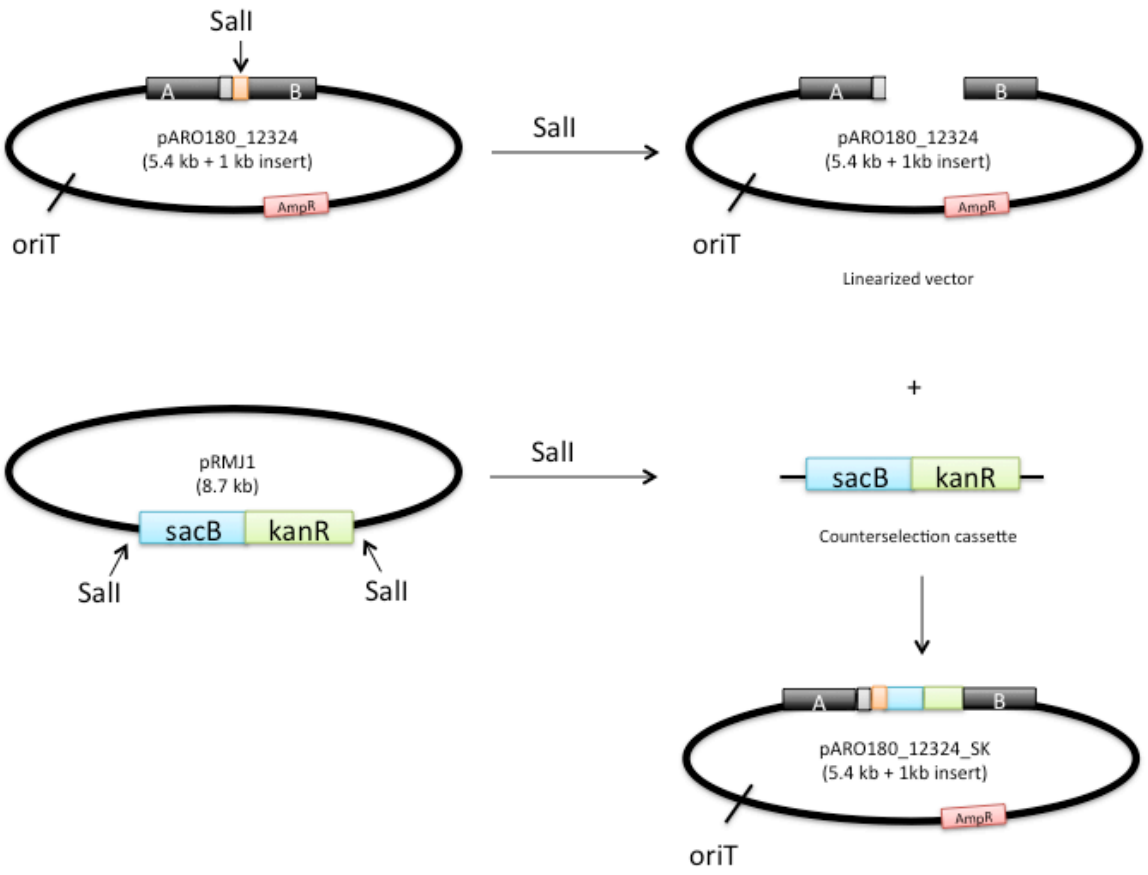


**Figure 2.2**. Illustration depicting the steps for generation of the allelic exchange plasmid construct, pARO180_12324_SK.

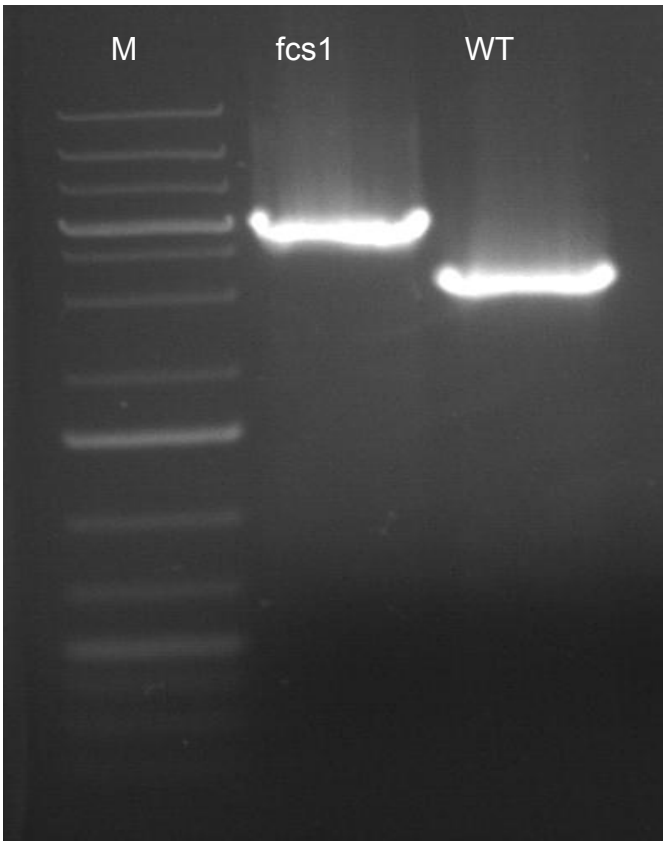


**Figure 2.3**. Agarose gel validating the replacement of the *fcs1* gene with the ::*sacBkanR* cassette from the mobilizable suicide plasmid construct. This amplification used primers Asac_F and Bkm_R targeting the E-37 genome flanking the *fcs1* gene. Replacement of *fcs1* with ::*sacBkanR* yields 5 kb product consistent with *sacBkan*R (3.5 kb) plus additional flanking regions (1,457 bp), whereas WT amplification yields 3.3 kb product consistent with the size of the *fcs1* (1,833 bp) gene plus additional flanking regions (1,457 bp) **M**; 1 kB plus ladder, **fcs1**; amplicon from *fcs1* mutant strain, **WT**; amplicons from E-37.

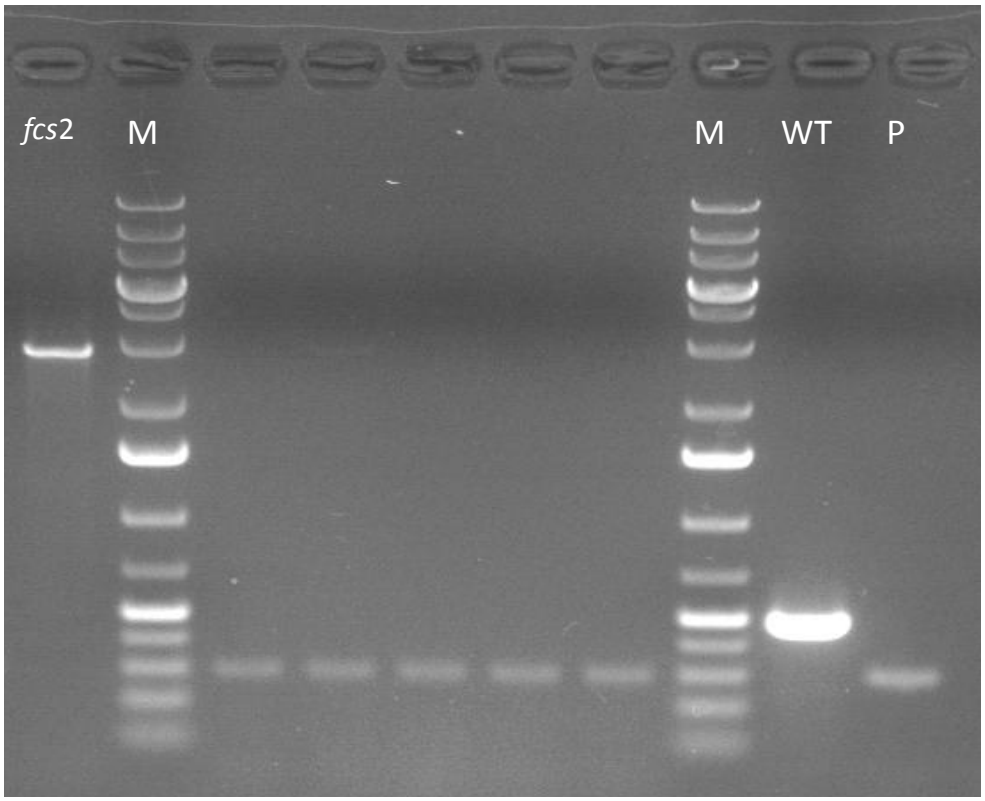


**Figure 2.4**. Agarose gel validating the interruption of the *fcs2* gene with the pKNOCK-Km. This amplification used primers 884_F/1383_R targeting the E-37 genome flanking 231 bp region used for homologous recombination. Insertion into the *fcs2* gene with pKNOCK-Km yields a 2.9 kb product consistent with the size of pKNOCK-Km (2.1 kb) plus the flanking region (800 bp). The wildtype band at 500 bp is consistent with amplification of the 231 bp region plus the flanking region. The bands at 300 bp represent a nonspecific product from the pKNOCK-Km plasmid (in lane P). **M**; 1 kb plus ladder, **fcs2**; amplicon from *fcs2* mutant strain, **WT**; amplicons from E-37. **P**; amplicon from pKNOCK-Km plasmid control. Unlabeled lanes represent unsuccessful clones with nonspecific amplification off the plasmid.

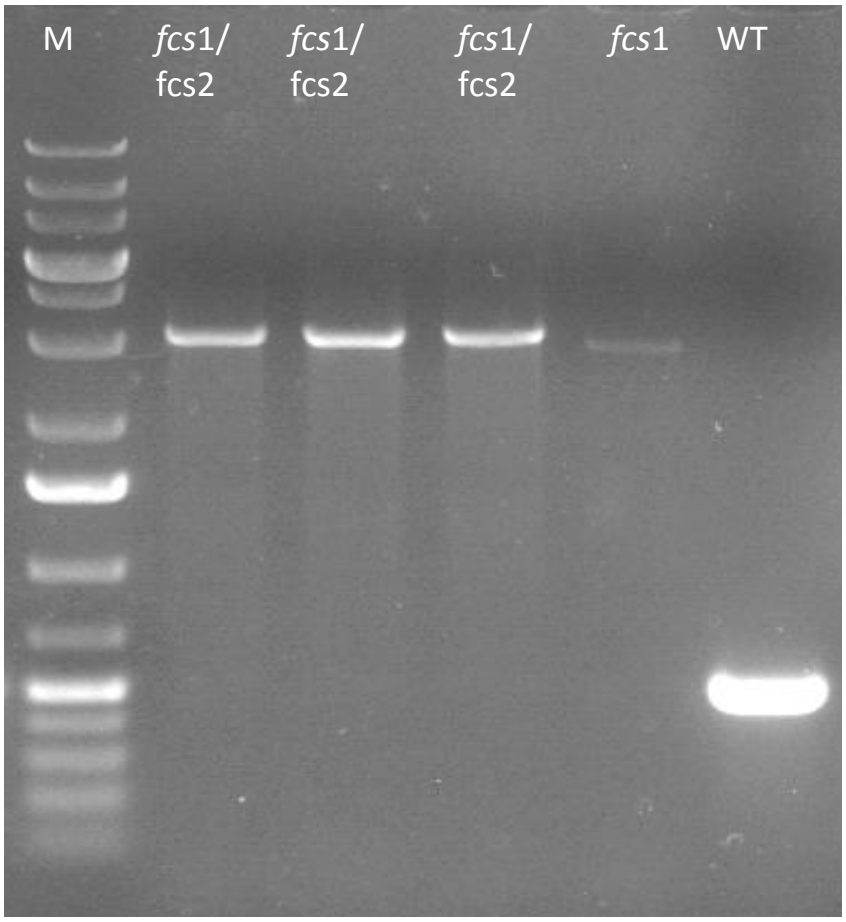


**Figure 2.5**. Agarose gel validating the interruption of the *fcs2* gene with pKNCOK-Tc in the *fcs*1- background. This amplification used primers 884_F/1383_R targeting the E-37 genome flanking 231 bp region used for homologous recombination. Insertion into the *fcs2* gene with pKNOCK-Tc yields a 3.1 kb product consistent with the size of pKNOCK-Tc (2.3 kb) plus the flanking region (800 bp). The *fcs1* band was also amplified from this strain using the Asac_F and Bkm_R primers to reconfirm the maintenance of this mutation. The wildtype band at 500 bp is consistent with amplification of the 231 bp region plus the flanking region **M**; 1 kb plus ladder, **fcs2**; amplicon from *fcs2* mutant strain, **WT**; amplicons from E-37.

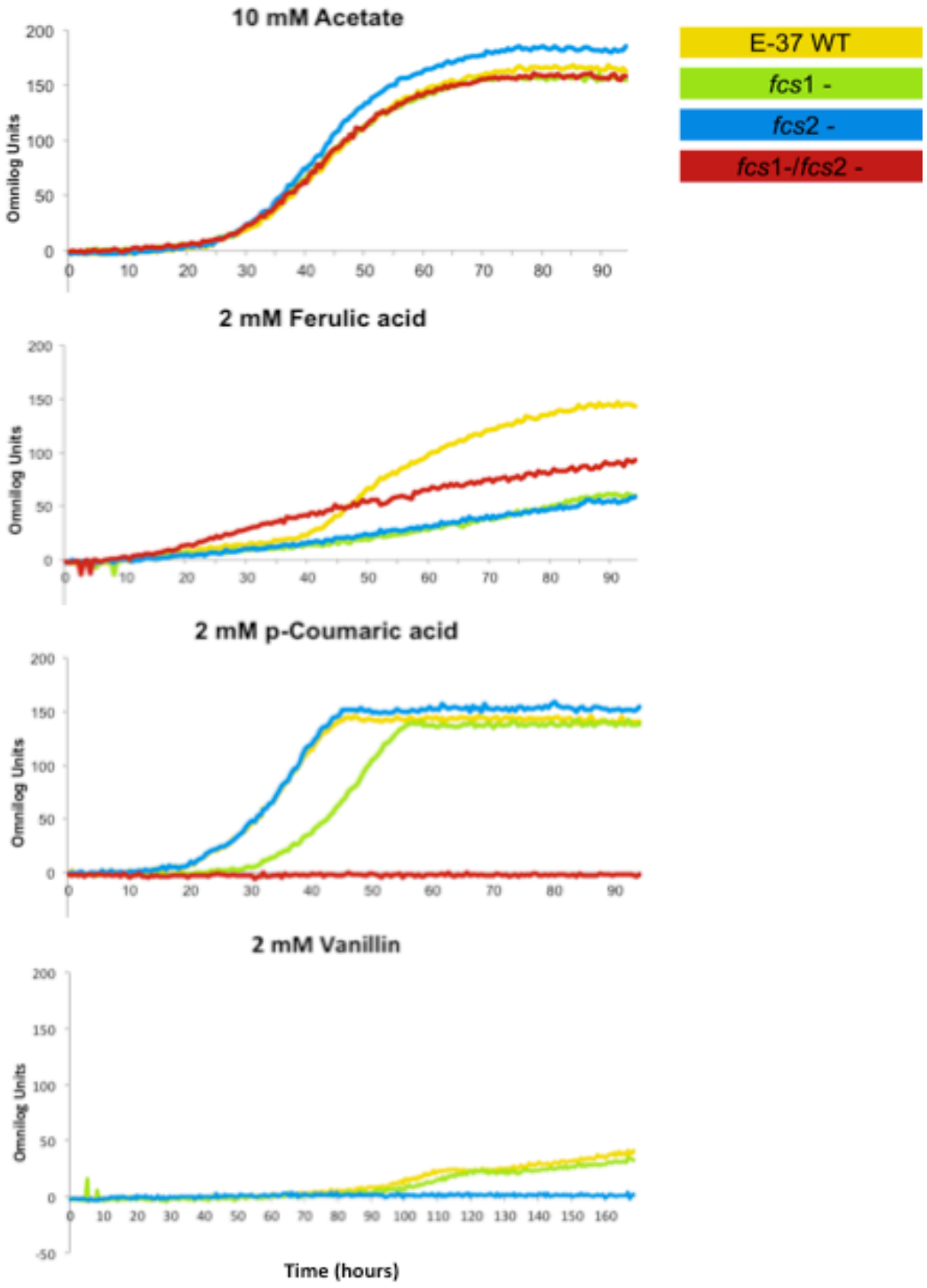


**Figure 2.6**. Biolog phenotypic assay of *fcs* mutant strains incubated with various aromatic compounds. Results demonstrate a loss of activity on *p*-coumaric acid for the *fcs1*/*fcs*2 mutant and a loss of activity on vanillin for the *fcs2* mutant. Data for the double mutant on vanillin is pending.

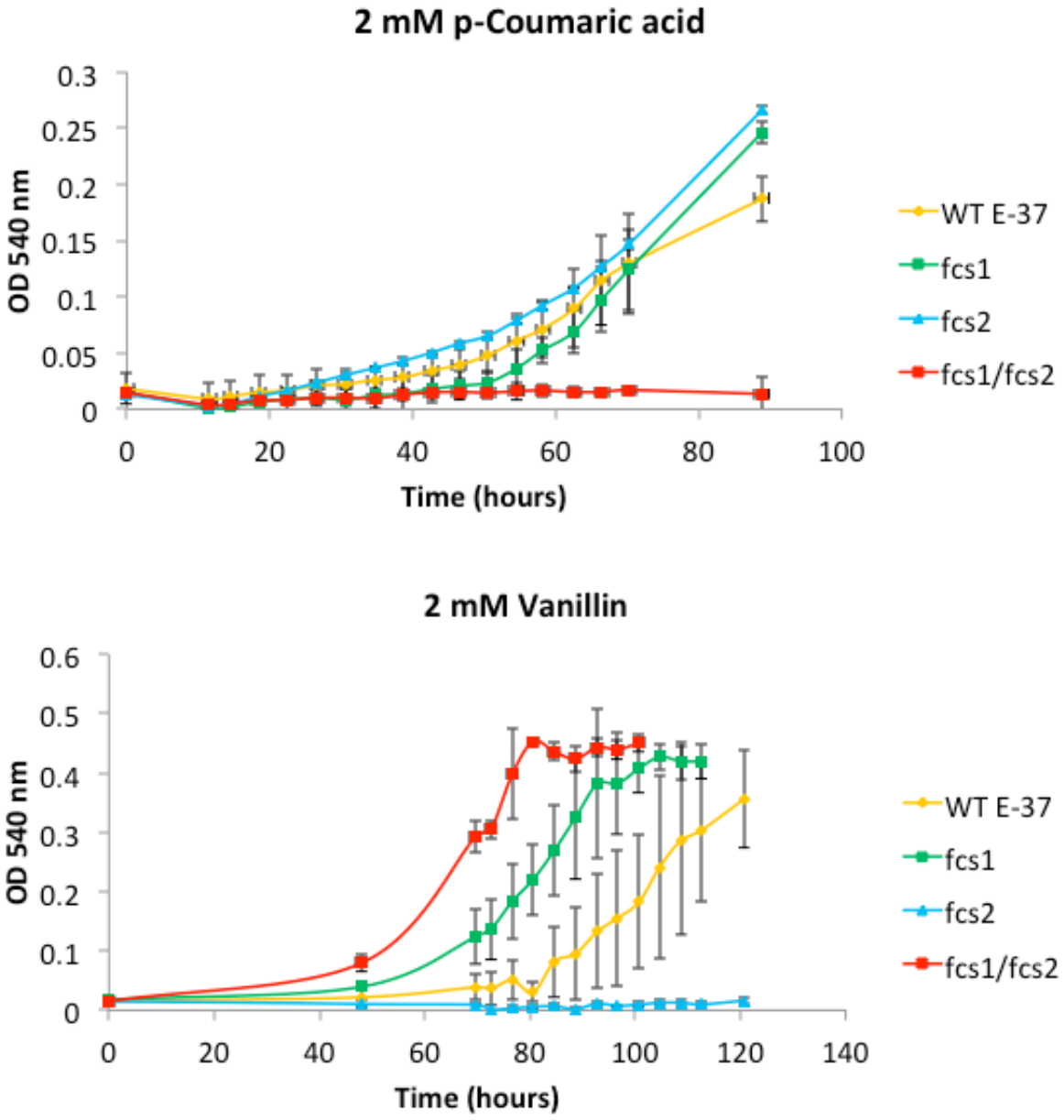


**Figure 2.7**. Growth curves of all *fcs* mutants on *p*-coumaric acid and vanillin. Results corroborate the loss of activities demonstrated in the Biolog assay

# CHAPTER THREE - TRANSFORMATION OF ORGANSOLV LIGNIN BY MARINE ROSEOBACTERS

# I. Abstract

The prospect of generating renewable products from plant biomass has received much attention as the need for cost-effective alternative energies increases. The lignocellulose from vascular plants often serves as the primary feedstock for the bioethanol refinery, where plant biomass is fractionated to remove lignin from the fermentable polysaccharides. The removal of lignin is accomplished through biomass pretreatments, ideally resulting in a clean separation of lignin from cellulose and hemicellulose. Due to the variability in plant cell wall architecture, there is no universal pretreatment method, however, one of the most promising fractionations is an organic extraction (organosolv) method that produces fairly pure streams of cellulose and lignin. This method is favorable as it produces two clean pools of carbon from which valuable products can be derived; cellulose can be saccharified and fermented to bioethanol and the lignin can be converted to hydrocarbon fuels and various other industrial chemicals. Thus, this introduces a new opportunity to upgrade the value of lignin from the biorefinery where it was formerly burned for energy. The conversion of lignin from a bioethanol refinery, however, is not a trivial task, as it requires the selective activity of either chemical or microbial catalysts. This work assesses the utility of marine roseobacter bacteria to utilize and transform different preparations of organosolv lignin. Microcosm incubations were performed and assayed for bacterial growth and structural changes to the lignin biomass via 2D NMR. Although the results were somewhat confounded by weak reproducibility, strong evidence for bacterial growth was observed and preliminary data suggests microbial conversions of ferulate esters, β-O-4 linkages, phenylcoumaran structures, and pinoresinol features. To our knowledge these findings present the first demonstration of bacterial utilization of an organosolv lignin and provide support for the continued investigation of their use for the valorization of lignin.

# II. Introduction

Lignin is the most abundant aromatic polymer on earth and offers an incredible resource for the production of renewable carbon (1). The abundance of carbon secured in this molecule (28 x $10^9$ tons deposited annually) (2) holds potential for conversion to industrially and commercially valuable commodities including hydrocarbon fuels and synthetic chemicals like benzene, toluene, xylene, and styrene (3). Harnessing the value from lignin, however, presents a grand challenge due to its inherent resistance to chemical and enzymatic hydrolysis. The stable architecture of lignin helps to fortify the cell walls of vascular plants, where it is concomitantly entrapped with two polysaccharides, cellulose and hemicellulose, providing an additional barrier to its extraction. Cell wall lignification occurs through radical formation and condensation of three hydroxycinnamic alcohols; *p*-coumaryl alcohol, coniferyl alcohol, and sinapyl alcohol (review Figures 1.1and 1.2), which vary only in the degree of ring methoxylation (4). Due to the variety of radicals that can form across these monolignols, a diversity of carbon-carbon and carbon-oxygen linkages is represented in the resulting lignin polymer. The heterogeneity supplied by the various aromatic constituents and interunit linkages combined with the inherent stability of the aromatic rings imparts an incredible recalcitrance to the material. These refractory properties are what have historically impeded the successful and economical upgrading of lignin to higher value applications.

One major opportunity for the valorization of lignin is offered from current bioethanol refinery where advancing technologies exist for a clean separation of lignin from cellulose and hemicellulose. In this industry, the lignin is considered an impediment to accessing the fermentable sugars in plant biomass, and thus methods to remove lignin from these polysaccharides have been a priority. Lignin extraction chemistries have been developing since the 1830s (5), however due to the considerable differences in lignin structures across different (and even related) plants (6), there is still no consensus on which biomass fractionation method is most universally appropriate. Among one of

the most promising pretreatment technologies is an organic solvent (organosolv) extraction method that typically performed through a high temperature reaction (up to 200°C) with an acid catalyst (commonly $H_2SO_4$) in an organic solvent (ethanol, methanol, etc.) and water. This reaction hydrolyzes bonds between (and partially within) the lignin and hemicellulose. The lignin fraction is separated through extraction into the organic phase (7, 8). Comparative analysis of reaction variables has suggested that an optimum organosolv fractionation for a mixed biomass input (9:1 switchgrass to poplar) would involve a 90-minute reaction at 160°C with 0.1M $H_2SO_4$ (9) and ethanol/water/methyl isobutyl ketone extraction (10).

While valiant strides have been made toward deconstructing lignin through chemical means, nature has evolved to exploit energy and carbon from this recalcitrant polymer. The primary lignin degraders in nature are fungi of the Basidiomycota phylum, although there is also emerging evidence for lignolysis in select phyla of bacteria including actinobacteria, γ-proteobacteria, and α-proteobacteria (11, 12). In either instance, the organism oxidizes the lignin polymer through the activity of various extracellular peroxidases (predominantly lignin peroxidase and manganese peroxidase), generating a pool of lower molecular weight aromatic compounds that can be further catabolized by surrounding microbes. Due to the large inputs of lignin from agricultural plants, previous studies have exhibited a large bias toward the examination of lignin degradation in soil systems (13). While this has established an indispensible foundation on aromatic catabolism pathways, there are newly recognized lignin-rich environments that are worthy of attention. Of note are lignin-rich coastal marsh systems along the southeastern United States whose surrounding grasses have been shown to account for up to 75% of the dissolved humic substances in this environment (14). It has also been demonstrated that the microbial communities in these regions are capable of mineralizing lignocellulose from the native cordgrass, *Spartina alterniflora* (15). This information supports the argument that additional studies with coastal bacteria may expand our knowledge of lignin degradation, as organisms from different environments often adapt diverse approaches metabolism due to environmental constraints.

Representing up to 30% of the total microbial community along the southeastern United States coast (16), members of the roseobacter lineage of marine bacteria are among the most abundant and active bacteria in this environment. While these organisms express a diverse collection of phenotypes and metabolisms (17), select representatives are notorious for their ability to degrade plant-derived aromatic compounds (18-20). One strain in particular, *Sagittula stellata* E-37, was isolated from a lignin enrichment culture and was shown to attach to lignocellulose particles and partially mineralize a synthetic lignin (21). Additional studies with *S. stellata* E-37 have confirmed growth on a variety of lignin-derived aromatic compounds including anthranilic acid, benzoic acid, *p*-hydroxybenzoic acid, protocatechuic acid, *p*-coumaric acid, vanillic acid, and ferulic acid (20, 22). Furthermore, bioinformatics analyses of all roseobacter strains has revealed evidence for up to 6 different aromatic ring-cleaving pathways in selected representatives (18). These findings suggest that roseobacter species would be of great utility for expanding insight into the degradation of lignin-derived compounds, including the underused residual lignin from bioethanol biomass fractionations.

Here we investigate the ability of roseobacters to utilize organosolv lignin as a sole carbon and energy source while monitoring structural changes to the biomass through 2D NMR analysis. While preliminary results show strong support for the utilization and transformation of organosolv lignin, subsequent studies did not provide the necessary confidence to confirm this activity. Additional methods of biomass analysis were explored, but were limited to the soluble phenolic faction of the biomass and were also confounded by an observed abiotic transformation of the lignin. While it is clear that selected roseobacter strains grow on the supplied carbon source, information regarding the changes to biomass are somewhat uncertain, however there is some indication of the conversion of β-O-4 linkages and ferulate esters by these organisms. These findings as well as recommendations for future studies are articulated within.

## III. Materials and methods

*Strains, substrates, and growth maintenance*

*Sagittula stellata* E-37, *Sulfitobacter* sp. EE-36, and *Phaeobacter* sp. Y4I were previously isolated from pulp mill effluent as described by Gonzalez *et al.* (16). *Citreicella* sp. SE45 was isolated from *Spartina alterniflora* from a coastal salt marsh near Savannah, Georgia as described by Buchan *et al.* (23). All strains were maintained at 30°C in YTSS medium (per liter, 2.5g yeast extract, 4 g tryptone, 15 g sea salts [Sigma-Aldrich, St. Louis, MO]) unless otherwise noted. Pre-conditioning cultures were grown in Marine Basal Medium (MBM) containing 1.5% (wt/vol) sea salts, 225 nM $K_2HPO_4$, 13.35 µM $NH_4Cl$, 71 mM Tris-HCl (pH 7.5), 68 µM Fe-EDTA, trace metals, vitamins and carbon source (3-10 mM acetate or 5 mg/mL lignin). Organosolv lignins were prepared with various reaction conditions (Table 3.1) by Anton Astner at the University of Tennessee's Center for Renewable Carbon as described by Astner (9) and Bozell *et al*. (10). Non-lignin carbon sources were sterilized by filtration through a 0.2 µm filter. All glassware was ashed for 4-24 hours to remove any interfering carbon sources. All materials including spatulas and weigh boats were sterilized through autoclaving or UV radiation. Experiments were typically set up in a laminar flow hood unless otherwise noted.

*Microcosm 1- pilot end point study with NMR analysis*

A four-month pilot study was performed to determine if organosolv lignin preparations could support the growth of roseobacter strains and if changes to the lignin structure could be detected through 2D NMR. For this set of incubations, four roseobacter isolates (*Sagittula stellata* E-37, *Sulfitobacter* sp. EE-36, *Phaeobacter* sp. Y4I, and *Citreicella* sp. SE45) were pre-conditioned in MBM supplemented with 3 mM acetate and 50 mg lignin. The grown cultures were used to inoculate 2 replicate milk bottles containing 40 mL MBM and 200 mg of the respective organosolv lignin preparation (#129, #131, and #139) (refer to Table 3.1), providing a starting cell concentration of

about $10^6$ cells/mL. Control bottles were included containing carbon free medium to differentiate lignin growth from carryover growth from the inoculum. Additional abiotic controls were included containing lignin but no bacterial inoculum to assess abiotic changes of the lignin and monitor for contamination of the starting lignin. The milk bottles were capped with rubber stoppers and incubated in the dark at room temperature, shaking at 100 rpm. The lignin used for these microcosms was not sterilized, as previous abiotic lignin incubations did not show evidence for microbial contamination (data not shown) and options for sterilizing lignin without compromising structure are limited. Samples were collected weekly for viable count analysis by removing 200 µl from the standing (planktonic) aqueous culture, diluting in 1.5% sea salts, and plating as spot titers or full plates onto YTSS agar. The experiment was terminated after 120 days at which point the liquid medium was evaporated through drying at 60°C for 5-7 days. Dried samples were washed with a total of 10 mL deionized $H_2O$ in small portions through a Buchner funnel to remove salts from the growth medium. These washed samples were then sent for NMR analysis.

*Microcosm 2 - refined temporal study with NMR analysis*

A refined microcosm study was designed guided by results of the pilot study. In this experiment, two roseobacter strains, *Sagittula stellata* E-37 and *Citreicella* sp. SE45 were incubated with organosolv lignin preparation #139 (see Table 3.1). Pre-conditioning cultures were prepared in 10 mL MBM supplemented with 3 mM acetate and 50 mg lignin as described previously. These cultures were used to inoculate serum bottles in triplicate containing 30 mL MBM and 150 mg lignin, at a starting concentration of $10^6$ cells/mL. Again, biotic no-carbon controls and abiotic no-cell controls were included to assess carryover growth and abiotic lignin transformations, respectively. Due to the required sacrificing of entire bottles for lignin NMR analysis, the experimental design includes biological triplicates for each of the 7 time points (day 0, 4, 7, 14, 21, 28, 35) for all lignin + bacteria treatments. Bottles were capped with gray butyl rubber stoppers without crimping and incubated in the dark at room temperature, shaking at 100 rpm for 35 days. Bottles were periodically vented and swirled to encourage mixing.

Samples were collected on days 4, 7, 14, 21, 28, and 35 for viable count analysis (Day 0 cell concentration was estimated based on available growth curve information for the organisms). Bottles were mixed vigorously prior to sample removal in effort to collect both planktonic and surface-attached cells. Samples (500 µl) were dispensed into UV-sterilized snap-cap vials and sonicated in a 25°C waterbath sonicator (Branson, Danbury, CT) for 6 minutes at 40KHz. Viable counts were performed from the sonicated samples as in microcosm 1. After removing samples for viable counts for any particular time point, the corresponding set of biological triplicates was sacrificed for NMR analysis. The liquid was evaporated in a 60°C oven to dryness, as previous. Dried samples were washed in a total of 10 mL $dH_2O$ through centrifugation and resuspension. Washed samples were freeze-dried (Labconco FreezeZone, Kansas City, MO) and sent to the University of Tennessee's Center for Renewable Carbon for HMQC-NMR analysis.

*Microcosm 3 –UV ionization difference spectrophotometry of lignin phenolics*

An additional microcosm was designed to determine if a method targeting the soluble phenolic fraction could be informative with respect to detecting changes in the lignin. For this study organosolv lignin #90 (100% switchgrass), #108 (100% poplar), and #157 (50/50 S/G) (see Table 2.1) were used as a carbon source for *Citreicella* sp. SE45. Turbid cultures of SE45 pre-conditioned on 7 mM acetate were used to inoculate 25 mm screw-cap borosilicate tubes containing 10 mL MBM and 50 mg lignin to a starting cell concentration of ~$1x10^7$ cells/mL in duplicate. Lignin was pre-sterilized by heating at 70°C for 2 hours as previously described (24). In this experiment samples were sacrificed at $T_{initial}$ (day 0) and $T_{final}$ (day 5) for lignin phenol analysis, and therefore sets of tubes were prepared for both sacrificial time points. For sacrificed samples, the medium was evaporated at 60°C until dryness, at which time UV ionization difference spectrophotometric analysis was performed to detect phenolics. Additionally, samples were collected on days 0, 1, 2, 3, and 5 for viable count analysis. For this 150 µl of well-mixed sample (containing both planktonic and particle-associated fractions) was removed, diluted in 1.5% sea salts and plated as spot titers on YTSS agar.

*2D NMR and spectral analysis*

Heteronuclear Multiple Quantum Coherence-Nuclear Magnetic Resonance (HMQC-NMR) was performed by various collaborators at the University of Tennessee's Center for Renewable Carbon following the methods described by Bozell *et al.* (25). Data were transformed and analyzed in Mnova 6.2.1 using a DMSO reference signal at 39.5/2.5 ppm.

*UV ionization difference spectrophotometry analysis*

Lignin phenols were extracted from the dried lignin samples from microcosm 3 according to previously reported methods (26). Briefly, lignin was resuspended in 95% ethanol and filtered through a 0.2 µm filter to remove lignin particles. The ethanol filtrate was then used to prepare individual dilutions in neutral (pH 6 potassium phosphate) and basic (pH 13 NaOH) solutions. UV ionization difference spectra were collected by wavelength scans (200-400 nm) on a DU800 UV-vis spectrophotometer (Beckman Coulter, Inc., Brea, CA) blanking with the neutralized sample and reading the ionized basic sample. This method should result in characteristic peaks for various phenolic groups as described by Lin (26). Although not performed here, the percent change (loss or gain) of a given phenolic hydroxyl group can be calculated using the extinction coefficient for the assigned phenolic type (% phenolic OH = $\Delta D/\Delta\varepsilon$, where $\Delta D$ is the difference in peak absorbance between two time points and $\varepsilon$ is the extinction coefficient). Literature values are available for Type I phenolics with $\lambda$max of 300 nm ($\varepsilon$ = 4100 L $mol^{-1}$ $cm^{-1}$) and Type IV phenolics with $\lambda$max of 370 ($\varepsilon$ = 37250 L $mol^{-1}$ $cm^{-1}$).

## IV. Results

*Microcosm 1 pilot study presents evidence of lignin transformation by roseobacters*

Growth analysis of the four strains on the 3 different organosolv lignin preparations provided evidence that this material could support the growth of all roseobacters. For each strain a rapid increase in CFU/mL was observed between day 0 and day 6 with a

steady decline afterwards. A hierarchical trend was generally noted in the growth yield, with the highest CFU achieved on lignin #139, followed by #129, and #121. The exception to this was EE-36, which exhibited consistent growth across all substrates. Although evidence for growth was provided for all strains, the most confident data were from incubations with SE45 and lignin #139. Accordingly, only these microcosms were supplied for NMR analysis.

2D HMQC-NMR experiments display correlations between the coupling of two different nuclei (here $^{1}H$ and $^{13}C$) to provide an enhanced resolution of features from the chemically complex organosolv lignin. For these analyses, spectra of bacterially treated lignin were overlayed on the spectra of the appropriate abiotic lignin controls to identify differences in the spectra, specifically with respect to disappearances of characteristic lignin features which have previously determined (25). Comparison of spectra for the abiotic lignin control and SE45-treated lignin clearly exhibit the loss of several features in the aromatic (~95-150 ppm/5.9-8.0 ppm) and methoxy/side-chain (~50-105 ppm/2.6-5.7 ppm) regions of the spectrum (Figure 3.1). Of note is the complete loss of ferulate ester features (114 ppm/6.3 ppm and 111/7.35) in the aromatic region. This result is further substantiated by depressed signals for syringyl (S), guaiacyl (G), and *p*-hydroxyphenyl (H) esters (144 ppm/7.5 ppm). An additional loss was noted for a particular pool of S (106 ppm/7.28 ppm) and G (111 ppm/7.5 ppm) units containing side-chains oxidized at the alpha position. When considering the methoxy/side chain region of the spectrum, additional signal reduction is exhibited in the presence of SE45. Of most significance are signals related to β-O-4 linkages for Cβ/Hβ linkages to S (86 ppm/4.15 ppm) and G (84 ppm/4.3 pmm) units as well as the Cα/Hα signals for S and G units at 72 ppm/4.9 ppm. Peaks for common structures such as phenylcoumaran and pinoresinol also exhibit marked losses and are indicated in Figure 3.2.

*Microcosm 2 displays only minor changes in lignin after 5 weeks*

Analysis of viable counts for E-37 and SE45 again provide evidence for the utilization for organosolv lignin #139 as a sole carbon source (Figure 3.3). Both strains increased

in number by two orders of magnitude over the first 4 days. E-37 CFUs began to decline from day 7 to day 35, whereas SE45 numbers stayed around their peak of $1x10^8$ CFU/mL for the duration of the experiment with a slight suggestion of slow decline after day 28.

In contrast to microcosm 1, all samples from microcosm 2 were analyzed by 2D NMR. Again, results were analyzed by comparing the overlay of bacterially treated lignin with the corresponding abiotic lignin control. Surprisingly, no substantial spectral differences between controls and experimental samples were observed for any of the treatments at any time with the exception of one of the day 35 replicates treated with SE45 (Figure 3.4). For this single replicate, lignin modifications were minor, but mimicked the features losses observed in the methoxy-region from the pilot study. Here small decreases in the some of the β-O-4, phenylcoumaran, and pinoresinol structures were exhibited. No substantial changes were presented in the aromatic region.

*Microcosm 3 identifies abiotic changes to lignin phenolics*

Viable counts from this experiment provide a third line of evidence supporting the growth of *Citreicella* sp. SE45 on organosolv lignins. Similar to the previous microcosms, CFU values rapidly increased by two order of magnitude over the first two days and are maximally maintained at ~$1x10^8$ CFU/mL for the duration of the experiment (Figure 3.5). This experiment supplied different types of organosolv biomass as the sole carbon source. Lignin substrates for this study consisted of an organosolv extraction from 100% switchgrass (#90), 100% poplar (#108), and a 50/50 mixture of switchgrass and poplar (#157) (refer to Table 3.1). A graded use of the substrates by SE45 was indicated with most growth on switchgrass, intermediate growth on poplar, and the least growth on the mixed biomass.

UV difference spectrophotometry is a technique that has been used to assess phenolics in lignin since the 1950s and relies on the acidity of the phenolic OH and its ability to be ionized by a basic solution (26). Ionized phenolics exhibit a bathochromic (longer

wavelength) and hyperchromic (increased absorbance) shift in a UV spectrum. Multiple phenolic peaks (λmax) are often observed in lignin samples, representing different phenolic structures. Many of these groups have been analyzed with standards for establishment of proper extinction coefficients. Given that this experiment was a trial to assess the utility of the technique, only those phenolics for which extinction coefficients have been reported will be considered. These include Type I phenolics (λmax ~ 300 nm) which include phenolics with saturated side chains and Type IV phenolic (λmax ~ 360) including stilbenes. Bacterial utilization of lignin phenolics would be represented by a decrease in absorbance for any given phenolic peak over time. Preliminary results from these studies exhibit the intended bathochromic/hyperchromic shift for ethanol extracted lignin phenolics upon ionization (data not shown). While the ionization difference spectra do indicate a decrease in phenolic peaks between day 0 and day 5, there is also a concomitant decrease in absorbance of the abiotic controls. Figure 3.6 displays the results for the organosolv switchgrass treated with SE45 and abiotic control. The observations noted for the switchgrass samples are consistent across the poplar and 50/50 mixed biomass microcosms as well (data not shown).

## V. Discussion and perspectives

This chapter aimed to explore the ability of marine roseobacters to utilize a pretreated (organosolv) lignin that would reflect residual material from a biorefinery. While data present repeated evidence for the growth of several roseobacter strains, particularly *Citreicella* sp. SE45, on organosolv lignin preparations, the corresponding structural modifications to the lignin substrate lack confidence due to inconclusive experimental replication. The 4 month microcosm incubations provided encouraging 2D NMR spectra from the SE45 treatment demonstrating the loss of diagnostic structural signatures including ferulate esters, β-O-4 linkages, as well as phenylcoumaran and pinoresinol structures. Ferulate esters have been identified as the connection between ferulates in lignin and the hemicellulose (27), and are responsible for imparting much of the

recalcitrance to lignocellulosic biomass, particularly in grasses where ferulic acid content is generally high (28, 29). The removal of ferulate esters in lignin is typically mediated by feruloyl esterases (EC 3.1.1.73), which cleave the ester bond between ferulate and the polysaccharide (30). Assuming the results from the first microcosm are accurate, it may not be surprising to observe a reduction of ferulate esters as genome surveys indicate the presence of a putative feruloyl esterase in the genomes of both *Citreicella* sp. SE45 (accession WP_008882956) and *Sagittula stellata* E-37 (accession WP_005854618). The strongest protein homolog for SE45 is for *Pelagibaca bermudensis* (82% identity, with 95% coverage, expected value of 0), a roseobacter species isolated from the western Sargasso sea (31). The annotated feruloyl esterase from E-37 exhibits most homology to *Ponticoccus* sp. UMTAT08 (78% identity, 99% coverage, expected value of 0). Protein sequence alignment of the putative feruloyl esterases from SE45 and E-37 also suggests robust homology between the two proteins with 74% identity over 95% sequence coverage and an expected value of 0. Given these results, future work may benefit from a functional characterization of these two enzymes. Several assays have been described for the identification and activity of feruloyl esterases. Among these is a simple spectrophotometric approach that monitors the release of 4-nitrophenol from the 4-nitrophenyl ferulate substrate by absorbance at 410 nm (32).

When considering the potential loss of β-O-4 linkages in the lignin, it is not immediately apparent which bacterial determinants might be responsible for this activity as there is no convincing evidence for presence of diagnostic β-O-4 cleaving proteins in the SE45 or E-37 genomes. Neither demonstrates any level of homology to the classical lignin peroxidase from the white rot fungus *Phaenerochate chrysosporium* suggesting this traditional extracellular peroxidase approach is not implemented in these organisms. Sequence comparison to the β-etherase (which aids in the degradation of β-O-4 linkages) of the α-proteobacterium *Sphingobium* SYK-6 displays limited homology to a protein of related function in the E-37 genome (accession EBA07640) with an amino acid identity of 29% and an expected value of $8x10^{-6}$. There is also a weak homology to

a protein in the SE45 genome (accession EEX12634) displaying an identity of 29% and expected value of $1x10^{-5}$. Given these unsatisfying comparisons, it remains difficult to predict which proteins might be involved in β-O-4 cleavage. Furthermore, attempts to culture these two organisms on the β-O-4 lignin model guaiacylglycerol-β-guaicacyl ether have not been successful. This may suggest that the culturing environment of the microcosm was more conducive to the consumption of β-O-4 linkages than conditions using a single carbon source. While the described microcosms provide evidence for roseobacter utilization and transformation of organosolv lignin, additional strength for these findings could be offered through supplemental experiments. One study that could be particularly enlightening would involve repeating the initial 4 month microcosm with SE45 and organosolv lignin #139 (50/50 switchgrass:poplar) but also include organosolv lignins of 100% switchgrass and 100% *Spartina alterniflora.* Since *S. alterniflora* is the native grass inhabiting the coastal systems from which SE45 and E-37 were isolated, this material would serve as a more natural substrate for these organisms and provide more environmentally relevant results. It might also be informative to include the roseobacter strain *Ruegeria pomeroyi* DSS-3, which was also isolated from the Georgia coast (33) and has gained acknowledgement for its prolific utilization of plant-derived aromatic compounds (18, 19).

Attempts to identify changes to lignin phenols facilitated by bacterial degradation provided inconclusive results. While the method of ionization difference spectrophotometry was validated for the given organosolv lignin source (the expected bathochromic/hyperchromic shift was noted), an abiotic change of lignin phenols was observed which masked an ability to differentiate abiotic transformations from those invoked by the added bacterial populations. In effort to discern between these abiotic and biotic changes, a more controlled account of starting and end material amounts is suggested, as losses may accrue as an artifact of the method and should be tracked. If this were to be a viable method for temporal analysis of lignin, increased sensitivity is required to differentiate between abiotic changes, sample losses, and the interrogated biotic changes. Freeze drying of samples has been briefly evaluated as a method to

preserve sample amounts (data not shown), however care must be taken in exact measurements of the medium salts that should be subtracted to measure final lignin mass. Washing of the lignin in water to remove salts would be ideal, however, this will also remove some of the phenols that are to be examined. While this method has proven successful for single time point analyses (24), it is clearly more complicated when adding variables associated with bacterial culturing over time.

Collectively these results provide hope for continued studies to strengthen our confidence in the transformation of biorefinery lignin by marine roseobacters. Although the replication power necessary to definitely support these transformations is currently lacking, there is strong evidence of growth on these substrates and limited evidence of structural changes as indicated by 2D NMR. Future studies may consider optimizing the UV ionization difference approach per previous suggestions to analyze lignin phenolics. In some cases, however, a more comprehensive examination of the biomass is preferable. In these instances 2D HMQC NMR is a viable option that can also be supplemented by the advancing technologies of mass spectrometry that have recently reported a method for analysis of organosolv lignin (34). Findings herein present various options for lignin analysis and encourage future efforts toward a more detailed understanding of the potential genetic determinants involved in lignin transformations.

## VI. Acknowledgements

I would like to thank and acknowledge my collaborators at the Center for Renewable Carbon (CRC) at the University of Tennessee for their contributions to this project. Specifically I would like to thank Dr. Joseph Bozell for running and analyzing the 2D NMR data that are presented in this document, as well as his technicians, Kun Cheng and Omid Hosseinaei, who also ran many NMR samples from the described microcosm experiments. Lastly, I would like to thank Anton Astner from the CRC for generating and providing the organosolv lignin preparations used in these studies.

# VII. References


1. **Ragauskas AJ, Beckham GT, Biddy MJ, Chandra R, Chen F, Davis MF, Davison BH, Dixon RA, Gilna P, Keller M, Langan P, Naskar AK, Saddler JN, Tschaplinski TJ, Tuskan GA, Wyman CE.** 2014. Lignin valorization: improving lignin processing in the biorefinery. Science **344:**1246843.
2. **Pauly M, Keegstra K.** 2008. Cell-wall carbohydrates and their modification as a resource for biofuels. Plant J **54:**559-568.
3. **Parsell T, Yohe S, Degenstein J, Jarrell T, Klein I, Gencer E, Hewetson B, Hurt M, Kim JI, Choudhari H, Saha B, Meilan R, Mosier N, Ribeiro F, Delgass WN, Chapple C, Kenttamaa HI, Agrawal R, Abu-Omar MM.** 2015. A synergistic biorefinery based on catalytic conversion of lignin prior to cellulose starting from lignocellulosic biomass. Green Chemistry **17:**1492-1499.
4. **Ralph J, Lundquist K, Brunow G, Lu F, Kim H, Schatz PF, Marita JM, Hatfield RD, Ralph SA, Christensen JH, Boerjan W.** 2004. Lignins: Natural polymers from oxidative coupling of 4-hydroxyphenyl- propanoids. Phytochem Rev **3:**29-60.
5. **McCarthy JL, Islam A.** 1999. Lignin chemistry, technology, and utilization: A brief history, p 2-99, Lignin: Historical, Biological, and Materials Perspectives, vol 742. American Chemical Society.
6. **Atalla RH, Agarwal UP.** 1986. Recording Raman spectra from plant cell walls. J Raman Spectrosc **17:**229-231.
7. **Galbe M, Zacchi G.** 2007. Pretreatment of lignocellulosic materials for efficient bioethanol production. Adv Biochem Eng Biotechnol **108:**41-65.
8. **Chaturvedi V, Verma P.** 2013. An overview of key pretreatment processes employed for bioconversion of lignocellulosic biomass into biofuels and value added products. 3 Biotech **3:**415-431.

9. **Astner AF.** 2012. Lignin yield maximization of lignocellulosic biomass by Taguchi robust product design using organosolv fractionation. Master's thesis. University of Tennessee.
10. **Bozell JJ, Black SK, Myers M, Cahill D, Miller WP, Park S.** 2011. Solvent fractionation of renewable woody feedstocks: Organosolv generation of biorefinery process streams for the production of biobased chemicals. Biomass Bioenerg **35:**4197-4208.
11. **Bugg TD, Ahmad M, Hardiman EM, Rahmanpour R.** 2011. Pathways for degradation of lignin in bacteria and fungi. Nat Prod Rep **28:**1883-1896.
12. **Brown ME, Chang MCY.** 2014. Exploring bacterial lignin degradation. Curr Opin Chem Biol **19:**1-7.
13. **Fuchs G, Boll M, Heider J.** 2011. Microbial degradation of aromatic compounds - from one strategy to four. Nat Rev Microbiol **9:**803-816.
14. **Moran MA, Hodson RE.** 1994. Dissolved humic substances of vascular plant origin in a coastal marine environment. Limnol Oceanogr **39:**762-771.
15. **Moran MA, Hodson RE.** 1989. Formation and bacterial utilization of dissolved organic carbon derived from detrital lignocellulose. Limnol Oceanogr **34:**1034-1047.
16. **Gonzalez JM, Whitman WB, Hodson RE, Moran MA.** 1996. Identifying numerically abundant culturable bacteria from complex communities: an example from a lignin enrichment culture. Appl Environ Microbiol **62:**4433-4440.
17. **Buchan A, Gonzalez JM, Moran MA.** 2005. Overview of the marine roseobacter lineage. Appl Environ Microbiol **71:**5665-5677.
18. **Newton RJ, Griffin LE, Bowles KM, Meile C, Gifford S, Givens CE, Howard EC, King E, Oakley CA, Reisch CR, Rinta-Kanto JM, Sharma S, Sun S, Varaljay V, Vila-Costa M, Westrich JR, Moran MA.** 2010. Genome characteristics of a generalist marine bacterial lineage. ISME J **4:**784-798.
19. **Yan D, Kang J, Liu D-Q.** 2009. Genomic analysis of the aromatic catabolic pathways from *Silicibacter pomeroyi* DSS-3. Ann Microbiol **59:**789-800.

20. **Gulvik CA, Buchan A.** 2013. Simultaneous catabolism of plant-derived aromatic compounds results in enhanced growth for members of the Roseobacter lineage. Appl Environ Microbiol **79:**3716-3723.
21. **Gonzalez JM, Mayer F, Moran MA, Hodson RE, Whitman WB.** 1997. *Sagittula stellata* gen. nov., sp. nov., a lignin-transforming bacterium from a coastal environment. Int J Syst Bacteriol **47:**773-780.
22. **Buchan A, Collier LS, Neidle EL, Moran MA.** 2000. Key aromatic-ring-cleaving enzyme, protocatechuate 3,4-dioxygenase, in the ecologically important marine Roseobacter lineage. Appl Environ Microbiol **66:**4662-4672.
23. **Buchan A, Neidle EL, Moran MA.** 2001. Diversity of the ring-cleaving dioxygenase gene pcaH in a salt marsh bacterial community. Appl Environ Microbiol **67:**5801-5809.
24. **Zhang Y, Yang D-Q, Wang X-M, Feng M, He G.** 2014. Fungus-modified lignin and its use in wood adhesive for manufacturing wood composites. Forest Prod J **65:**43-47.
25. **Bozell JJ, O'Lenick CJ, Warwick S.** 2011. Biomass fractionation for the biorefinery: heteronuclear multiple quantum coherence-nuclear magnetic resonance investigation of lignin isolated from solvent fractionation of switchgrass. J Agric Food Chem **59:**9232-9242.
26. **Lin SY.** 1992. Ultraviolet Spectrophotometry, p 217-232. *In* Lin SY, Dence CW (ed), Methods in Lignin Chemistry. Springer, Berlin, Heidelberg.
27. **Carpita NC.** 1996. Structure and biogenesis of the cell walls of grasses. Annu Rev Plant Physiol Plant Mol Biol **47:**445-476.
28. **de Oliveira DM, Finger-Teixeira A, Rodrigues Mota T, Salvador VH, Moreira-Vilar FC, Correa Molinari HB, Craig Mitchell RA, Marchiosi R, Ferrarese-Filho O, Dantas Dos Santos W.** 2015. Ferulic acid: a key component in grass lignocellulose recalcitrance to hydrolysis. Plant Biotechnol J **13:**1224-1232.
29. **de OBMM.** 2009. Feruloylation in grasses: current and future perspectives. Mol Plant **2:**861-872.

30. **Mathew S, Abraham TE.** 2004. Ferulic acid: an antioxidant found naturally in plant cell walls and feruloyl esterases involved in its release and their applications. Crit Rev Biotechnol **24:**59-83.
31. **Cho JC, Giovannoni SJ.** 2006. *Pelagibaca bermudensis* gen. nov., sp. nov., a novel marine bacterium within the Roseobacter clade in the order *Rhodobacterales*. Int J Syst Evol Microbiol **56:**855-859.
32. **Mastihuba Vr, Kremnický Lr, Mastihubová M, Willett JL, Côté GL.** 2002. A spectrophotometric assay for feruloyl esterases. Anal Biochem **309:**96-101.
33. **González JM, Covert JS, Whitman WB, Henriksen JR, Mayer F, Scharf B, Schmitt R, Buchan A, Fuhrman JA, Kiene RP, Moran MA.** 2003. *Silicibacter pomeroyi* sp. nov. and *Roseovarius nubinhibens* sp. nov., dimethylsulfoniopropionate-demethylating bacteria from marine environments. Int J Syst Evol Microbiol **53:**1261-1269.
34. **Jarrell TM, Marcum CL, Sheng H, Owen BC, O'Lenick CJ, Maraun H, Bozell JJ, Kenttamaa HI.** 2014. Characterization of organosolv switchgrass lignin by using high performance liquid chromatography/high resolution tandem mass spectrometry using hydroxide-doped negative-ion mode electrospray ionization. Green Chemistry **16:**2713-2727.

# VIII. Appendix: Tables

**Table 3.1**. Reaction conditions for the preparation of organosolv lignins

| Lignin ID | Feedstock (SG/P)* | Temperature (C) | [Acid] (M) | Time (min) | Microcosm 1 | Microcosm 2 | Microcosm 3 |
|---|---|---|---|---|---|---|---|
| 129 | 50/50 | 120 | 0.05 | 56 | x | | |
| 131 | 50/50 | 140 | 0.025 | 56 | x | | |
| 139 | 50/50 | 160 | 0.025 | 90 | x | x | |
| 90 | 100/0 | 160 | 0.025 | 56 | | | x |
| 108 | 0/100 | 160 | 0.050 | 56 | | | x |
| 157 | 50/50 | 160 | 0.050 | 90 | | | x |

*SG = switchgrass, P = poplar

# IX. Appendix: Figures

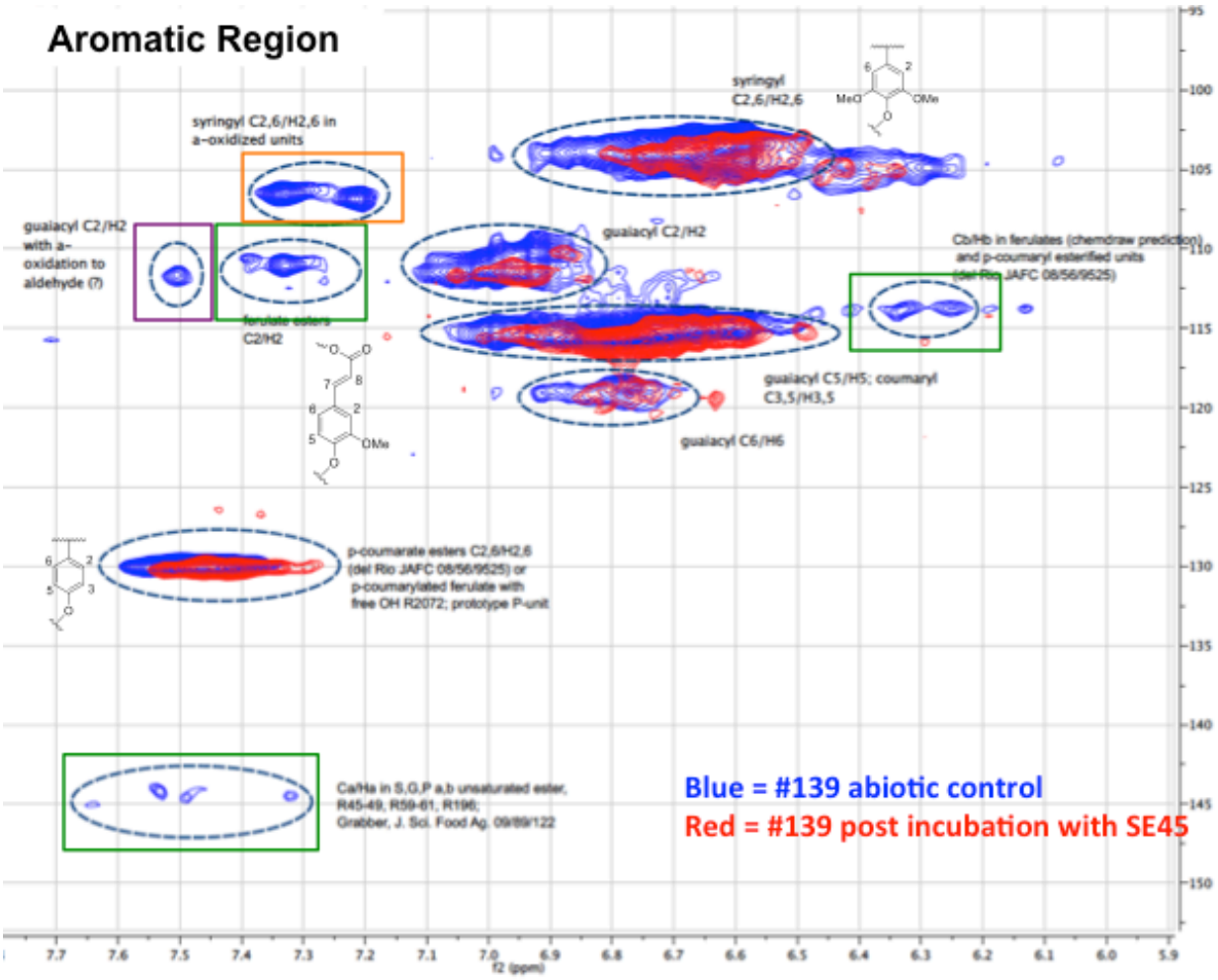


**Figure 3.1**. Aromatic region of the 2D NMR spectrum from microcosm 1. Signals for ferulate esters are outlined in green, guaiacyl units with oxidized alpha side chains are outline in purple, syringyl units with alpha oxidized side chains are outline in orange. Spectra were generated and provided by Dr. Joseph Bozell at the University of Tennessee.

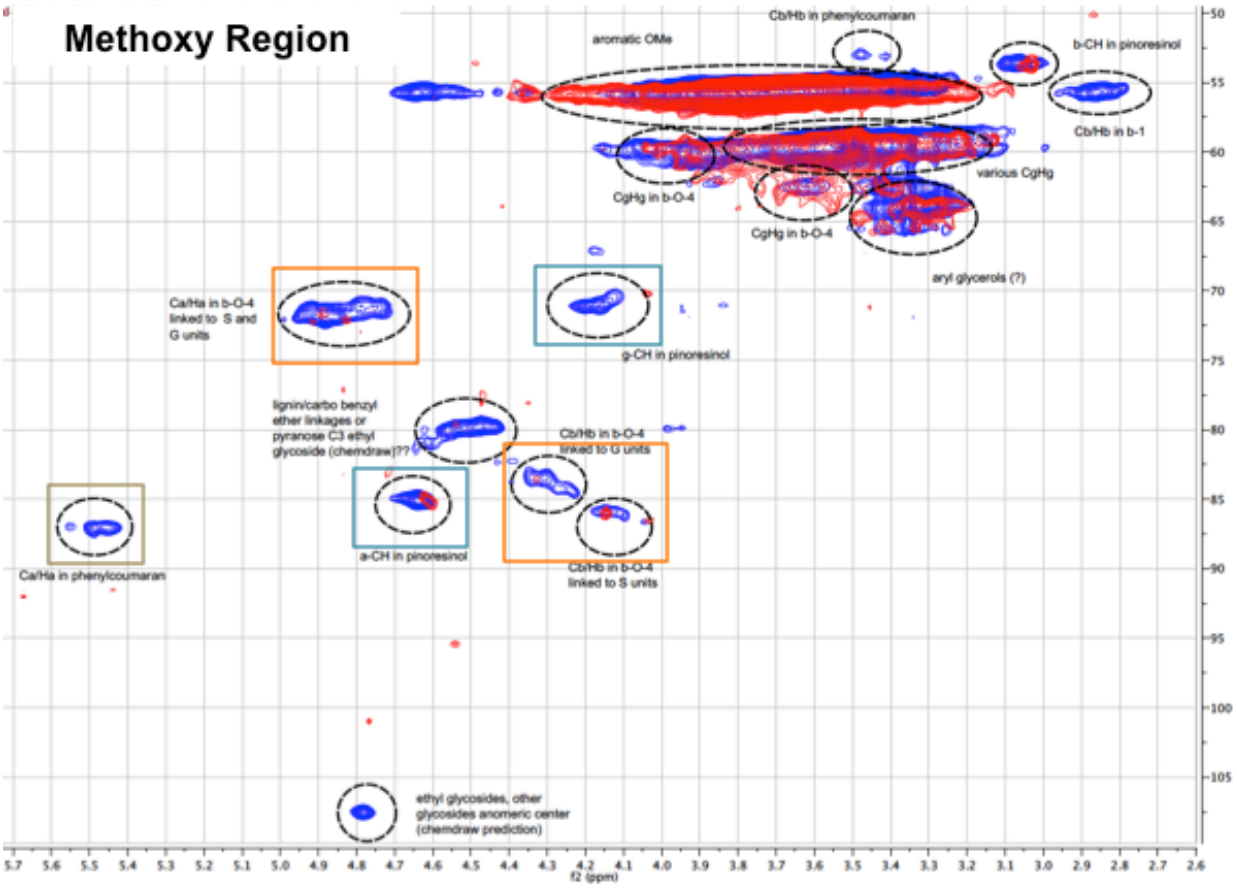


**Figure 3.2**. Methoxy region of the 2D NMR spectrum from microcosm 1. Signals for β-O-4 linkages are outlined in orange, phenylcoumaran features are in tan, and pinoresinol features are outline in blue. Spectra were generated and provided by Dr. Joseph Bozell at the University of Tennessee.

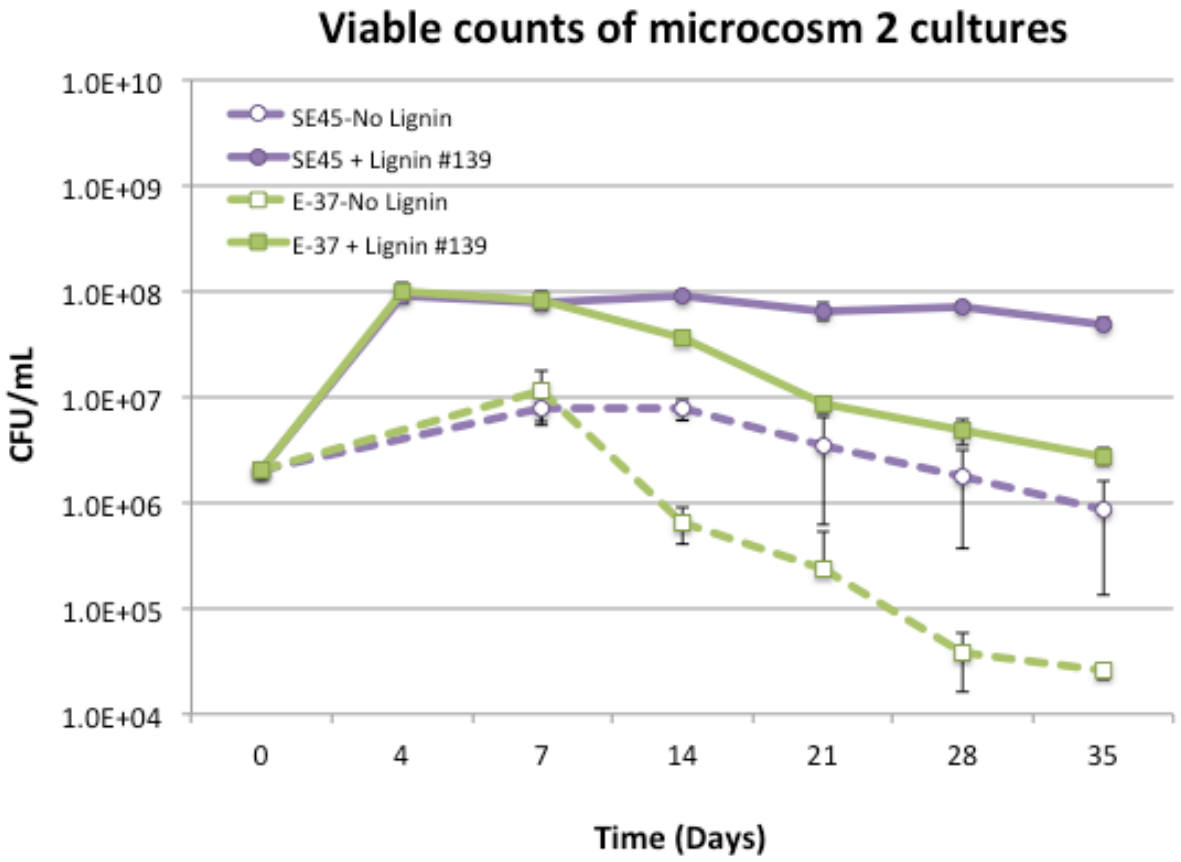


**Figure 3.3**. Viable counts from microcosm 2. SE45 growth is depicted in purple, E-37 growth is depicted in green. Dashed lines represent carryover growth into no carbon controls.

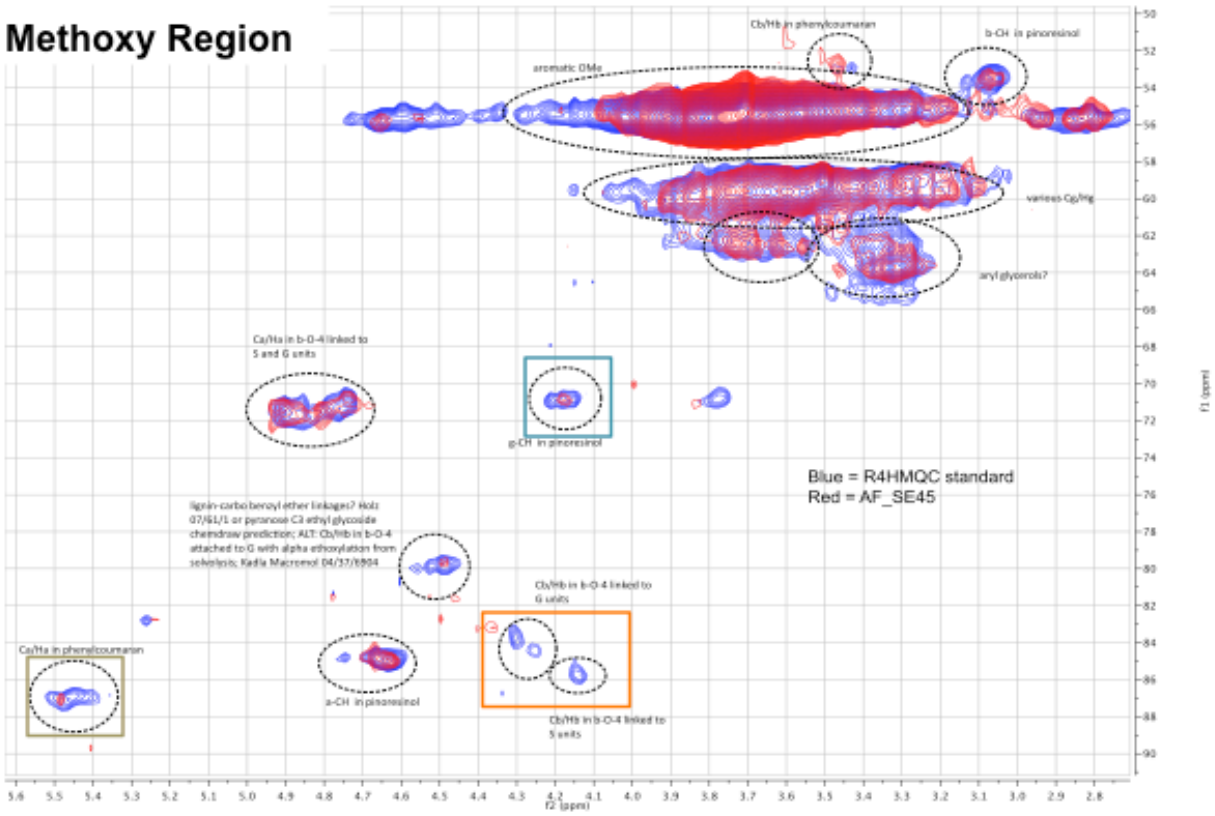


**Figure 3.4**. Methoxy region of the 2D NMR spectrum from microcosm 2. Signals for β-O-4 linkages are outlined in orange, phenylcoumaran features are in olive, and pinoresinol features are outline in blue. Spectra were generated and provided by Dr. Joseph Bozell at the University of Tennessee.

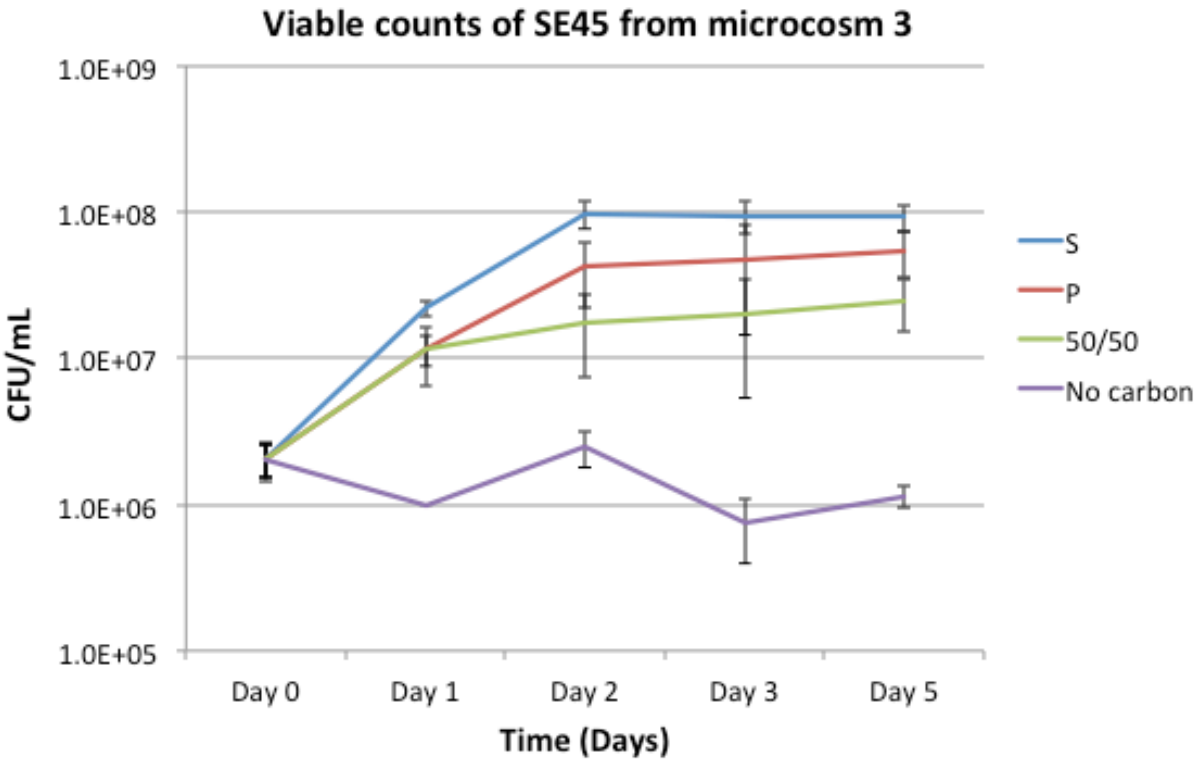


**Figure 3.5**. Viable counts from microcosm 3 with SE45. **S**; 100% switchgrass organosolv lignin #90, **P**; 100% poplar organosolv lignin #108, **50/50**; 50/50 switchgrass:poplar organosolv lignin #157 (see Table 3.1).

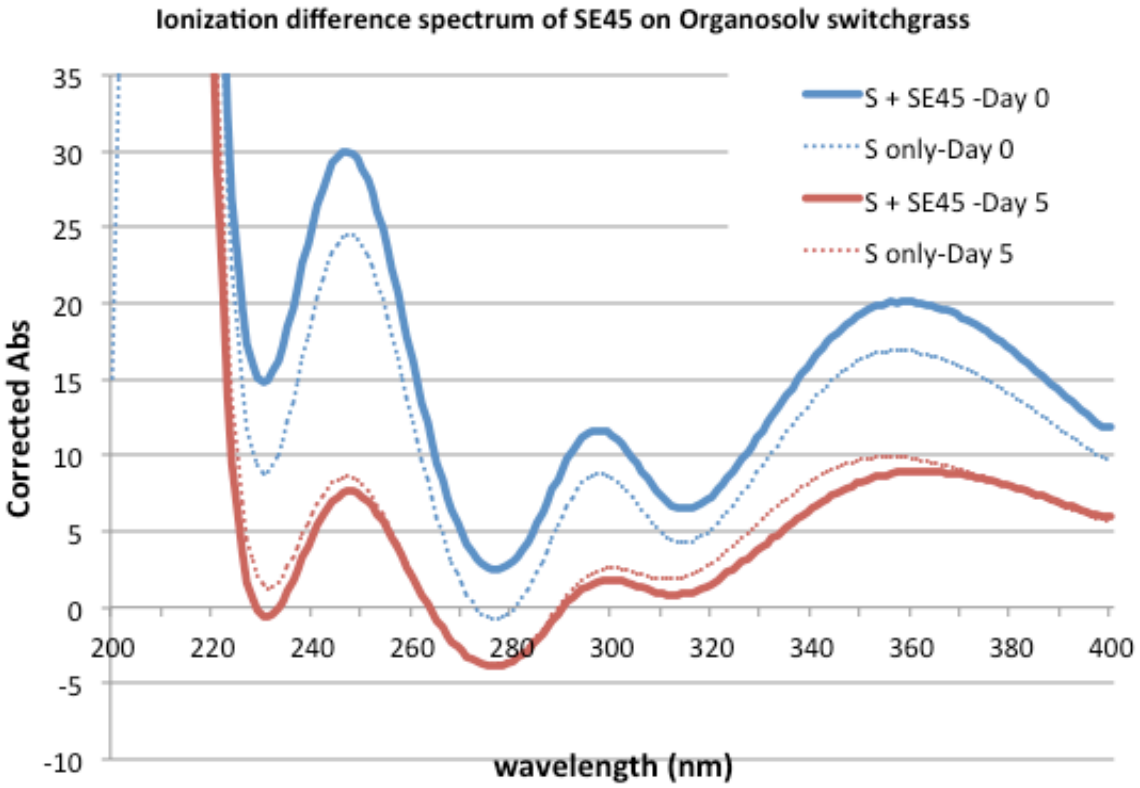


**Figure 3.6**. UV ionization difference spectrum from day 0 and 5 of microcosm 3. Blue lines represent the phenolic spectrum from day 0, red lines represent the phenolic spectrum from day 5. Solid lines represent samples treated with SE45 while dashed lines represent abiotic controls. **S**; 100% switchgrass (organosolv).

# CHAPTER FOUR - APPLICATION OF BACTERIAL RING HYDROXYLATING DIOXYGENASES FOR THE PRODUCTION OF *CIS*-DIHYDRODIOLS FROM LIGNIN MODEL COMPOUNDS

# I. Abstract

Bacterial ring-hydroxylating dioxygenases (RHDs) are multicomponent enzyme systems responsible for activating aromatic compounds through the addition of two vicinal hydroxyl groups, resulting in a dearomatized *cis*-dihydrodiol. This activated intermediate is a very attractive chemical species, demonstrating enhanced functionality for chemical catalysis to a variety of valuable chemicals including BTEX, flavor compounds, and precursors to pharmaceutical products. Due to this potential, RHDs have been targeted for biotechnological applications through heterologous expression for the increased production of *cis*-dihydrodiol intermediates. Most of the described RHD systems have been highlighted for their ability to transform aromatic pollutants and are valued for their indiscriminate substrate specificity. Thus, most of the information derived from these systems has been from bioremediation studies aiming to detoxify contaminants from the environment. While this has provided a strong foundation on the mechanisms employed by these enzymes, there is a very limited knowledge regarding their ability to dihydroxylate lignin-derived compounds that share structural similarity to the native RHD substrates. Here we investigate the ability of RHDs to transform a set of lignin model compounds with the intention of identifying *cis*-dihydrodiols for downstream chemical catalysis. Recombinant *E. coli* strains expressing four different RHDs were used in biotransformation studies with a library of 12 lignin model compounds. A UV-based screen suggested product formation from 3 of these strains with at least 3 (but up to 7) of the model compounds, with a *cis*-dihydrodiol confirmed via NMR for 2 of these compounds. Although many obstacles were encountered in the analysis of these data, it is encouraging to suggest that the substrate range of these enzymes could be expanded to include lignin-derived compounds. An enhanced understanding of potential RHD conversions of lignin compound could be provided through *in silico* docking of substrates to the known protein structures. This information could guide decisions for potential mutations in the proteins to tailor the enzymes to accept the desired substrates and generate a *cis*-dihydrodiol.

## II. Introduction

Research on the bacterial degradation of aromatic compounds has a rich history in soil systems, particularly with respect to the detoxification of anthropogenic contaminants (1, 2). The information collected from these studies has fortified a knowledge base on the diverse reactions involved in the transformation of aromatic compounds. It is now understood that bacteria degrade aromatics by a process known as catabolic funneling whereby a suite of substrates are converted into a few key intermediates prior to ring cleavage (Figure 4.1). This funneling is separated into two parts, the upper/peripheral pathways that prepare the ring for fission, and the lower/central pathway after ring cleavage where catabolites are directed toward central metabolism. Due to the diverse array of compounds entering the catabolic funnel, the transformations for ring-preparation can be numerous and involve a set of versatile enzymes (2, 3). Consequently, the reactions involved in the diverse peripheral pathways are less well understood than those of the lower pathway where only a few intermediates require conversion.

Despite this inverse bottleneck, there exists a basic understanding of ring-activating reactions in the peripheral pathways that can be separated into three categories, each of which is thought to reflect the oxygen availability in the organism's environment (2) (refer to Diaz *et al*. 2013). The first type of ring-activation is the classical aerobic hydroxylation of the aromatic ring mediated by a ring-hydroxylating oxygenase (1.14.13.- and EC 1.14.12.-). The hydroxylated intermediate is later cleaved by a ring-*cleaving* oxygenase (EC 1.13.11.-); thus both the ring-activation and ring-cleavage are performed by different classes of oxygenases under oxic conditions. While this is a widespread approach for aerobic organisms, the seminal example is derived from work on toluene degradation in *Pseudomonas putida* F1 (4). The second category of ring-activation is the traditional anaerobic method initiated by converting the aromatic carboxylic acid to a CoA thioester through the activity of an acyl-CoA ligase (EC 6.2.1.-

.). This reductive approach promotes further electron transfer via a CoA-reductase (EC 1.3.7.-) followed by β-oxidative-like reactions toward central metabolism. The archetypical example of this approach is derived from studies on benzoate degradation in *Rhodopseudomonas palustris* (5) and *Thauera aromatica* (6). The final and most recently recognized category is a hybrid pathway that is thought to exist in aerobic organisms exposed to sub-optimal oxygen levels, as it presents strategies from both aerobic and anaerobic organisms (7). Here the aromatic acid is converted to a CoA thioester using the same oxygen-*in*dependent CoA ligase used in anaerobic catabolism. The CoA compound is then converted to an epoxide intermediate through an oxygen-*de*pendent reaction mediated by a CoA epoxidase (EC 1.14.13.cu). In most instances, the aromatic compound is subsequently cleaved through hydrolysis (consistent with anaerobic methods) and not oxygenolysis. This route to aromatic catabolism has been demonstrated for benzoic acid in *Azoarcus evansii* (8) and for phenylacetic acid in *E. coli* K12 and *Pseudomonas* Y2 (9).

While the emerging information on novel reactions for aromatic catabolism are drawing deserved attention, studies have historically favored work on aerobic transformations due to interest in isolating the chemically desirable *cis*-dihydrodiol intermediate generated by ring-hydroxylating dioxygenases (RHDs) of the aforementioned peripheral pathways. This biological compound is chemically attractive due to its ability to be converted into a variety of industrial products and has practical advantages over a chemically-synthesized product that is very difficult to isolate without further reactivity resulting in product loss (10). Among the many compounds that can be synthesized from *cis*-dihydrodiols are natural products, fine chemicals, and pharmaceuticals (11, 12). Perhaps the most obvious product derived from *cis*-dihydrodiols is indigo, as this compound is visible in RHD-expressing bacterial cultures upon standard growth in tryptophan-containing media. Here, the bacterium converts tryptophan (via tryptophanase) to indole, which serves as a natural substrate for RHD-mediated dihydroxylation to indoxyl, which spontaneously loses water to form indigo (13). Another successful example of RHD applications in synthetic chemistry is the production of

flavor compounds. The preparation of strawberry furanone flavoring has been documented from modifications of the *p*-xylene *cis*-dihydrodiol after biocatalysis with a toluene/tetrachlorobenzene dioxygenase (14). *Cis*-dihydrodiols can also be chemically upgraded to medically-relevant compounds, such as indinivir, an HIV-1 protease inhibitor, however further work is required to prevent undesired by-products of this oxidation (15).

Given the tremendous value of the *cis*-dihydrodiol intermediate, it is not surprising that researchers have dedicated much effort to understanding the mechanism of these enzymes in hopes of manipulating the reactions for increased product formation. RHDs belong to a family of enzymes known as Rieske non-heme iron oxygenases (16). These are multicomponent, co-factor-requiring, oxygen-dependent systems comprised of a reductase, a ferredoxin (sometimes), and a trimeric ($\alpha_3$) or hexameric ($\alpha_3\beta_3$) oxygenase. The alpha subunit of the oxygenase enzyme contains a characteristic Rieske [2Fe-2S] cluster that is coordinated to the protein by 2 cysteine and 2 histidine residues. In these systems, 2 electrons (H-) are transferred from an NAD(P)H cofactor and shuttled across the reducing enzyme(s) to the oxygenase, allowing for the addition of dioxygen onto an aromatic substrate producing the reactive dihydrodiol intermediate (Figure 4.2) (17). While RHDs are present in both bacteria and fungi, only bacterial species generate the reactive *cis*-dihydrodiol, whereas the fungi produce a less chemically reactive (and less biotechnologically desirable) *trans*-dihydrodiol (18). Consequently, most attention has been devoted to studying bacterial ring-hydroxylating dioxygenases.

Much of what is known about bacterial RHDs comes from a relatively small pool of well-characterized enzyme systems. Among these RHDs are the toluene dioxygenase (TDO) from *Pseudomonas putida* F1 (4, 19), the naphthalene dioxygenase (NDO) from *Pseudomonas* sp. NCIB 9816-4 (20, 21), and the biphenyl dioxygenase (BPDO) from

*Burkholderia* (*Pseudomonas*) sp. LB400 (22-25), whose names reflect the substrate from which the enzyme was first documented to produce an oxidized product. Thus, despite the specificity implied by their names, RHDs are notorious for their broad substrate range, making them even more attractive biocatalysts for the production of a diverse collection of active *cis*-dihydrodiols (20). For instance, the *Pseudomonas*-derived naphthalene dioxygenase has been found to convert over 60 different aromatic substrates when purified or expressed in a heterologous host (20), although it is important to note that not all products are *cis*-dihydrodiols. In addition to performing dihydroxylations, these enzymes can also often assist in monooxygenations, desaturations, sulfoxidations, dealkylations, and other transformations (21, 25). With this knowledge it is important to understand the substrate and product range of the enzymes applied for *cis*-dihydrodiol biotransformations.

In effort to upscale and isolate the production of *cis*-dihydrodiols from bacteria, many RHDs have been cloned into heterologous hosts (usually *E. coli* or *Pseudomonas* sp.) for overexpression of the enzyme that can then be used to transform the desired substrate. Application of a recombinant system for these biotransformations is advantageous, and arguably essential, for many reasons. First, because the native host catabolizes the aromatic compound for central metabolism, the *cis*-dihydrodiol does not accumulate in the cell, and in instead is quickly rearomatized by a dehydrogenase encoded in the corresponding operon. Thus, it is necessary to extract only the desired genes of the enzymes system (reductase, ferredoxin, and dioxygenase components) for expression in a non-native host lacking the RHD dehydrogenase. Secondly, the use of well-established bacterial expression systems allows for the overproduction of these enzymes, increasing the biocatalysis potential for *cis*-dihydrodiol. Lastly, this approach implants the necessary RHD genes into a plasmid with an inducible promoter (usually *lac*) for controlled expression of the protein, offering convenience and further ability to optimize reaction conditions, as the timing of protein expression is known.

Due to the large interest employing RHDs for the decontamination of aromatic environmental pollutants, a wealth of information is available on the ability of these enzymes to dihydroxylate substrates like toluene (4), naphthalene (20), polycyclic aromatic hydrocarbons (26, 27), chlorinated compounds (28) etc. What is lacking from the literature, however, is an assessment of RHD-mediated conversions of abundant and naturally occurring lignin compounds that exhibit structures similar to those of aromatic contaminants. Here we examine the activity of well-characterized RHDs with a set of lignin model compounds to determine [1] if the selected enzymes accept non-cognate lignin compounds as substrates; [2] which enzymes demonstrate the broadest substrate range across tested lignin models; and [3] if the enzymes produce *cis*-dihydrodiols from our substrates. To address the above questions, small-scale biotransformations were performed with four different recombinant RHD systems and 12 different lignin substrates. Crude product conversion was screened through a UV-based assay to provide preliminary information regarding the ability of the enzyme to convert a given substrate. For select positive reactions, the enzyme-substrate combination was scaled (by collaborators) for product isolation, purification, and identification via NMR (James Daleiden, unpublished data). Results suggest the ability of 3 of the 4 tested RHDs to convert at least 3 lignin model compounds, with a *cis*-dihydrodiol confirmed for 3 of these reactions. Insight into the ability of RHDs to transform lignin models has potential implications for the biorefinery as residual lignin could be valorized through conversion to *cis*-dihydrodiols for subsequent chemical reduction to high value

## III. Materials and methods

*Strains and growth maintenance*

Strains used for this study are listed in Table 4.1. The toluene dioxygenase strain, *E. coli* JM109 pDTG601 (4), was gifted by Dr. Tomas Hudlicky (Brock University, Canada). The naphthalene dioxygenase strain, *E. coli* JM109 (DE3) pDTG141 (20, 21), was gifted by Dr. Rebecca Parales (University of California Davis). Both biphenyl dioxygenase

strains (*E.coli* BL21 (DE3) pLysS pAIA111 (24) and *P. putida* KT2442 pDM10 (29)) were gifted by Dr. Bernd Hofer (Hemholtz Center for Infection Research). All strains were maintained in Luria Bertani (LB) medium supplemented with the appropriate antibiotic to maintain selection of the recombinant plasmid (pDTG601 and pDTG141, 200 µg/mL ampicillin; pAIA111, 200 µg/mL ampicillin and 50 µg/mL ampicillin (for pLysS), pDM10 50 µg/mL chloramphenicol). Control strains lacking the recombinant plasmid were cultured in parallel when necessary with the caveat that *Pseudomonas putida* F1 was used as the control strain for *Pseudomonas putida* KT2442 due to inability to acquire the appropriate strain. Biotransformations were performed in either LB or Minimal Salts Broth medium (MSB) containing 4.5 g/L $K_2HPO_4$, 3.4 g/L $KH_2PO_4$, 2 g/L $(NH_4)2SO_4$, 0.16 g/L $MgCl_2*6H_2O$, 1x minerals, 1x trace metals (30) supplemented with 10 mM glucose and 0.1 mM thiamine. *E. coli* strains were generally maintained at 30-37°C at 200 rpm and *P. putida* strains at 30°C, 200 rpm. Biotransformations were performed at 25°C with shaking (200 rpm) and induced with 1 mM isopropyl β-D-1-thiogalactopyranoside (IPTG).

*RHD enzyme assay via indigo formation*

In effort to establish a baseline understanding of the relative efficacy of our RHD systems, a variety of enzyme assays were attempted (indoxyl (31) NADH, indigo (13)), of which only the indigo demonstrated success. Methods for the indigo assay were followed as described by Ensley *et al*. (13) and were only performed on the TDO and NDO strains. Briefly, 2 mL of an 18-hour culture was used to inoculate 200 mL of LB/ampicillin. These cultures were incubated at 37°C, 200 rpm and induced with 1mM IPTG at an $OD_{600}$ of 0.4-0.8. Induction was terminated after 4 hours. Samples for OD measurements (500 µl) were taken every hour pre- and post-induction to monitor cell growth. Samples for indigo extraction (2 mL) were taken in triplicate every 30 minutes post-induction (with one sample just prior to IPTG addition). These samples were spun down and supernatant removed prior to storing the cell pellet at -20°C for indigo extraction. Indigo was extracted from thawed pellets through two rounds of resuspension in 200 µl dimethylsulfoxide (DMSO), centrifugation, and collection of the

supernatant. Indigo extractions were pooled for each biological replicate and measured through spectrophotometric absorbance at 620 nm (DU 800 UV-vis spectrophotometer Beckman Coulter, Inc., Brea, CA). Indigo concentrations were determined using the extinction coefficient for indigo at 620 nm ($\varepsilon = 2{,}260 M^{-1}cm^{-1}$) and the measured absorbance of the sample ($c = A/\varepsilon$).

*Biotransformations of lignin model compounds*

Biotransformations were performed under a variety of conditions in effort to optimize the reaction conditions for each enzyme and/or substrate. Generally, overnight cultures of the RHD strains were used to inoculate a 9 mL LB pre-culture which was incubated at 37°C (for *E. coli* strains) or 30°C (for the *P. putida* strain) at 200 rpm until an $OD_{600}$ of 0.4-0.8, at which time cultures were sub-cultured to 25 mm screw cap tubes containing 7 mL LB or MSB and appropriate antibiotic. These tubes were incubated under the same conditions as above until an $OD_{600}$ 0.4-0.6 was observed, at which time the temperature was incrementally dropped every 15 minutes until a final temperature of 25°C was achieved. The cultures were incubated another 30 minutes at 25°C before induction with 1 mM IPTG. Substrate was added after 12-16 hours of protein induction to initiate the biotransformation which proceeded at 25°C, 200 rpm. Table 4.2 displays the substrates, solvents, and typical final concentrations used in these assays. Concentrations were determined based on preliminary studies assessing substrate toxicity (data not shown). Samples (300-500 µl) were taken periodically throughout the biotransformation to screen for product formation via a UV assay (described below).

*UV analysis of biotransformation products*

Products from the biotransformation were monitored with a general UV assay to screen for the change in absorbance between the starting material and the incubated product. Throughout the biotransformation, samples were collected and cells removed via centrifugation. An absorbance spectrum in the UV range (200-400 nm) was collected using the respective control culture (host organism with no RHD plasmid without substrate) supernatant as a blank. Differences in spectra between the control and RHD

strain supernatants were considered positive for substrate transformation. Spectra of the substrate alone in the appropriate growth medium were also collected for comparison of starting material and products.

## IV. Results

*Indigo assay detects RHD activity*

In the interest of validating the activity of our RHDs and determining an approximation their conversion rates, an assay was used that monitors a well-recognized reaction of RHDs in which indigo is formed as a final product. In this reaction, the RHD converts indole (a natural metabolite of tryptophan) in the medium to a transient indoxyl intermediate that is quickly dehydrated to form insoluble indigo (Figure 4.4). While it would be beneficial and convenient to detect the soluble indoxyl intermediate (31), for which there is also a described assay, efforts toward that end were never fruitful. The extraction of indigo, however, did provide results demonstrating the efficacy of indole conversion (Figure 4.5). Here, temporal samples were collected to monitor cell growth and indigo formation after induction with IPTG. Results demonstrate that for the two assayed strains (TDO and NDO), the RHDs generated increasing levels of indigo over time that correlated with cell growth. Growth was consistent across strains and indigo formation rates were similar for both the TDO (113 uM/hr) and NDO (116 uM/hr) strains.

*Biotransformations reveal new lignin substrates for classic RHD systems*

Biotransformations were conducted to assess the ability of a subset of well-known RHD systems (TDO, NDO, and 2 BPDO strains) (see Table 4.1) to convert a library of lignin model compounds (see Table 4.2), with which these enzymes have never been tested. Substrates were supplied to pre-induced cultures of the recombinant strains, with samples collected temporally for UV analysis. Due to the characteristic absorbance of aromatic compounds between 200-400 nm (32), detection of biotransformation products was determined through UV scans in the ultraviolet region. It must be noted that this

assay does not differentiate between *cis*-dihydrodiol products and any other aromatic product as it detects all compounds absorbing in the UV range. Because most of the starting materials are hydrophobic while the intended *cis*-dihydrodiol product is water-soluble, we anticipated that only the detectable products would be the water-soluble products derived from RHD oxidations. While this was true for many of the substrates like toluene (Figure 4.5), others like 4-methyanisole provided confounding results (Figure 4.6). In the case of toluene biotransformation, a clear product peak is observed at ~265 nm with no absorbance for the starting material alone. The 4-methylanisole, however, exhibits a peak for the substrate alone (in growth medium) and product peaks that are just above the peaks for the non-RHD control cultures. These observations present a challenge in assigning an honest score for the biotransformation; however, one could argue that the hypsochromic shift in absorption maxima for this substrate suggests a loss of conjugation indicative of RHD-mediated transformation. Regardless, the unexpected solubility and inherent multiple-peak absorption of compounds like 4-methylanisole interfered with confident interpretation of the data. Consequently, biotransformation scores were awarded conservatively with intentions to further optimize conditions to yield cleaner spectra.

Despite this obstacle, potential products were detected in all of the strains, with 3 of the 4 demonstrating transformation of at least 3 lignin models (Table 4.3). The TDO strain provided the most positives with evidence of 7 transformed model compounds, whereas the NDO strain demonstrated conversion of 6 lignin models, and the BPDO from *Burkholderia* LB400 exhibiting products from 3 models. Interestingly, the BPDO from *Rhodococcus globerulus* only displayed evidence of transforming its native substrate. Of the reactions that provided evidence for product formation, 4 were scaled up for product isolation, purification, and identification by collaborators at the University of Tennessee Center for Renewable Carbon. These scaled biotransformations all employed the TDO strain, but varied the substrate using toluene, 4-methylanisole, 4-chloroanisole, or 4-propylanisole. From these reactions, the *cis*-dihydrodiol was

confirmed for toluene, 4-methylanisole, and 4-chloroanisole via NMR (James Daleiden, unpublished data).

## V. Discussion and perspectives

The application of ring-hydroxylating dioxygenases for the production of biological *cis*-dihydrodiols has been strongly pursued since 1968 when Gibson confirmed the *cis* conformation of the dihydrodiol *Pseudomonas putida* F1 (19). Subsequent studies aimed to generate mutant strains like *Pseudomonas* F39/D (33) that were deficient in the RHD dehydrogenase responsible for rearomatizing the prized *cis*-dihydrodiol intermediate. As molecular techniques boomed in the 1970s with the discovery and application of restriction endonucleases in 1971 (34), Sanger sequencing in the late 1977 (35), and the first cloning vectors in the late 70s (36) opportunities arose for expressing RHD systems in cloning plasmids. Soon thereafter cloning strains housing RHD plasmids were being applied for the formation of *cis*-dihydrodiols from aromatic pollutants (4, 21). The recombinant strains used in this study represent some of the most well understood RHD systems, with 3D protein information currently available for the catalytic oxygenase component of most, offering valuable information about the potential substrates that can be transformed (37-40) (Table 4.4). This information can be compared to results of the current study to help contribute to the growing knowledge of RHD substrates and guide decisions for future manipulations of these enzymes for increased substrate range and diol formation.

While our screening approach for product formation lacked desired specificity, it served as an acceptable first approximation of RHD activity with the given library of lignin models. Results suggest that all of our RHDs, except the BPDO from *Rhodococcus,* can transform at least 3 of the provided lignin compounds. Much overlap between the potential substrate ranges of these enzymes was apparent, with most shared substrates between the TDO and NDO. The LB400 BPDO demonstrated a more unique (and

limited) substrate profile, which is somewhat surprising as one might expect the BPDO and NDO to share more similar substrates considering the resemblances in their cognate substrates (multi-ring, non-substituted, hydrophobic). Cross over between substrates for these two RHDS has, in fact, been previously reported (41). Additionally, the BPDO from LB400 has drawn attention for its lack of substrate discrimination, however (24, 25), most studies with this enzyme system focus on congeners of chlorinated polycyclic aromatic hydrocarbons, which were not tested in this study.

Owing to the lack of sensitivity and confidence demonstrated by the UV assay, only those reactions for which the *cis*-dihydrodiol was confirmed can truly be critically analyzed. These included reactions of the TDO with toluene, 4-methylanisole, and 4-propylanisole. The typical substrates for TDO are substituted benzenes (25), a class to which anisoles belong. In fact, the TDO-mediated dihydroxylation of anisole (methoxybenzene) and phenetole (ethoxybenzene) has been reported (42), however, the steric and electronic effects of other substituents has not been considered. The ability of the TDO to transform both 4-methylanisole and 4-chloroanisole, but not 4-propylanisole might suggest a steric hindrance of the propyl side chain in the binding site of the enzyme. Considering that both the methoxylated (electron donating) and chlorinated (electron withdrawing) anisoles were successfully transformed to *cis*-dihydrodiols, it is unlikely that differences in electronic effects influences the substrate conversion for this enzyme. The larger propyl group of 4-propylanisole, however, may have presented a size obstruction in the active site; however, this cannot be confirmed without proper binding studies.

Given this information, it is clear that further investigation is required to understand the substrate range of these enzymes with respect to lignin model compounds. The necessary insight may be provided through molecular docking studies using the available crystal protein structures and desired substrates, for which chemical files are available. Depending on the computational literacy of the researcher and the desired depth of information, one may choose from variety of available software. Autodock (43)

and SwissDock (44) are commonly used tools to provide binding energy information for various ligands. Additionally, *in silico* mutations can be made to the protein sequence in effort to determine which residue changes could facilitate stronger substrate binding to the active site. Previous mutational studies done on the TDO (45), NDO (41, 46) and BPDO (47) have helped to unveil key residues involved in substrate binding for these information. These insights could enable the construction of *in vitro* mutations and subsequent functional studies to tailor the enzymes for lignin substrates. The ability to enhance RHD conversions of lignin-related compounds could provide an enhanced application of residual lignin from the current bioethanol refineries and paper mills.

## VI. Acknowledgements

I would like to thank and acknowledge Mary Hadden, former lab manager of the Buchan lab, for her assistance in performing many of the initial biotransformations discussed in this chapter. I would also like to thank my peer/collaborator, James (Jim) Daleiden, former graduate student in Dr. Joseph Bozell's lab, for his contributions to this project. Jim was responsible for scaling up biotransformations and extracting, isolating, and chemically characterizing products from these reactions. Without his help, much of the presented data would not have been possible, as his work was critical to optimizing conditions for *cis*-dihydrodiol production.

# VII. References


1. **Diaz E.** 2004. Bacterial degradation of aromatic pollutants: a paradigm of metabolic versatility. Int Microbiol **7:**173-180.
2. **Diaz E, Jimenez JI, Nogales J.** 2013. Aerobic degradation of aromatic compounds. Curr Opin Biotechnol **24:**431-442.
3. **Carmona M, Zamarro MT, Blazquez B, Durante-Rodriguez G, Juarez JF, Valderrama JA, Barragan MJ, Garcia JL, Diaz E.** 2009. Anaerobic catabolism of aromatic compounds: a genetic and genomic view. Microbiol Mol Biol Rev **73:**71-133.
4. **Zylstra GJ, Gibson DT.** 1989. Toluene degradation by *Pseudomonas putida* F1. Nucleotide sequence of the *todC1C2BADE* genes and their expression in *Escherichia coli*. J Biol Chem **264:**14940-14946.
5. **Egland PG, Gibson J, Harwood CS.** 1995. Benzoate-coenzyme A ligase, encoded by *badA,* is one of three ligases able to catalyze benzoyl-coenzyme A formation during anaerobic growth of *Rhodopseudomonas palustris* on benzoate. J Bacteriol **177:**6545-6551.
6. **Schuhle K, Gescher J, Feil U, Paul M, Jahn M, Schagger H, Fuchs G.** 2003. Benzoate-coenzyme A ligase from *Thauera aromatica*: an enzyme acting in anaerobic and aerobic pathways. J Bacteriol **185:**4920-4929.
7. **Ismail W, Gescher J.** 2012. Epoxy coenzyme A thioester pathways for degradation of aromatic compounds. Appl Environ Microbiol **78:**5043-5051.
8. **Rather LJ, Knapp B, Haehnel W, Fuchs G.** 2010. Coenzyme A-dependent aerobic metabolism of benzoate via epoxide formation. J Biol Chem **285:**20615-20624.
9. **Teufel R, Mascaraque V, Ismail W, Voss M, Perera J, Eisenreich W, Haehnel W, Fuchs G.** 2010. Bacterial phenylalanine and phenylacetate catabolic pathway revealed. Proc Natl Acad Sci U S A **107:**14390-14395.

10. **Boyd DR, Bugg TD.** 2006. Arene cis-dihydrodiol formation: from biology to application. Org Biomol Chem **4:**181-192.
11. **Parales RE, Resnick SM.** 2006. Applications of aromatic hydrocarbon dioxygenases, Biocatalysis in the Pharmaceutical and Biotechnology Industries. CRC Press.
12. **Hudlicky T, Gonzalez D, Gibson DT.** 1999. Enzymatic dihydroxylation of aromatics in enantioselective synthesis: Expanding asymmetric methodology. Aldrichimica Acta **32:**35-62.
13. **Ensley BD, Ratzkin BJ, Osslund TD, Simon MJ, Wackett LP, Gibson DT.** 1983. Expression of naphthalene oxidation genes in *Escherichia coli* results in the biosynthesis of indigo. Science **222:**167-169.
14. **Newman LM, Garcia H, Hudlicky T, Selifonov SA.** 2004. Directed evolution of the dioxygenase complex for the synthesis of furanone flavor compounds. Tetrahedron **60:**729-734.
15. **Zhang NY, Stewart BG, Moore JC, Greasham RL, Robinson DK, Buckland BC, Lee C.** 2000. Directed evolution of toluene dioxygenase from *Pseudomonas putida* for improved selectivity toward cis-indandiol during indene bioconversion. Metab Eng **2:**339-348.
16. **Bugg TDH, Ramaswamy S.** 2008. Non-heme iron-dependent dioxygenases: unravelling catalytic mechanisms for complex enzymatic oxidations. Curr Opin Chem Biolog **12:**134-140.
17. **Ferraro DJ, Gakhar L, Ramaswamy S.** 2005. Rieske business: Structure–function of Rieske non-heme oxygenases. Biochem Biophys Res Commun **338:**175-190.
18. **Cerniglia CE, Morgan JC, Gibson DT.** 1979. Bacterial and fungal oxidation of dibenzofuran. Biochem J **180:**175-185.
19. **Gibson DT, Koch JR, Kallio RE.** 1968. Oxidative degradation of aromatic hydrocarbons by microorganisms .I. Enzymatic formation of catechol from benzene. Biochemistry **7:**2653-&.

20. **Resnick SM, Lee K, Gibson DT.** 1996. Diverse reactions catalyzed by naphthalene dioxygenase from *Pseudomonas* sp strain NCIB 9816. J Ind Microbiol Biotechnol **17:**438-457.
21. **Gibson DT, Resnick SM, Lee K, Brand JM, Torok DS, Wackett LP, Schocken MJ, Haigler BE.** 1995. Desaturation, dioxygenation, and monooxygenation reactions catalyzed by naphthalene dioxygenase from *Pseudomonas* sp strain-9816-4. J Bacteriol **177:**2615-2621.
22. **Mondello FJ.** 1989. Cloning and expression in *Escherichia coli* of *Pseudomonas strain* LB400 genes encoding polychlorinated biphenyl degradation. J Bacteriol **171:**1725-1732.
23. **Haddock JD, Nadim LM, Gibson DT.** 1993. Oxidation of biphenyl by a multicomponent enzyme-system from *Pseudomonas* sp strain LB400. J Bacteriol **175:**395-400.
24. **Seeger M, Zielinski M, Timmis KN, Hofer B.** 1999. Regiospecificity of dioxygenation of di- to pentachlorobiphenyls and their degradation to chlorobenzoates by the bph-encoded catabolic pathway of *Burkholderia* sp strain LB400. Appl Environ Microbiol **65:**3614-3621.
25. **Johnson RA.** 2004. Microbial arene oxidations. *In* Overman LE (ed), Organic Reactions, vol 63. John Wiley & Sons, Inc., Hoboken, New Jersey.
26. **Bordel S, Munoz R, Diaz LF, Villaverde S.** 2007. New insights on toluene biodegradation by *Pseudomonas putida* F1: influence of pollutant concentration and excreted metabolites. Appl Microbiol Biotechnol **74:**857-866.
27. **Singleton DR, Hu J, Aitken MD.** 2012. Heterologous expression of polycyclic aromatic hydrocarbon ring-hydroxylating dioxygenase genes from a novel pyrene-degrading betaproteobacterium. Appl Environ Microbiol **78:**3552-3559.
28. **Werlen C, Kohler HP, van der Meer JR.** 1996. The broad substrate chlorobenzene dioxygenase and cis-chlorobenzene dihydrodiol dehydrogenase of *Pseudomonas* sp. strain P51 are linked evolutionarily to the enzymes for benzene and toluene degradation. J Biol Chem **271:**4009-4016.

29. **McKay DB, Seeger M, Zielinski M, Hofer B, Timmis KN.** 1997. Heterologous expression of biphenyl dioxygenase-encoding genes from a gram-positive broad-spectrum polychlorinated biphenyl degrader and characterization of chlorobiphenyl oxidation by the gene products. J Bacteriol **179:**1924-1930.
30. **Faizal I, Dozen K, Hong CS, Kuroda A, Takiguchi N, Ohtake H, Takeda K, Tsunekawa H, Kato J.** 2005. Isolation and characterization of solvent-tolerant *Pseudomonas* putida strain T-57, and its application to biotransformation of toluene to cresol in a two-phase (organic-aqueous) system. J Ind Microbiol Biotechnol **32:**542-547.
31. **Jenkins RO, Dalton H.** 1985. The use of indole as a spectrophotometric assay substrate for toluene dioxygenase. FEMS Microbiol Lett **30:**227-231.
32. **Jones RN.** 1943. The ultraviolet absorption spectra of aromatic hydrocarbons. Chemical Reviews **32:**1-46.
33. **Gibson DT, Hensley M, Yoshioka H, Mabry TJ.** 1970. Oxidative degradation of aromatic hydrocarbons by microorganisms. III. Formation of (+)-cis-2,3-dihydroxy-1-methyl-4,6-cyclohexadiene from toluene by *Pseudomonas putida*. Biochemistry **9:**1626-1630.
34. **Danna K, Nathans D.** 1971. Specific cleavage of simian virus 40 DNA by restriction endonuclease of *Hemophilus influenzae*. Proc Natl Acad Sci U S A **68:**2913-2917.
35. **Sanger F, Nicklen S, Coulson AR.** 1977. DNA sequencing with chain-terminating inhibitors. Proc Natl Acad Sci U S A **74:**5463-5467.
36. **Bolivar F, Rodriguez RL, Greene PJ, Betlach MC, Heyneker HL, Boyer HW, Crosa JH, Falkow S.** 1977. Construction and characterization of new cloning vehicle. II. A multipurpose cloning system. Gene **2:**95-113.
37. **Friemann R, Lee K, Brown EN, Gibson DT, Eklund H, Ramaswamy S.** 2009. Structures of the multicomponent Rieske non-heme iron toluene 2,3-dioxygenase enzyme system. Acta Crystallographica Section D: Biological Crystallography **65:**24-33.

38. **Kauppi B, Lee K, Carredano E, Parales RE, Gibson DT, Eklund H, Ramaswamy S.** 1998. Structure of an aromatic-ring-hydroxylating dioxygenase-naphthalene 1,2-dioxygenase. Structure **6:**571-586.
39. **Karlsson A, Parales JV, Parales RE, Gibson DT, Eklund H, Ramaswamy S.** 2003. Crystal structure of naphthalene dioxygenase: side-on binding of dioxygen to iron. Science **299:**1039-1042.
40. **Kumar P, Mohammadi M, Viger J-F, Barriault D, Gomez-Gil L, Eltis LD, Bolin JT, Sylvestre M.** 2011. Structural insight into the expanded PCB-degrading abilities of a biphenyl dioxygenase obtained by directed evolution. J Mol Biol **405:**531-547.
41. **Parales RE, Lee K, Resnick SM, Jiang H, Lessner DJ, Gibson DT.** 2000. Substrate specificity of naphthalene dioxygenase: effect of specific amino acids at the active site of the enzyme. J Bacteriol **182:**1641-1649.
42. **Resnick SM, Gibson DT.** 1993. Biotransformation of anisole and phenetole by aerobic hydrocarbonoxidizing bacteria. Biodegradation **4:**195-203.
43. **Goodsell DS, Morris GM, Olson AJ.** 1996. Automated docking of flexible ligands: applications of AutoDock. J Mol Recognit **9:**1-5.
44. **Grosdidier A, Zoete V, Michielin O.** 2011. SwissDock, a protein-small molecule docking web service based on EADock DSS. Nucleic Acids Res **39:**W270-277.
45. **Jiang H, Parales RE, Lynch NA, Gibson DT.** 1996. Site-directed mutagenesis of conserved amino acids in the alpha subunit of toluene dioxygenase: potential mononuclear non-heme iron coordination sites. J Bacteriol **178:**3133-3139.
46. **Parales RE.** 2003. The role of active-site residues in naphthalene dioxygenase. J Ind Microbiol Biotechnol **30:**271-278.
47. **Zielinski M, Kahl S, Hecht HJ, Hofer B.** 2003. Pinpointing biphenyl dioxygenase residues that are crucial for substrate interaction. J Bacteriol **185:**6976-6980.

# VIII. Appendix: Tables

**Table 4.1**. Recombinant RHD strains used in this study and their source organism

| Enzyme classification | Source organism | Host strain | Plasmid |
|---|---|---|---|
| Toluene dioxygenase | *Pseudomonas putida* F1 | *E. coli* JM109 | pDTG601 |
| Naphthalene dioxygenase | *Pseudomonas* sp. strain NCIB 9816-4 | *E. coli* JM109 (DE3) | pDTG141 |
| Biphenyl dioxygenase | *Burkholderia* sp. LB400 | *E. coli* BL21 (DE3) pLysS | pAIA111 |
| Biphenyl dioxygenase | *Rhodococcus globerulus* P6 | *P. putida* KT2442 | pDM10 |

**Table 4.2**. Lignin model substrates used in this study

| Substrate | Structure | Solvent | [Final] |
|---|---|---|---|
| Toluene | 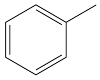 | NA (neat) | 18 mM |
| Naphthalene | 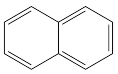 | DMSO | 7.8 mM |
| Biphenyl | 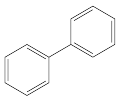 | DMSO | 0.5 mM |
| 4-methylanisole | 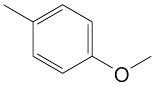 | NA (neat) | 6.3 mM |
| 4-chloroanisole | 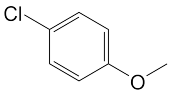 | NA (neat) | 9.2 mM |
| 4-propylanisole | 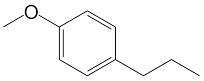 | NA (neat) | 5 mM |
| 1,3-dimethoxybenzene | 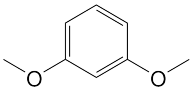 | NA (neat) | 2 mM |
| 1,4-dimethoxybenzene | 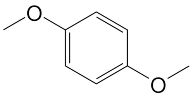 | DMSO | 2 mM |
| Syringaldehyde | 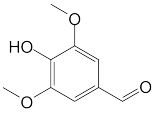 | DMSO | 2 mM |
| 2-methoxy-4-propylphenol | 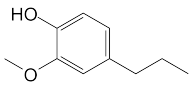 | NA (neat) | 0.2 mM |
| Vanillin | 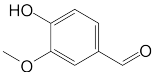 | DMSO | 6 mM |
| Vanillin acetate | 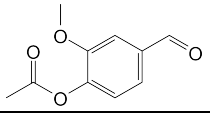 | DMSO | 6 mM |

**Table 4.3**. Results of the UV biotransformation screen using RHDs overexpressed on recombinant plasmids (pDTG601, pDTG141, pAIA111, pDM10) and a library of lignin model compounds. Purple boxes indicate evidence of product formation. Black outline indicates *cis*-dihydrodiol confirmation via NMR (Jim Daleiden).

| Substrate | Structure | TDO (pDTG601) | NDO (pDTG141) | BPDO (pAIA111) | BPDO (pDM10) |
|---|---|---|---|---|---|
| **Toluene** | 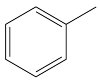 | + | + | + | + |
| **Naphthalene** | 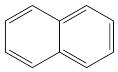 | + | + | - | - |
| **Biphenyl** | 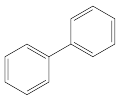 | ND* | ND | + | + |
| **4-methylanisole** | 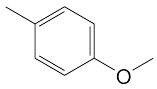 | + | + | - | - |
| **4-chloroanisole** | 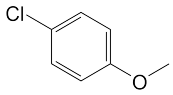 | + | + | - | - |
| **4-propylanisole** | 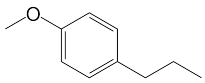 | - | - | ND | ND |
| **1,3-dimethoxybenzene** | 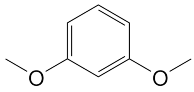 | + | + | - | - |
| **1,4-dimethoxybenzene** | 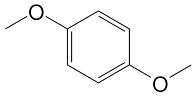 | - | - | - | - |
| **Syringaldehyde** | 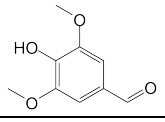 | + | + | + | - |
| **2-methoxy-4-propylphenol** | 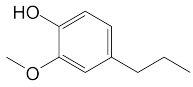 | - | + | - | - |
| **Vanillin** | 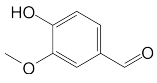 | + | - | + | - |
| **Vanillin acetate** | 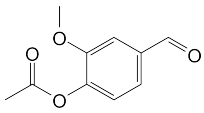 | + | - | + | - |

* ND indicates no data

**Table 4.4**. Crystal structure availability for the RHDs used in this study

| Enzyme classification | Source organism | PDB ID* | Reference |
|---|---|---|---|
| Toluene dioxygenase | *Pseudomonas putida* F1 | 3EN1 | Friemann *et al*. 2009 |
| Naphthalene dioxygenase | *Pseudomonas* sp. strain NCIB 9816-4 | 1O7G | Kauppi *et al*. 1998<br>Karlsson *et al.* 2003 |
| Biphenyl dioxygenase | *Burkholderia* sp. LB400 | 2XrX | Kumar *et al*. 2011 |
| Biphenyl dioxygenase | *Rhodococcus globerulus* P6 | No data | none |

* PDB = Protein Data Bank

# IX. Appendix: Figures

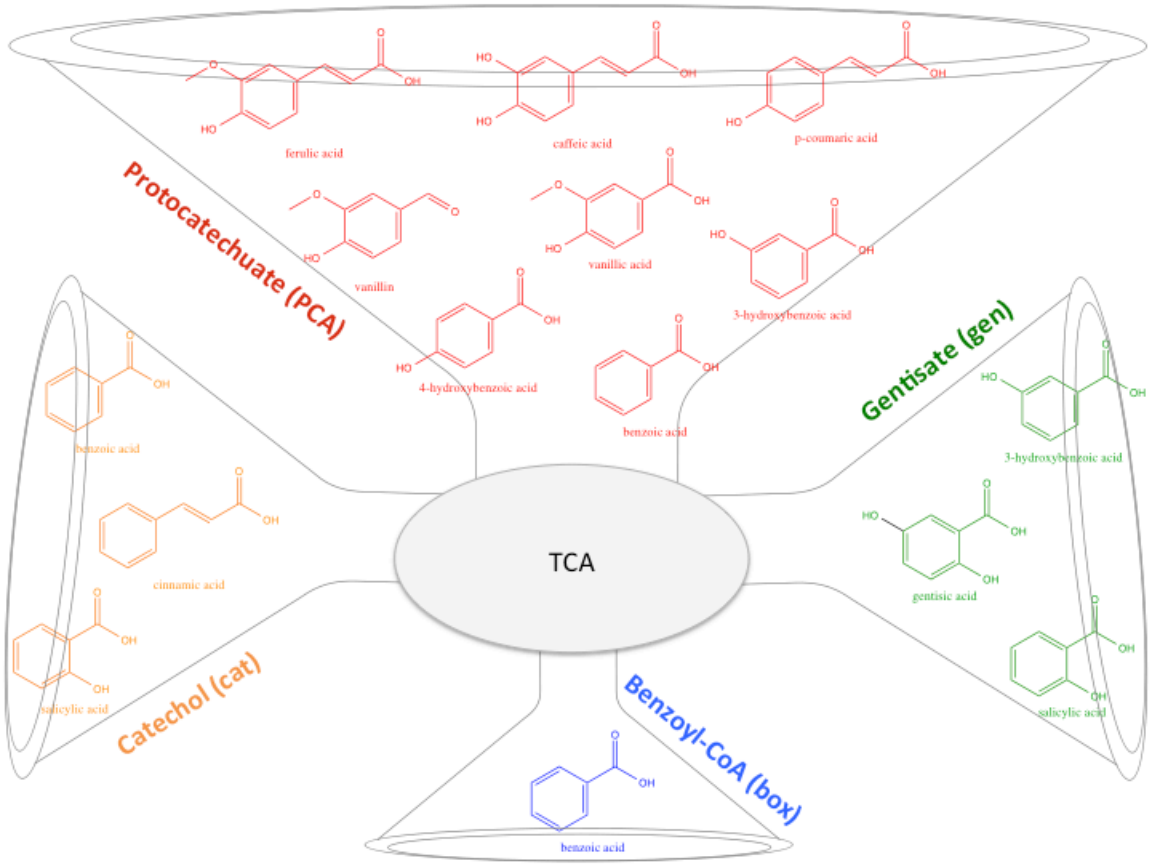


**Figure 4.1.** Illustration exhibiting the concept of catabolic funneling.

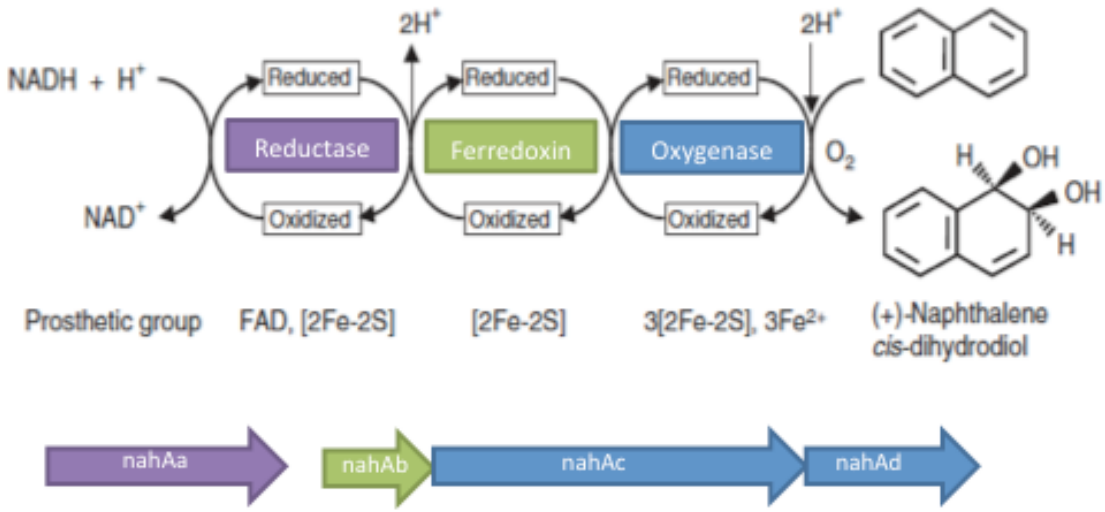


Gene map of naphthalene catabolic Genes in *Pseudomonas putida* PpG7 NAH7 plasmid

**Figure 4.2.** Mechanism of the RHD enzyme system whereby the electrons are transferred across reducing enzymes to the oxygenase component that is responsible for addition of dioxygen onto the ring. The example provided is from the naphthalene dioxygenase from *Pseudomonas putida* PpG7 (adapted from Parales and Resnick 2006). A genetic map is provided below to display the genes responsible for the given reactions.

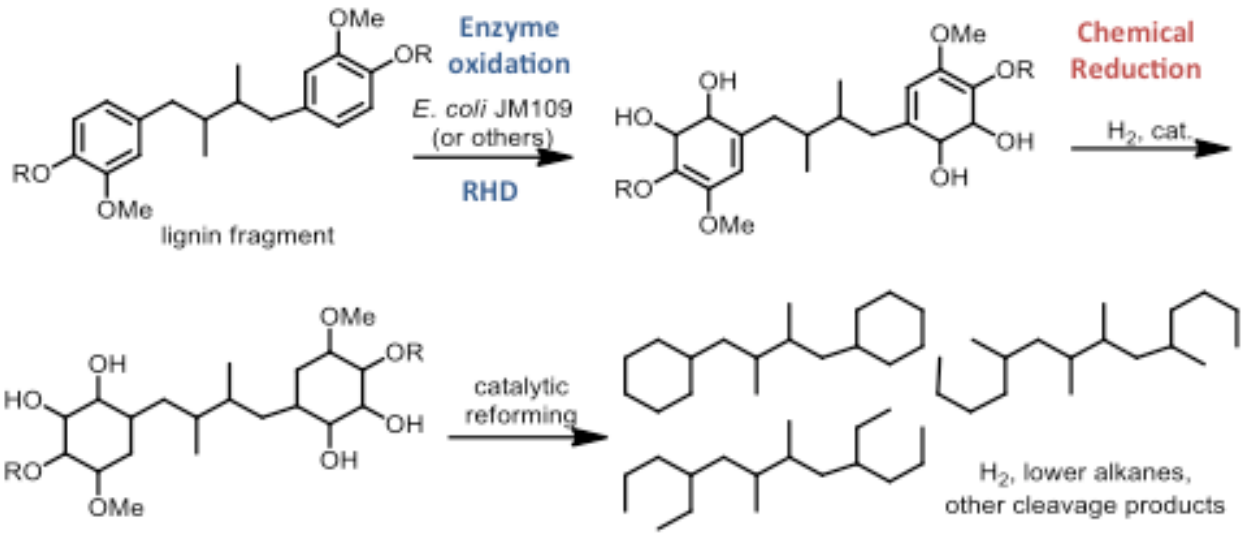


**Figure 4.3.** Reaction demonstrating the dihydroxylation of lignin models to *cis*-dihydrodiols for subsequent chemical conversion to hydrocarbons.

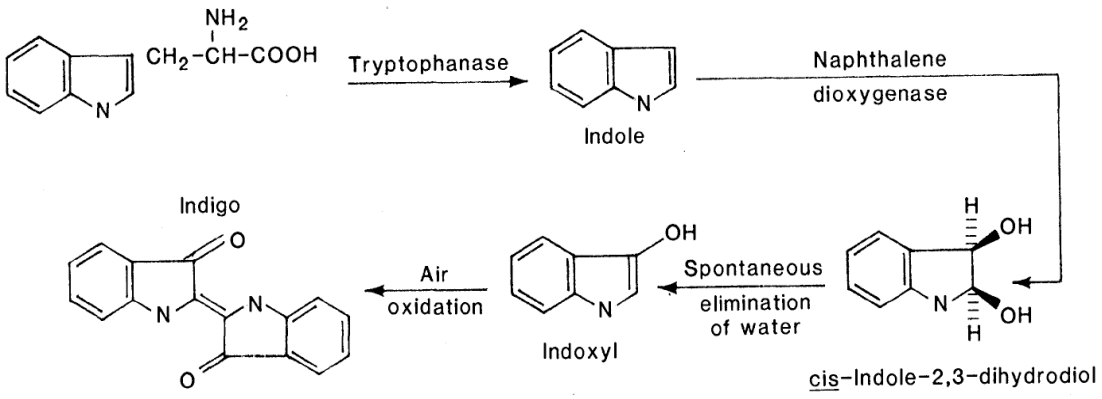


**Figure 4.4.** Proposed reaction for the formation of indigo from tryptophan. From Ensley *et al*. 1983

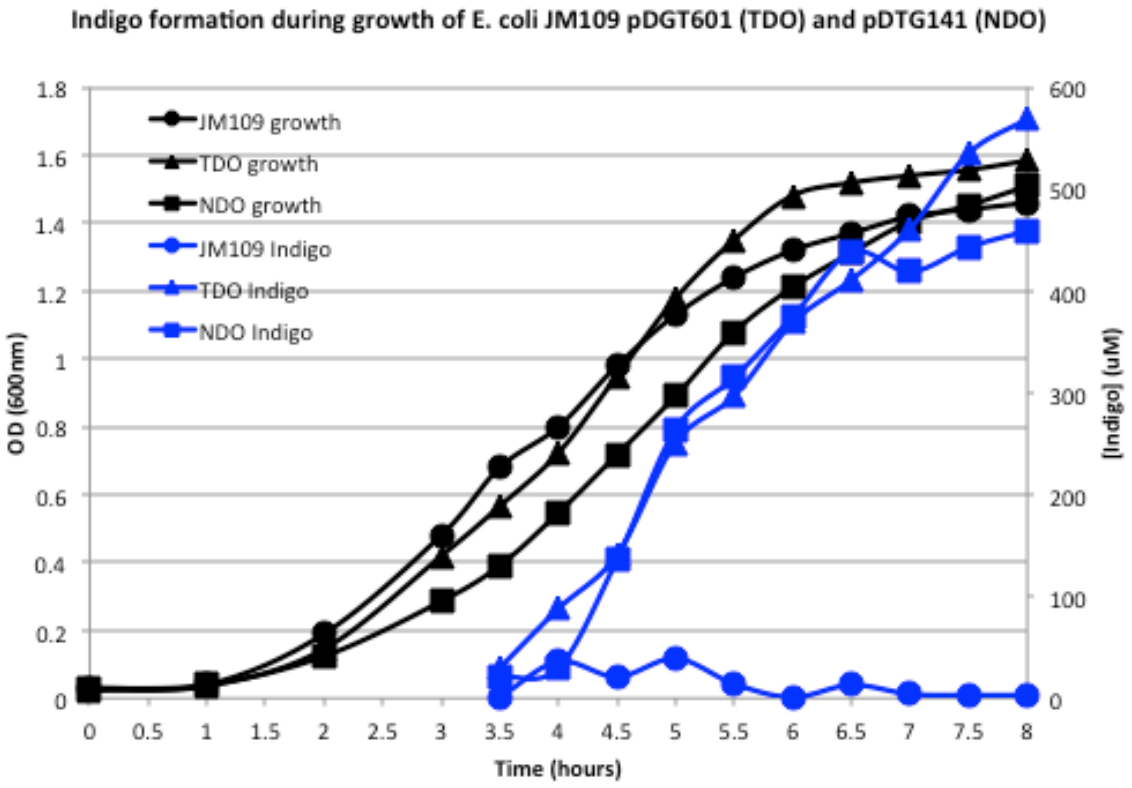


**Figure 4.5.** Results of the indigo assay with the toluene dioxygenase and naphthalene dioxygenase recombinant strains. Growth is measured by optical density on the left axis (black lines) and indigo concentration on the right axis (blue lines). Controls are represented by the JM109 host strain that lacks the respective RHD plasmid.

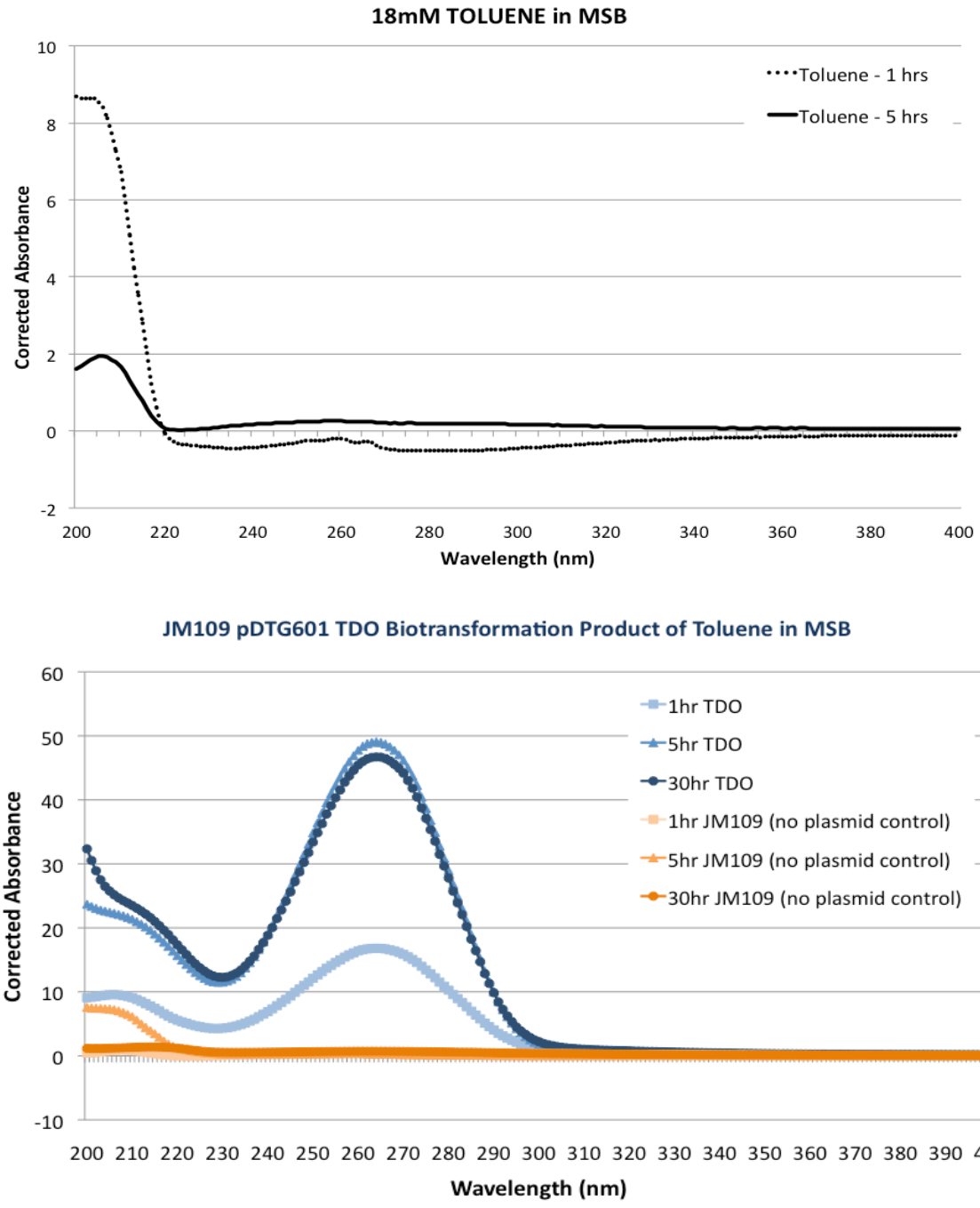


**Figure 4.6.** UV assay of from the biotransformation of toluene with the toluene dioxygenase. Products from the TDO strain are in blue and products from the control strain in orange. The top spectrum shows the absorbance of toluene alone in sterile growth medium.

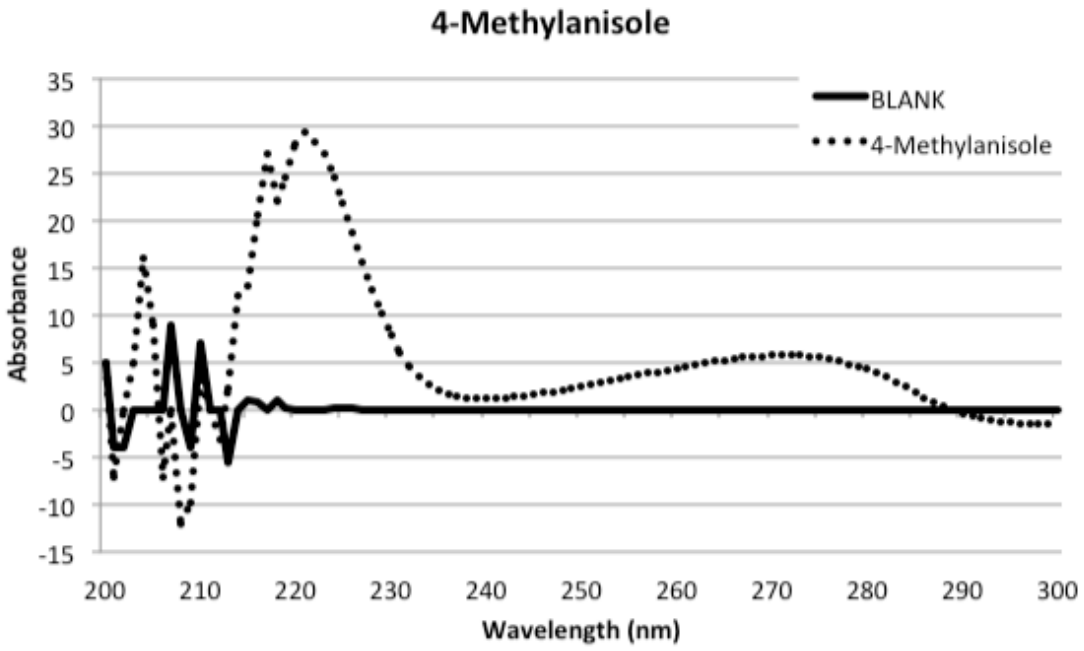


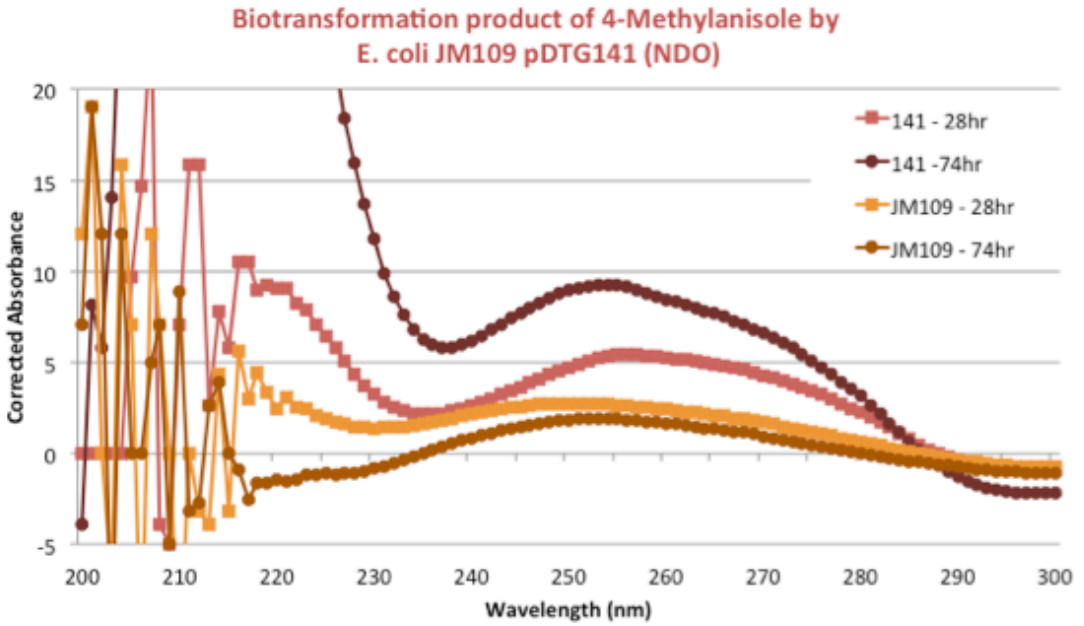


**Figure 4.7**. UV assay of from the biotransformation of 4-methylanisole with the naphthalene dioxygenase. Products from the NDO strain are in red and products from the control strain in orange. The top spectrum shows the absorbance of 4-methylanisole alone in sterile growth medium.

# CHAPTER FIVE - CONCLUSIONS AND FUTURE DIRECTIONS

Lignin, the most abundant aromatic polymer on earth, offers an outstanding opportunity to serve as a reservoir of renewable carbon. Due to the recalcitrance of this material, however, exploiting the potential of lignin has presented a considerable obstacle. The work described within this dissertation examined the diverse mechanisms by which bacteria transform lignin-derived compounds, with an emphasis on conversions that could result in the production of valuable products such as hydrocarbon fuels (1), synthetic chemicals (2), and commercial commodities like vanillin (3). The research applied to interrogate these biocatalytic conversions displayed varying levels of success, with several instances of ambiguous or interpretable outcomes. The occurrence of these setbacks is very much *unsurprising* as the challenges associated with lignin transformations (4, 5) and structural analyses (6) have long been acknowledged. Nevertheless, interesting and novel insights were uncovered that will aid in the optimization of future studies and generate new hypotheses with a higher probability of tangible outcomes.

Of the many conversions that were addressed, the most specific and informative of these involved the conversion of ferulic acid by the marine roseobacter isolate, *Sagittula stellata* E-37. Investigations into ferulate catabolism in this organism were primarily spurred by the intriguing observation of two annotated feruloyl-CoA synthase (*fcs*) genes located in disparate regions of the genome. With the knowledge that ferulic acid can be catabolized through pathways involving a vanillin intermediate (7) and that E-37 can utilize vanillin as a sole carbon source, it was hypothesized that E-37 utilizes at least one of the two encoded *fcs* genes to degrade ferulic acid through a vanillin intermediate. The presence of a vanillin intermediate was also a motivation for enhanced insight into this pathway due to its importance as chemical commodity (3, 8). Mutational studies were performed to generate strains with single and double knockouts for the *fcs* genes. To our surprise, the resulting phenotypes suggested only a partial involvement of either of the genes in ferulic acid catabolism, as growth was observed for all strains on ferulic acid that was only slightly depressed from that of the wildtype strain. Even more interestingly was the loss of growth on *p*-coumaric acid for the double

mutant, suggesting that both of these genes are required for the utilization of this compound, and not ferulic acid. These findings could reflect a misannotation of the two *fcs* genes in the E-37 genome and/or could indicate a level of enzyme promiscuity that requires further functional analysis to validate. The mutagenesis techniques performed on this strain also offers an advancement in roseobacter genetics (9), as two genetic approaches were successful implemented, one of which had only been documented for one roseobacter strain (10) and another that is completely novel to this lineage.

Another bacterial conversion that was examined was the transformation of a larger, more complex organosolv lignin substrate. The studies outlined in Chapter 3 describe a set of microcosm experiments where selected roseobacter strains were incubated with different preparations of organosolv lignin (11, 12). All of the microcosms provided strong evidence of bacterial growth on organosolv lignin, which in itself suggests a conversion of the material. 2D NMR analysis of the material across the different microcosms, however, provided mixed results. The strongest evidence for roseobacter transformations of lignin was derived from a 4 month microcosm incubation with *Citreicella* sp. SE45. At the end point of this experiment, the lignin profiles from 2D NMR suggest a complete loss of ferulate ester features, a considerable loss of β-O-4 linkages, and a diminished presence of phenylcoumaran and pinoresinol signals. While the disappearance of β-O-4 linkages cannot be readily explained by the genotype of the organism, the loss of ferulate esters could be a consequence of feruloyl esterase activity which is known to hydrolyze the cross-linkages between ferulate in lignin and the hemicellulose polysaccharide (13). There exists as a single gene annotated as a feruloyl esterases in the SE45 genome that exhibits strong sequence homology to other annotated feruloyl esterases. Although these experiments may require more replication to assign lignolytic activity to this organism, they provide a strong line of support for the pursuance of related studies aiming to add confidence to this claim.

The last reaction described in this work is the dihydroxylation of aromatic compounds by bacterial ring-hydroxylating dioxygenases (RHDs). This reaction has drawn much

attention due to its generation of a desirable *cis*-dihydrodiol intermediate. The broken aromaticity of this chemical species and the *cis* orientation of hydroxyl group provide advanced chemical functionality for subsequent conversion to a variety of chemical and pharmaceutical products (14). Work in this chapter involved screening a set of heterologously expressed RHDs for their ability to convert non-native lignin model compounds with the end-goal of accumulating *cis*-dyhydrodiols for subsequent chemical conversion. Results from this study was not as fruitful as desired, although some new information was exposed regarding the substrate range of these enzyme systems. Of the 4 tested RHDs, 3 showed evidence of converting three or more of the lignin compounds. Of these reactions, *cis*-dihydrodiols were confirmed from two of the starting lignin substrates (4-methylanisole and 4-chloroanisole). In effort to tailor these enzymes to accept a larger range of lignin-derived compounds, it is suggested to perform *in silico* protein docking studies with the selected lignin models. Information provided form this approach should illuminate key residues that could be mutated *in vitro* to allow for increased substrate conversion to *cis*-dihydrodiols.

When considering the future of lignin studies, there remains much hope. Due to the need for alternative energies, vigorous efforts have been put forth to expand our knowledge of lignin structure (15) and to tailor biomass (16) and microorganisms (17) for more efficient conversion to useful products. An extremely exciting advent in lignin technology is development of analytical techniques for resolving lignin structures. Between 2012 and 2014 mass spectrometry methods have improved from technologies optimized for lignin model compounds (18) to the resolution of structures from an complex organosolv switchgrass preparation (19). These advancements suggest that we may be approaching an era of lignin sequencing (6) which would highly strengthen efforts to discern both chemical and enzymatic conversions of the material. Given these positive prospects in lignin analysis, encouragement is extended for continued studies regarding bacterial transformations of lignin-derived compounds.

# I. References


1. **Parsell T, Yohe S, Degenstein J, Jarrell T, Klein I, Gencer E, Hewetson B, Hurt M, Kim JI, Choudhari H, Saha B, Meilan R, Mosier N, Ribeiro F, Delgass WN, Chapple C, Kenttamaa HI, Agrawal R, Abu-Omar MM.** 2015. A synergistic biorefinery based on catalytic conversion of lignin prior to cellulose starting from lignocellulosic biomass. Green Chemistry **17:**1492-1499.
2. **Bozell JJ, Holladay JE, Johnson D, White JF.** 2007. Top value added chemicals from biomass. Volume II - results of screening for potential candidtates from biorefinery lignin. Pacific Northwest National Laboratory, Richland.
3. **Priefert H, Rabenhorst J, Steinbuchel A.** 2001. Biotechnological production of vanillin. Appl Microbiol Biotechnol **56:**296-314.
4. **Bozell JJ.** 2014. Approaches to the selective catalytic conversion of lignin: A grand challenge for biorefinery development. Top Curr Chem **353:**229-255.
5. **Ragauskas AJ, Beckham GT, Biddy MJ, Chandra R, Chen F, Davis MF, Davison BH, Dixon RA, Gilna P, Keller M, Langan P, Naskar AK, Saddler JN, Tschaplinski TJ, Tuskan GA, Wyman CE.** 2014. Lignin valorization: improving lignin processing in the biorefinery. Science **344:**1246843.
6. **Banoub J, Delmas G-H, Joly N, Mackenzie G, Cachet N, Benjelloun-Mlayah B, Delmas M.** 2015. A critique on the structural analysis of lignins and application of novel tandem mass spectrometric strategies to determine lignin sequencing. J Mass Spectrom **50:**5-48.
7. **Rosazza JP, Huang Z, Dostal L, Volm T, Rousseau B.** 1995. Review: biocatalytic transformations of ferulic acid: an abundant aromatic natural product. J Ind Microbiol **15:**457-471.
8. **Plaggenborg R, Overhage J, Loos A, Archer JA, Lessard P, Sinskey AJ, Steinbuchel A, Priefert H.** 2006. Potential of *Rhodococcus* strains for biotechnological vanillin production from ferulic acid and eugenol. Appl Microbiol Biotechnol **72:**745-755.

9. **Piekarski T, Buchholz I, Drepper T, Schobert M, Wagner-Doebler I, Tielen P, Jahn D.** 2009. Genetic tools for the investigation of Roseobacter clade bacteria. BMC Microbiol **9:**265.
10. **Lidbury I, Murrell JC, Chen Y.** 2014. Trimethylamine N-oxide metabolism by abundant marine heterotrophic bacteria. Proc Natl Acad Sci U S A **111:**2710-2715.
11. **Bozell JJ, O'Lenick CJ, Warwick S.** 2011. Biomass fractionation for the biorefinery: heteronuclear multiple quantum coherence-nuclear magnetic resonance investigation of lignin isolated from solvent fractionation of switchgrass. J Agric Food Chem **59:**9232-9242.
12. **Astner AF.** 2012. Lignin yield maximization of lignocellulosic biomass by Taguchi robust product design using organosolv fractionation. Master's thesis. University of Tennessee.
13. **Mathew S, Abraham TE.** 2004. Ferulic acid: an antioxidant found naturally in plant cell walls and feruloyl esterases involved in its release and their applications. Crit Rev Biotechnol **24:**59-83.
14. **Parales RE, Resnick SM.** 2006. Applications of aromatic hydrocarbon dioxygenases, Biocatalysis in the Pharmaceutical and Biotechnology Industries. CRC Press.
15. **Ralph J, Lundquist K, Brunow G, Lu F, Kim H, Schatz PF, Marita JM, Hatfield RD, Ralph SA, Christensen JH, Boerjan W.** 2004. Lignins: Natural polymers from oxidative coupling of 4-hydroxyphenyl- propanoids. Phytochem Rev **3:**29-60.
16. **Anderson NA, Tobimatsu Y, Ciesielski PN, Ximenes E, Ralph J, Donohoe BS, Ladisch M, Chapple C.** 2015. Manipulation of guaiacyl and syringyl monomer biosynthesis in an *Arabidopsis* cinnamyl alcohol dehydrogenase mutant results in atypical lignin biosynthesis and modified cell wall structure. Plant Cell **27:**2195-2209.

17. **Himmel ME, Ding SY, Johnson DK, Adney WS, Nimlos MR, Brady JW, Foust TD.** 2007. Biomass recalcitrance: engineering plants and enzymes for biofuels production. Science **315:**804-807.

18. **Haupert LJ, Owen BC, Marcum CL, Jarrell TM, Pulliam CJ, Amundson LM, Narra P, Aqueel MS, Parsell TH, Abu-Omar MM, Kenttämaa HI.** 2012. Characterization of model compounds of processed lignin and the lignome by using atmospheric pressure ionization tandem mass spectrometry. Fuel **95:**634-641.

19. **Jarrell TM, Marcum CL, Sheng H, Owen BC, O'Lenick CJ, Maraun H, Bozell JJ, Kenttamaa HI.** 2014. Characterization of organosolv switchgrass lignin by using high performance liquid chromatography/high resolution tandem mass spectrometry using hydroxide-doped negative-ion mode electrospray ionization. Green Chemistry **16:**2713-2727.

# VITA

Ashley Frank was born in Elmhurst, Illinois to Robin and Ray Frank. She spent her childhood in the nearby town of Glen Ellyn. Growing up, Ashley was very active in both athletics and academic activities. She played softball from grade school through undergraduate and was a member of the volleyball team in middle school and high school. Ashley attended Elmhurst College for undergraduate studies where she received a double major in Biology and Art and a double minor in Chemistry and French. As evidenced by the diversity of unrelated degrees, Ashley often struggles with decisions due to her interest in a variety of fields. During undergraduate Ashley was accepted into an internship program at Argonne National laboratory where she worked for two consecutive summers. During these summers she worked for Dr. Frank Collart in the Biosciences division where she gained a strong interest in molecular biology. After undergraduate, Ashley worked as a full time contract worker at Argonne under Dr. Collart for about a year and a half before deciding to pursue graduate studies. In Fall 2009, Ashley entered graduate school at the University of Tennessee, Knoxville where she joined Alison Buchan's lab. The following six years consisted of a lot of research, interacting with new friends and scientists, going to local concerts, attending scientific meetings, and even participating in a US-EC course in Lausanne, Switzerland (the highlight of her graduate career). The less social aspects of these six years are documented within the many pages of this document and can be perused at your convenience.